

General Disclaimer

One or more of the Following Statements may affect this Document

- This document has been reproduced from the best copy furnished by the organizational source. It is being released in the interest of making available as much information as possible.
- This document may contain data, which exceeds the sheet parameters. It was furnished in this condition by the organizational source and is the best copy available.
- This document may contain tone-on-tone or color graphs, charts and/or pictures, which have been reproduced in black and white.
- This document is paginated as submitted by the original source.
- Portions of this document are not fully legible due to the historical nature of some of the material. However, it is the best reproduction available from the original submission.

CR-171730

NAS-9-14907

Development of A Contact Heat Exchanger for A Constructable Radiator System

Report No. 2-53200/3R-53490

1 July 1983



SUBMITTED TO

**National Aeronautics and Space Administration
Johnson Space Center
Houston, Texas**

BY


**Vought Corporation
Dallas, Texas**

(NASA-CR-171730) DEVELOPMENT OF A CONTACT
HEAT EXCHANGER FOR A CONSTRUCTABLE RADIATOR
SYSTEM (Vought Corp., Dallas, Tex.) 120 p
HC A06/MF A01 CSCL 20D

N84-17523

Unclass
11641

G3/34

 **Vought**

DEVELOPMENT OF A CONTACT
HEAT EXCHANGER FOR A
CONSTRUCTABLE RADIATOR SYSTEM

Report No. 2-53200/3R-53490

1 July 1983

SUBMITTED TO

National Aeronautics and Space Administration
Johnson Space Center
Houston, Texas

By

Vought Corporation
Dallas, Texas

Prepared By:

H. R. Howell

H. R. Howell

Approved By:

R. L. Cox

R. L. Cox

FOREWARD

The Contact Heat Exchanger Development Program described herein was conducted during the two and a half year period from January 1981 thru June 1983. Approximately 15 months of this period resulted from the long delivery times of the compact heat exchanger core and metal diaphragm used in the prototype test unit.

Mr. Mike Fleming performed the initial concept trade studies, designed, and tested the feasibility demonstration unit and initiated the prototype unit design. Mr. John Oren finalized the prototype unit design and planned the prototype test. Mr. Harold Howell conducted the prototype test and had the unenviable task of program documentation. The program was directed by Mr. Roy Cox.

4941
Mr. Gary Rankin of NASA-JSC Crew Systems Division, served as the Contracting Officer's Representative and provided valuable technical assistance and guidance throughout the program.

TABLE OF CONTENTS

	Page
1.0 Summary	1
2.0 Introduction	1
3.0 Concept Evaluation and Selection	2
3.1 Concept Description	3
3.2 Concept Selection	7
4.0 Feasibility Demonstration Test	7
4.1 Test Article Design and Fabrication	11
4.2 Test Description	11
4.3 Test Results	12
4.4 Experience With Test Hardware Fabrication	15
5.0 Prototype Test	17
5.1 Test Article Design	17
5.2 Test Set-up and Instrumentation	18
5.3 Test Results	19
5.4 Prototype Performance with Current Radiator Design	26
6.0 Conclusions and Recommendations	28
References	29
Appendix A - Fluid Pressure Contact Heat Exchanger Test	A-1
Appendix B - Prototype Contact Heat Exchanger Test Data	B-1

LIST OF FIGURES

	<u>Page</u>
1 Space Constructable Radiator	30
2 Effect of Thermal Interface ΔT on Constructable Radiator System Size	31
3 Constructable Radiator System Temperature Profile	32
4 Monogroove Heat Pipe	33
5 Concept 1	34
6 Fluid Pressure Clamping Contact Heat Exchanger	35
7 Concept 1 - Overall ΔT	36
8 Concept 2	37
9 Concept 2 - Overall ΔT	38
10 Concept 3	39
11 Concept 4	40
12 Concept 4	41
13 Concept 5	42
14 Concept 4 and 5	43
15 Concept 4 and 5	44
16 Concept 2A - Combining Heat Exchanger and Flexible Diaphragm	45
17 Sketch of Selected Concept Heat Exchanger Cross Section	46
18 Photographs of Feasibility Demonstration Test Article Contact Heat Exchanger	47
19 Instrumentation of Heating Tube and Heat Exchanger Elements	48
20 Thermal Vacuum Test Set-up	49
21 Test Results - Contact Conductance Vs Diaphragm Pressure For Two Heat Loads	50
22 Test Results - Contact Conductance Vs Diaphragm Pressure For Two Heat Loads	51
23 Constructable Interface Contact Conductance Comparison With Previous Data	52
24 Simulated Heat Pipe Instrumentation	53
25 Prototype Heat Exchanger Cross Section	54

LIST OF FIGURES CONT'D

26	Prototype Contact Heat Exchanger Overall View	55
27	Prototype Contact Heat Exchanger Manifold Assembly	56
28	Prototype Contact Heat Exchanger Insertion End View	57
29	Prototype Constructable Radiator Interface Test Article Description	58
30	Test Data Reduction Example	59
31	Prototype Constructable Radiator Interface Overall Conductance	60
32	Prototype Constructable Radiator Interface Contact Conductance	61
33	Constructable Interface Contact Conductance Comparison With Previous Data	62
34	Comparison of Vacuum and Ambient Pressure Contact Conductance	63
35	Prototype Constructable Radiator Interface Heat Exchanger Pressure Drop	64

LIST OF TABLES

	<u>Page</u>
1 Fluid Clamping Heat Exchanger Test Results	5
2 Comparison of HX Weights	8
3 Concept Evaluation	9
4 On-Orbit Construction and Replacement Operations	10
5 Constructable Radiator Interface Heat Exchanger Testing	13
6 Constructable Radiator Interface Test Summary	14
7 Instrumentation Verification	20
8 Contact Heat Exchanger Test Summary	21
8 Contact Heat Exchanger Test Summary Cont'd	22
8 Contact Heat Exchanger Test Summary Cont'd	23
9 Test Data Repeatability	25
10 Prototype Contact Heat Exchanger Performance For a Typical Design	27

1.0 SUMMARY

A two stage development program has been successfully completed for a connectable/disconnectable contact heat exchanger to be used in the constructable radiator system under development by the NASA Johnson Space Center. The contact heat exchanger provides for heat transfer from the spacecraft coolant loop to a heat pipe radiator system. Individual heat pipe radiators are "plugged" into, or removed from the contact heat exchanger to provide on orbit construction of a radiator system and replacement of individual panels for long-lived systems.

The contact heat exchanger uses an all welded flexible metal diaphragm pressurized with gaseous nitrogen to clamp segmented heat exchangers around a circular heat pipe radiator element. Each radiator panel replacement cycle requires the expenditure of 0.06 pounds of nitrogen. A feasibility demonstration test article and prototype unit have been fabricated and tested to verify the design concept and thermal performance. A contact conductance of 1520 BTU/hr.. ft² °F at 300 psi was obtained for the prototype unit. This excellent thermal performance provides for a minimum area radiator system due to the small temperature difference between the spacecraft coolant loop and the heat pipe radiator.

The concept also appears promising for solving a variety of spacecraft heat transfer problems including replaceable electronic equipment cold plates, spacecraft to spacecraft heat transfer and heat transfer between individual coolant loops and modular add-on thermal control systems.

2.0 INTRODUCTION

This report describes a development program for a contact heat exchanger to be used to transfer heat from a spacecraft coolant loop to a heat pipe radiator. The contact heat exchanger provides for a connectable/disconnectable joint which allows for on-orbit assembly of the radiator system and replacement or exchange of radiator panels for repair and maintenance. The contact heat exchanger does not require the transfer of fluid across the joint; the spacecraft coolant loop remains contained in an all welded system with no static or dynamic fluid seals. The contact interface is also "dry" with no conductive grease or interstitial material required.

Figure 1 shows the Constructable Radiator System under development by the NASA Johnson Space Center. It consists of a series of single heat pipe radiators assembled to form the spacecraft radiator system. Each heat pipe radiator is "plugged into" the spacecraft where the evaporator section of the heat pipe mates with the spacecraft coolant loop contact heat exchanger.

The constructable interface contact heat exchanger was developed in two stages. First, concepts were evolved and screened. A concept was selected and a feasibility demonstration unit was fabricated and tested to verify the concept. Secondly, a full scale prototype unit was fabricated and tested to verify the design. Each of the development stages are described in this report.

3.0 CONCEPT EVALUATION AND SELECTION

Five concepts were established and evaluated for use as the constructable radiator interface:

- (1) Fluid Clamping - Round Evaporator Section
- (2) Fluid Clamping - Separate Heat Exchanger - 8 Shape
- (3) Fluid Clamping Using Conductive Fluid
- (4) Finned Evaporator With Gas Pressurized Bladder
- (5) Finned Evaporator With Overcenter Clamp/Deformation

The evaluation is based on the heat pipe radiator design information provided by NASA/JSC. Separate high and low temperature loops are specified. The high temperature loop would have a radiator inlet temperature of 250°F and an outlet temperature of 40°F. An acetone heat pipe radiator will be used for the high temperature loop with a maximum single panel heat rejection of 2 kW.

The low temperature loop will operate with a radiator inlet temperature of 150°F and an outlet of 0°F. Ammonia will be the heat pipe fluid and the maximum single panel heat rejection will be approximately 1 kW.

Figure 2 shows the low temperature loop radiator area requirements for a typical 25 kW heat load as a function of the temperature difference between the fluid and the first radiator panel (contact heat exchanger ΔT). With the radiator panels flowed in series, each panel successively operates at a lower temperature and hence rejects successively less heat. Therefore, the contact heat exchanger for each panel has a corresponding smaller fluid to heat pipe ΔT . Figure 3 shows that the first panel rejects 0.90 to 1.08 kW depending on the heat exchanger ΔT , and the last panel rejects only 0.22 to 0.24 kW. Thus, if the first panel had a 15°F ΔT the last panel would have only a 3.4°F ΔT .

It is desirable to flow the constructable radiator panels in series, because each heat pipe must operate at a temperature lower than the panel fluid outlet temperature. Thus, an all parallel system would have all radiator panels operating below 0°F , in order to cool the fluid to 0°F , and the radiator area requirements would be excessive. For example, for a 25 kW heat load, the low temperature loop flowed in parallel would require 132 radiator panels assuming a 15°F contact heat exchange ΔT , whereas the all series system would require only 53 panels (Figure 2). In a conventional pumped fluid radiator panel (such as the Space Shuttle Orbiter), the temperature difference between the fluid and radiator tube is on the order of 5 to 10°F . The pumped fluid radiator with the relatively large fluid heat transfer area available due to parallel flow tubes over the entire radiator area results in the minimum radiator area requirements. Thus, a contact heat exchanger ΔT of 5 to 10°F represents a practical lower limit for comparison purposes. Figure 2 indicates that 51-52 panels are required for a first panel ΔT of 5°F - 10°F and 53 panels are required for a 15°F ΔT . Therefore, a contact heat exchanger design goal of 15°F would result in only a 1.9% to 3.9% increase in radiator area. More detailed trades may indicate that higher ΔT 's are allowable (a 25°F ΔT results in only a 9.8% increase in panel area). However, a 15°F ΔT has been established as a preliminary design goal and will be used in evaluating the interface concepts. It should be noted that the temperature difference between the heat pipe evaporator wall and the condenser wall has not been included in the above analysis in order to isolate the heat exchanger ΔT effects.

3.1 CONCEPT DESCRIPTION

Both the high temperature acetone and low temperature ammonia heat pipes utilize the monogroove design illustrated in Figure 4. The basic monogroove design contains two large axial channels, one for vapor, and one for liquid. A small slot separating the channels creates a high capillary pressure difference that, coupled with the minimized flow resistance of the two separate channels, gives the high axial heat transport. High evaporation and condensation film coefficients are provided by circumferential grooves in the vapor channel walls.

The resultant figure eight cross section and restriction of heat transfer to only the vapor channel presents a design challenge for the contact heat exchanger. A round or flat interface is desirable for clamping the surfaces and providing efficient heat transfer.

Concept 1, Figure 5, provides a round cross section heat pipe and utilizes the coolant loop fluid for clamping pressure*. The contact heat exchanger consists of a cylindrical sleeve into which the evaporator section of the heat pipe is inserted. The sleeve is made up of concentric inner and outer walls, separated by an annular fluid passageway. The inner wall is an axially convoluted metal diaphragm, 0.003 inches thick, which deforms under fluid pressure and clamps against the heat pipe. The heat pipe is easily extracted or installed by removing the fluid pressure. A high contact conductance is obtained due to the uniform contact pressure. The flexibility of the thin diaphragm allows it to conform to the waviness or other irregularities of the heat pipe surface.

The fluid clamping concept has been verified by test. Figure 6 shows the contact heat exchanger test article. A 6 ft. long 1.0 inch diameter heat pipe/radiator panel was included in the test to provide a heat sink for the contact heat exchanger. Table 1 shows the test results, demonstrating that high contact conductances can be obtained by the fluid clamping technique. A complete test description is given in Appendix A.

Figure 7 presents a design nomograph for Concept 1. The top curve shows the required heat pipe length (contact area) as a function of the heat flux. Surface area and length are also shown. The bottom graph shows the overall temperature difference between the fluid and the heat pipe as a function of heat flux. Values are shown for contact conductances from 50 to 600 BTU/hr. ft.² °F. The annular flow heat transfer coefficient was calculated to be 339.7 BTU/hr. ft.² °F based on an R-21 flow rate of 1000 lb./hr.

The required length of the heat pipe in contact with the heat exchanger is obtained by entering the desired overall ΔT (15°F) of the bottom curve, reading across to the design contact conductance (500 BTU/hr. ft.² °F), reading up to the appropriate heat pipe curve (ammonia or acetone), and reading across to the required length. A 7.3 ft. evaporator length is required for the acetone heat pipe, and the ammonia heat pipe requires a 3.2 ft. evaporator.

*This concept was conceived, fabricated and tested under Vought IR & D funds.

TABLE I
FLUID CLAMPING HEAT EXCHANGER TEST RESULTS

T sink = -256°F

R-21 FLOW, LB/HR	340	1005	2001	3002	3001
INLET TEMP, °F	33	43	46	48	69
R-21 PRESS, psia	300	300	300	300	300
R-21 ΔP , psid	0.25	0.75	2.38	3.14	5.22
R-21 TEMP DROP, °F	5.63	2.18	1.16	0.79	0.89
HEAT REJECTION, BTU/hr	465	537	571	586	671
OVERALL CONDUCTANCE, BTU/hr ft ² °F	56.5	95.5	136.0	160.0	160.0
CONTACT CONDUCTANCE, BTU/hr ft ² °F	580	580	580	580	580
CONTACT ΔT , °F	3.3	3.9	4.1	4.2	4.8

Concept 2 (Figure 8) provides heat exchanger contact with only the vapor channel of the heat pipe and allows the heat pipe figure 8 shape to be retained. The heat exchanger core is segmented and is forced against the heat pipe by a separate fluid pressure between the outer sleeve and diaphragm. The heat exchanger core increases the fluid hA over the annular flow of Concept 1 and potentially decreases the required contact area provided the high contact conductance between the heat exchanger and heat pipe can be retained.

Figure 9 shows the design nomograph for Concept 2. As indicated the required evaporator lengths are 14.3 ft. for the acetone heat pipe and 7.25 ft. for the ammonia heat pipe. Although the required lengths are considerably longer than for Concept 1, the required contact area has been reduced from approximately 1.01 ft.² to 0.90 ft.². The longer length requirement results from less area available per unit length due to the smaller diameter of the vapor channel and that only 270° of arc of the channel can be contacted.

Concept 2 requires a separate fluid pressurization system to provide the contact pressure, but does not require shutting down the entire coolant loop, or isolating the coolant in the heat exchanger for radiator removal/insertion as does Concept 1. The pressure can be supplied by a gas or liquid. Liquid pressurization systems could include a spring loaded accumulator to allow for fluid thermal expansion and contraction with pressurization and pressure relief provided by a piston driven by an overcenter latch or other mechanical advantage device. The gas pressurization system could be high pressure N₂ storage with the small volume of heat exchanger gas expended during each radiator change-out. Mechanical compression/decompression of the contact heat exchanger gas can be accomplished if expendables are not desired. It is anticipated that the number of radiator change-outs will be relatively small during the spacecraft life and that the total gas expended will be small.

A third thermal interface concept, illustrated in Figure 10, incorporates an interstitial fluid between the diaphragm and the heat exchanger. This allows the heat exchanger position to be fixed (no relative motion) during the radiator removal/insertion. Fluid pressurization and relief is accomplished in the same manner as discussed above for Concept 2. A brief survey of fluids indicated that a 50% copper powder/krytox mixture will provide acceptable thermal performance. The temperature drop through the fluid is small compared to the total ΔT of 15°F, being 0.64°F for the ammonia heat pipe and 1.24°F for the acetone heat pipe.

Concepts 4 and 5 involve flat plate contact heat exchangers which accommodate the radiator panel fin. Thus, the contact area is not required to conform to the heat pipe cross section and larger contact areas can be obtained. However, there is an additional temperature drop in the radiator fin, i.e. heat must be conducted through the fin to the heat pipe.

Figure 11 shows Concept 4. An over-center latch is used to bring the fin and heat exchanger surfaces in contact and the pressurized bladder provides the final contact pressure. Figure 12 shows the results of a cursory structural analysis on the latch. Although the total force (144,000 lb.) is large, the latch dimensions are reasonable.

Concept 5, shown in Figure 13, utilizes a curved back-up panel to provide a uniform contact pressure. The over-center latches provide the final contact pressure and would require considerable force to engage. With a latch mechanical advantage of 100:1, each latch would require a force of 112.5 lb. This could be reduced by having more latches, but assembly operations and weight would increase. Figures 14 and 15 show the contact length required for Concepts 4 and 5 for the acetone and ammonia heat pipes. Figure 14 shows the length required for one-sided heat input and Figure 15 shows the length required for two-sided heat input.

3.2 CONCEPT SELECTION

Table 2 summarizes the required evaporator lengths for each of the five concepts and the thermal interface weights. Table 3 summarizes the advantages and disadvantages of each concept. The on-orbit radiator panel construction and replacement operations are summarized in Table 4. Concept 2 was judged to have more advantages than the other concepts except for the complex diaphragm shape required for the figure 8 heat pipe cross section. Concept 2A, Figure 16, incorporates the best features of Concept 1 and Concept 2. The round heat pipe cross section is maintained, a high fluid conductance (hA) is obtained from the heat exchanger core, and a separate pressurization system is utilized.

4.0 FEASIBILITY DEMONSTRATION TEST

The objectives of the feasibility demonstration test were:

1. To assemble a contact heat exchanger using a flexible diaphragm and heat exchanger segments.
2. To demonstrate operation of heat exchanger/heat pipe assembly and disassembly using the concentric heat pipe radiator.

TABLE 2
COMPARISON OF HX WEIGHTS

CONCEPT	WT/FT Evap Length LB	LENGTH Reqd. for 15 ⁰ FΔT-FT		WT HX-LB	
		Acetone	Amonia	Acetone	Amonia
1.	.781	7.3	3.2	5.7	2.5
2.	.364	14.3	7.2	5.2	2.6
3.	1.494	6.8	4.2	10.2	6.3
4.	2.515	9.8	4.9	24.6	12.3
5.	2.805	6.9	3.0	19.4	8.4

TABLE 3
CONCEPT EVALUATION

ADVANTAGES		DISADVANTAGES	
CONCEPT 1	<p>LOWER EVAP. LENGTH</p> <p>EASIER DIAPHRAM SHAPE</p> <p>NO HX CORE</p> <p>PROVEN CONCEPT</p>	<p>ANNULUS NOT AS EFFICIENT FILM COEFF. REQUIRES SEPERATE FLUID SYSTEM OR HIGHER RISK</p> <p>WEIGHT PENALTY TO MAKE HP ROUND</p>	
CONCEPT 2	<p>ONLY PRESSURIZATION SYSTEM REQUIRED</p> <p>HX CORE HIGH FILM COEFFICIENT</p> <p>LOWER OPERATING RISK THAN CONCEPT 1</p>	<p>COMPLEX DIAPHRAM SHAPE REQUIRES SMALL HX CORE - REQUIRES LONGER EVAP</p>	
CONCEPT 3	<p>USES THERMALLY EFFICIENT SIMPLE HX</p> <p>PROVEN CLAMPING CONCEPT</p> <p>LOWER RISK THAN CONCEPT 1</p>	<p>DEPENDS ON THERMAL FLUID PROPERTIES</p>	ORIGINAL PAGE 13 OF POOR QUALITY
CONCEPT 4	<p>SIMPLE PRESSURIZATION SYSTEM</p> <p>USES CURRENT HP SHAPE</p> <p>SIMPLE CONSTRUCTION MORE RELIABLE</p>	<p>WEIGHT</p> <p>SLIGHTLY LONGER EVAPORATOR</p>	
CONCEPT 5	<p>SIMPLE CONSTRUCTION</p> <p>USES CURRENT HP SHAPE NO PRESSURIZATION REQUIRED-HIGHEST RELIABILITY</p>	<p>WEIGHT</p> <p>SIGNIFICANT FORCE TO ASSEMBLE</p>	

TABLE 4

ON-ORBIT CONSTRUCTION AND REPLACEMENT OPERATIONS

<u>CONCEPT 1</u>	-	(1) ISOLATION OF HEAT EXCHANGER (2) VENTING OR COOLING OF FLUID TO LOW PRESSURE (3) REMOVAL OF HEAT PIPE RADIATOR (4) RE-INSTALLATION OF HEAT PIPE RADIATOR (5) OPEN ISOLATION VALVES	
		<u>REQUIRES:</u> - ISOLATION VALVES - VENTING TO SPACE OR A COOLING SYSTEM	
	<u>OPTION:</u>	SECONDARY LOOP WITH LOW VAPOR PRESSURE FLUID REQUIRES PUMP/ACCUMULATOR ASSEMBLY	
<u>CONCEPT 2</u> <u>CONCEPT 3</u>	-	(1) VENT OR RELIEVE PRESSURE (HYDRAULIC SYSTEM OPTION) (2) REMOVE HP RADIATOR (3) REINSTALL HP RADIATOR (4) REPRESSURIZE	
		<u>REQUIRES:</u> - PRESSURIZATION SYSTEM - THERMALLY CONDUCTIVE FLUID (CONCEPT 3)	
<u>CONCEPT 4</u>	-	(1) VENT OR RELIEVE PRESSURE (HYDRAULIC SYSTEM OPTION) (2) REMOVE HP RADIATOR/UNLATCH CLAMPS (3) REINSTALL HP RADIATOR (4) REPRESSURIZE/RELATCH CLAMPS	<u>REQUIRES:</u> - PRESSURIZATION SYSTEM
<u>CONCEPT 5</u>	-	(1) UNLATCH CLAMPS (UP TO 16 OPERATIONS) (2) REMOVE HP RADIATOR (3) REINSTALL HP RADIATOR (4) RELATCH CLAMPS	<u>REQUIRES:</u> - LATCHING TOOL OR HIGH FORCE

3. To conduct an evaluation of the thermal performance of the heat exchanger using a simulated heat pipe.

All three of these objectives were successfully accomplished. The design of the feasibility test article was successfully fabricated and operation demonstrated.

4.1 TEST ARTICLE DESIGN AND FABRICATION

The test article design is illustrated in the sketch of Figure 17 and the photograph of Figure 18. Further detail of the design is given in Vought Drawings CR51772-002 and -003. Referring to Figure 17, the heat exchanger segments are made using split cylindrical thirds of a soft (2024T0) aluminum tubing. Small, 1/16 in. O.D. aluminum flow tubes are brazed on the outside. These tubes carry the heat transport fluid. The sections are formed to match the one inch diameter of the heat pipe evaporator. The sections are then installed into the diaphragm assembly which consists of 0.003 inch thick stainless steel diaphragm assembly which has been pressure formed to accommodate the three segments and retain flexibility to allow sufficient movement to clamp the segments on a heat pipe installed in the center. The 0.003 inch diaphragm is transitioned into a cylindrical shape at the ends and welded into a 0.020 inch thick stainless steel outer shell. A fitting is installed into the wall of the outer shell to allow pressurization of the area between the outside of the diaphragm and the inside of the shell. After the segments are installed into the diaphragm assembly, the flow tubes are connected to a doughnut shaped manifold at the ends. A protective cover is installed over the manifold.

Operation of the heat exchanger is effected by inserting the heat pipe evaporator into the center of the heat exchanger segments. The segments are then forced into contact with the heat pipe by pressurizing the diaphragm with gaseous nitrogen. Heat is transferred from the heat transport fluid to the element surfaces and into the heat pipe evaporator. Relieving the diaphragm pressure allows the heat pipe to be removed.

4.2 TEST DESCRIPTION

The approach taken to test the heat exchanger involved determination of the conductance across the contacting surfaces, commonly referred to as h_c .

This conductance has the same units and application as a convective film coefficient, h , or overall heat transfer coefficient. In these formulations:

$$Q = h_c A_c \Delta T_c$$

Q - heat load

h_c - contact conductances

A_c - contact surface area

ΔT_c - temperature difference between the contacting surfaces

Given the value of A_c , measurements of Q and ΔT are required to define h_c values. The approach taken to obtain this data was to place thermocouples on the heat exchanger surface and on the simulated heat pipe contacting surface. The thermocouple locations were as shown in Figure 19. The simulated heat pipe consists of an aluminum tube with an electric resistance heater installed inside the tube to provide a heat load. Heat is transferred to the inside wall of the tube and removed by the fluid flowing through the heat exchanger. The direction of heat flow in this arrangement is the opposite of the normal operation of the heat pipe evaporator, however, this should cause no error in the measurement of contact conductance. The ΔT_c is determined by the difference in the heat exchanger element temperatures and the simulated heat pipe temperatures. As shown in the overall test setup in Figure 20, additional immersion thermocouples were installed at the inlet and outlet of the heat exchanger and a flowmeter used to determine flowrate. This allowed measurement of heat load, Q , by $m C_p \Delta T$. An additional measurement of Q from electrical measurements of power input to the heater was also taken. The test was conducted in a vacuum chamber at 10^{-5} torr or less pressure. Assembly and disassembly operations were conducted post test in atmospheric conditions.

The test sequence established was as shown in Table 5. Data was taken over parametric variations of heat load, diaphragm pressures and flowrate.

4.3 TEST RESULTS

Twenty-five test points were taken over a range of pressures from 0 to 300 psig at power inputs of 200, 250, 300, and 400 watts. A summary of the test points taken and the results are shown in Table 6.

Test points at flowrates of 300 lbm/hr and 200 lbm/hr were taken during the testing.

TABLE 5
CONSTRUCTABLE RADIATOR INTERFACE HEAT EXCHANGER TESTING

<u>Test Matrix</u>				
<u>TEST POINT</u>	<u>DIAPHRAGM PRESSURE (PSI)</u>	<u>H₂O TEMPERATURE TO TEST ARTICLE (°F)</u>	<u>HEAT INPUT (WATTS)</u>	<u>H₂O FLOWRATE (LBM/HR)</u>
1	50	60	200	300
2	50	"	400	300
3	50	"	500	300
4	100	"	300	300
5	100	"	400	300
6	100	"	500	300
7	200	"	300	300
8	200	"	400	300
9	200	"	500	300
10	300	"	300	300
11	300	"	400	300
12	300	"	500	300

TABLE 6
CONSTRUCTABLE RADIATOR INTERFACE TEST SUMMARY

TEST POINT	PRESSURE (PSIG)	CONTACT SURFACE AT (°F)	POWER mCP AT (WATTS)	POWER EI (WATTS)	FLOWRATE (LBM/HR)	PRESSURE DROP (PSI)	CONTACT CONDUCTANCE (BTU/HR-FT ² -°F)	OVERALL HEAT TRANSFER COEFFICIENT (BTU/HR-FT ² -°F)
101	200	6.4	272.4	250.5	300	.53	547.5	277.2
102	300	5.7	272.4	250.5	300	.51	609.8	294.8
103	0	31.4	272.4	250.4	300	.54	110.9	89.1
104	100	8.6	272.4	250.7	300	.49	406.9	232.6
105	300	6.4	307.6	306.7	300	.52	66.8	308.3
106	200	7.0	316.3	306.4	300	.51	610.6	295.5
107	100	8.9	325.1	306.3	300	.50	476.3	262.6
108	50	12.2	325.1	306.3	300	.49	348.7	216.1
109	0	34.5	342.7	306.5	300	.52	123.6	97.4
110	0	44.8	430.6	404.1	300	.48	125.4	98.8
111	50	17.3	430.6	403.6	300	.57	323.3	202.0
112	100	12.9	439.4	403.2	300	.49	435.5	244.0
113	200	9.6	413.0	402.5	310	.53	581.9	290.7
114	300	8.3	430.6	402.2	300	.52	671.8	312.4
115	300	8.5	397.9	401.6	209	.35	650.0	296.7
116	300	6.6	333.9	304.3	300	.53	641.8	305.9
117	0	32.3	333.9	304.3	300	.52	131.0	102.8
118	50	13.2	333.9	304.6	300	.53	321.2	200.2
119	50	13.0	306.1	304.7	209	.32	324.6	196.1
120	100	9.9	295.7	304.7	206	.34	430.0	233.0
121	200	7.6	300.2	304.7	205	.34	559.4	271.6
122	200	5.2	198.2	201.4	205	.31	539.5	265.1
123	300	4.7	192.2	201.6	205	.31	601.8	280.5
124	100	6.2	201.6	201.4	222	.37	448.7	245.3
125	50	8.4	203.0	201.6	210	.32	333.0	202.4

ORIGINAL PAGE IS
OF POOR QUALITY

Relatively low flowrates were used to provide a higher fluid temperature difference across the heat exchanger for more accurate heat load measurements by the $m C_p \Delta T$ method. Heat load calculated from electrical measurements differed from that from the flow measurements by up to 11% at the higher flowrate but less than 1% at the lower flowrate. The electrically measured heat load was used in the performance calculations.

Using the average of inlet and outlet fluid temperatures as the bulk temperature and the heat exchanger segment temperatures as the wall temperatures allowed calculation of the convection heat transfer film coefficient and subsequently an overall heat transfer coefficient for the heat exchanger. The film coefficient values ranged from 232 to 292 BTU/hr-ft²-°F. These values are lower than could be obtained at a more representative flowrate since flow was in the laminar flow regime. It is expected that a flight heat exchanger design will achieve approximately 800 BTU/hr-ft²-°F at operating flowrates.

The contact conductance vs diaphragm pressure for various heat loads are shown in Figures 21 and 22. The results followed the pattern of contact conductance measurements of previous investigations showing variation in conductances depending on whether the pressure is being increased or decreased. Higher conductances are also observed for higher heat loads. In all cases the conductance measured exceeded the goal of 500 BTU/hr-ft²-°F at pressures below 200 psi with conductances of over 600 BTU/hr-ft²-°F at the 300 psi maximum test pressure.

Figure 23 shows the test results compared with two previous tests. The values are in the expected range for bare aluminum surfaces in a vacuum.

Assembly and disassembly of the heat exchanger and simulated heat pipe indicated a very tight fit. This was likely due to lack of straightness of the heat exchanger elements which caused pinching at some points on the surfaces. In addition, the assembly of the device did not result in the designed clearance and made for a tighter fit. Future designs will be made with provision for adjustment of the clearance during assembly.

The results of the feasibility demonstration revealed no reason this concept could not be carried into the prototype program with a high degree of confidence of success.

4.4 EXPERIENCE WITH TEST HARDWARE FABRICATION

Some difficulties were encountered during the fabrication of the test article involving brazing of the heat exchanger, assembly of the part and welding of the manifolds.

During the brazing operation some distortion of the tubular shape of the segments was experienced. Efforts to straighten the segments resulted in some surface damage on the inside of the segments. The problem was resolved by roll forming the elements on a mandrel and polishing them to the desired one inch diameter. A few small areas of surface imperfections were still present but were judged not to be large enough to impact performance. After fabrication of the heat exchanger segments and application of the silicone rubber filler, difficulty was encountered in assembling the heat exchanger and inserting a simulated heat pipe. Part of the difficulty was due to excess filler material which was subsequently trimmed. This allowed assembly, however, there was less clearance than originally planned. Insertion of the simulated heat pipe caused scuffing of the heat exchanger surfaces. To avoid this problem the heat exchanger elements were placed on the simulated heat pipe and installed into the diaphragm assembly simultaneously. Welding the 1/16 tubes into the manifold proved to be difficult to achieve without leakage at the weld joints. The problem was never satisfactorily solved and epoxy was installed around the joints to stop the leakage. The test fluid was changed from R21 to water for lower pressure inside the tubes to make leakage from the epoxy joints less likely. Since the heat exchanger elements are expected to be made of compact core, this problem is not expected to have any impact on the prototype program.

A third problem experienced involved the installation of the thermocouples on the simulated heat pipe evaporator. The initial and final methods for this installation are shown in Figure 24. The objective of these thermocouples was to measure the wall temperature on the tube which was used to simulate a heat pipe test. Initially, an attempt was made to epoxy bond the thermocouples to the tube and cover with a metal tape. Since the heat load is provided from a heater in the center of this tube any insulation from the aluminum wall can result in errors in the temperature measurement. Initially these were not expected to be significant, however, the results of the first test series indicated large temperature differences between measurements which did not follow the expected cooling pattern along the flow direction. In addition, indicated performance of the heat exchanger contact conductance was very poor and did not improve significantly with contact pressure. These thermocouples were suspect. The device was disassembled and the thermocouples reinstalled using the method shown as the final thermocouple installation in Figure 19. In this method a small groove was cut in the tube outer surface into which the thermocouples were installed.

Two small holes were drilled in the bottom of the groove to pass the leads into the center of the tube and out the ends. This method resulted in good measurements which had the expected variation in the direction of the flow.

5.0 PROTOTYPE TEST

A prototype contact heat exchanger has been designed, fabricated and tested for thermal performance. The prototype test results verify the application of the metal diaphragm concept to a flight representative heat exchanger. The test method was identical to the feasibility test in that the contact conductance between a heat exchanger surface and a simulated heat pipe was determined by measuring the temperature difference between the two surfaces and the heat flow. Compact heat exchanger core and a metal diaphragm, both specifically fabricated for the prototype unit were purchased from United Aircraft Products and Stainless Steel Products respectively. The unit was assembled and tested in the Vought Space Environment Simulation Laboratory.

5.1 TEST ARTICLE DESIGN

The prototype contact heat exchanger design shown in Figure 25 consists of three cylindrical segment compact heat exchangers enclosed by a pressurizing diaphragm assembly. The heat exchangers are designed to exchange heat from the Refrigerant - 21, which flows through the heat exchangers, to the enclosed heat pipe. The active heat transfer length of the heat exchanger assembly is four feet and the inside diameter is designed to mate with a 1.6 inch diameter heat pipe. These dimensions were selected by NASA to match the configuration of the evolving heat pipe radiator design.

The unit was assembled by clamping the three heat exchanger elements in place around a 1.6 inch diameter simulated heat pipe. The heat exchanger/heat pipe was then forced into the diaphragm assembly and the doughnut manifolds were welded to the heat exchanger tubes and the tubes mechanically attached to the diaphragm assembly. This procedure insured that the heat exchanger elements were positioned correctly in the diaphragm assembly prior to tube welding. However, after completion of the welding, considerable force (approximately 150 lb.) was required to remove the simulated heat pipe. Approximately 100 lb. force was required to re-insert the heat pipe. Since these forces are unacceptable for on orbit operations it was decided to reduce the heat pipe diameter. Reduction of the heat pipe diameter from the nominal 1.6 inches to 1.56 inches provided a

non-interference fit and required approximately a 5 lb. force for heat pipe removal and installation. Future assembly operations will utilize an oversized simulated heat pipe to insure that the final assembly accommodates the heat pipe design diameter.

The compact heat exchanger supplied by United Aircraft Products is constructed with a ruffled configuration with a density of 20 fins/inch. Fin thickness is 0.006 inch. Each cylindrical segment is designed to achieve an ηhA of 1130 BTU/hr $^{\circ}F$ at an R-21 flow rate of 1000 lb/hr. The assembled three elements flowed in parallel therefore, have an ηhA of 3390 BTU/hr $^{\circ}F$. Thus, for a 2 kW load, there is a $2^{\circ}F$ temperature drop between the R-21 and heat exchanger surface. Total contact area of the four feet long heat exchangers is 1.42 ft². The heat exchanger contact surface had a 16 finish.

Figures 26 thru 28 are photographs of the assembled contact heat exchanger. Figure 26 is an overall view. The manifold and heat exchanger tube details are shown in Figure 27. Figure 28 shows the insertion end with the simulated heat pipe in place.

5.2 TEST SETUP AND INSTRUMENTATION

The instrumentation of the test article is illustrated in Figure 29. Twenty-four thermocouples were installed inside the heat exchanger/heat pipe test assembly to measure the temperature drop across the contact surface. Twelve of the thermocouples were located on the heat exchanger and twelve were located on the simulated heat pipe. Thermocouples were located at 4 stations along the 4 ft. length, beginning at 6 inches from the end and spaced 12 inches apart. Six thermocouples were located at each station with three pairs equally spaced around the circumference as shown in Figure 29.

Additional instrumentation included the temperature of the R-21 into and out of the heat exchanger, the R-21 delta temperature and pressures, the flow rate and the electrical power to the heater.

Heat was supplied to the contact surface through an electrical heater in the simulated heat pipe. The heater was constructed by wrapping 14 gage chromel wire around a 1.0 inch diameter by .035 in. wall 6061 T-6 aluminum pipe which was inserted inside the simulated heat pipe. The void between the heater elements and the simulated heat pipe was filled with Dow Corning DC4 thermal grease. The power source to the heater was regulated DC power which varied up to 50 volts for 2000 watts of power input.

By measuring the electrical input power (volts and amps) a very accurate measure of the heat exchanger heat load was obtained. The heat load was also measured via the fluid temperatures and flow rates, providing a heat load verification.

Table 7 shows the stabilized temperatures recorded prior to the test with no R-21 flow and no heat input. The average of the 12 heat pipe thermocouples is seen to agree closely with the average of the 12 heat exchanger thermocouples. The 0.14°F difference would tend to make the calculated conductance lower. However, no adjustment was made to the test data; conductances are based on the observed temperature differences.

5.3 TEST RESULTS

Tests were conducted to evaluate the performance of the prototype contact heat exchanger for a range of contact pressures from 0 to 300 psig. Heat input ranged from 500 to 2000 watts. Thirty-four test points were made at vacuum conditions (10^{-6} torr) and nine ambient pressure points were made. Table 8 summarizes the test conditions and data. 1000 lb/hr was used for all test points except 22 and 23.

An example of the procedure used to reduce the test data is shown in Figure 30. At each of four lengthwise locations, the three thermocouples on the heat exchanger were averaged. The three thermocouples on the simulated heat pipe were also averaged. The difference between the two averages is the contact temperature difference at that location. The temperature differences are determined at each of the four locations in this manner. An overall average temperature difference is then determined by averaging the four location averages. The contact conductance is then determined by the relation:

$$h_c = \frac{Q}{A \Delta T_{\text{avg.}}}$$

Where: Q = Power input

h_c = Contact Area

ΔT_{avg} = the average contact temperature difference

Appendix B presents the test data for all 43 test points.

Figure 31 is a summary of the measured performance of the prototype contact heat exchanger. Overall conductance from the heat pipe to the fluid is shown as a function of the contact pressure. Figure 32 shows the contact conductance as a function of the contact (diaphragm) pressure. The test data repeatability as indicated by the band on Figure 32 is good.

TABLE 7

INSTRUMENTATION VERIFICATION

40 JAN 1983

TIME 8 : 19 : 9

TEMPERATURE STABILIZATION BEFORE

TC1-100H	62.9284	DEGF	TC2-200H	62.7514	DEGF	TC3-200H	62.7074	DEGF	HEAT PIPE
TC4-100H	62.7514	DEGF	TC5-100H	62.7047	DEGF	TC6-200H	62.7074	DEGF	HEAT PIPE
TC7-200H	62.5637	DEGF	TC8-100H	62.7514	DEGF	TC9-100H	62.7514	DEGF	HEAT PIPE
TC10-200H	62.7074	DEGF	TC11-200H	62.5637	DEGF	TC12-100H	62.7074	DEGF	HEAT PIPE
TC13-100H	62.7514	DEGF	TC14-200H	62.7074	DEGF	TC15-200H	62.5637	DEGF	HEAT PIPE
TC16-100H	62.62	DEGF	TC17-100H	62.9284	DEGF	TC18-200H	62.9131	DEGF	HEAT EXCHANGER
TC19-100H	62.9284	DEGF	TC20-100H	62.9284	DEGF	TC21-100H	62.9131	DEGF	HEAT EXCHANGER
TC22-200H	62.9131	DEGF	TC23-200H	62.9284	DEGF	TC24-100H	62.9284	DEGF	HEAT EXCHANGER
TC25-100H	62.9284	DEGF	TC26-200H	62.9284	DEGF	TC27-200H	62.9284	DEGF	HEAT EXCHANGER
TC28-100H	62.9284	DEGF	TC29-200H	62.9284	DEGF	TC30-200H	62.9284	DEGF	HEAT EXCHANGER
TC31-100H	62.9284	DEGF	TC32-200H	62.9284	DEGF	TC33-200H	62.9284	DEGF	HEAT EXCHANGER
TC34-100H	62.9284	DEGF	TC35-200H	62.9284	DEGF	TC36-200H	62.9284	DEGF	HEAT EXCHANGER
TC37-100H	62.9284	DEGF	TC38-200H	62.9284	DEGF	TC39-200H	62.9284	DEGF	HEAT EXCHANGER
TC40-100H	62.9284	DEGF	TC41-200H	62.9284	DEGF	TC42-200H	62.9284	DEGF	HEAT EXCHANGER
TC43-100H	62.9284	DEGF	TC44-200H	62.9284	DEGF	TC45-200H	62.9284	DEGF	HEAT EXCHANGER
TC46-100H	62.9284	DEGF	TC47-200H	62.9284	DEGF	TC48-200H	62.9284	DEGF	HEAT EXCHANGER
TC49-100H	62.9284	DEGF	TC50-200H	62.9284	DEGF	TC51-200H	62.9284	DEGF	HEAT EXCHANGER
TC52-100H	62.9284	DEGF	TC53-200H	62.9284	DEGF	TC54-200H	62.9284	DEGF	HEAT EXCHANGER
TC55-100H	62.9284	DEGF	TC56-200H	62.9284	DEGF	TC57-200H	62.9284	DEGF	HEAT EXCHANGER
TC58-100H	62.9284	DEGF	TC59-200H	62.9284	DEGF	TC60-200H	62.9284	DEGF	HEAT EXCHANGER
TC61-100H	62.9284	DEGF	TC62-200H	62.9284	DEGF	TC63-200H	62.9284	DEGF	HEAT EXCHANGER
TC64-100H	62.9284	DEGF	TC65-200H	62.9284	DEGF	TC66-200H	62.9284	DEGF	HEAT EXCHANGER
TC67-100H	62.9284	DEGF	TC68-200H	62.9284	DEGF	TC69-200H	62.9284	DEGF	HEAT EXCHANGER
TC70-100H	62.9284	DEGF	TC71-200H	62.9284	DEGF	TC72-200H	62.9284	DEGF	HEAT EXCHANGER
TC73-100H	62.9284	DEGF	TC74-200H	62.9284	DEGF	TC75-200H	62.9284	DEGF	HEAT EXCHANGER
TC76-100H	62.9284	DEGF	TC77-200H	62.9284	DEGF	TC78-200H	62.9284	DEGF	HEAT EXCHANGER
TC79-100H	62.9284	DEGF	TC80-200H	62.9284	DEGF	TC81-200H	62.9284	DEGF	HEAT EXCHANGER
TC82-100H	62.9284	DEGF	TC83-200H	62.9284	DEGF	TC84-200H	62.9284	DEGF	HEAT EXCHANGER
TC85-100H	62.9284	DEGF	TC86-200H	62.9284	DEGF	TC87-200H	62.9284	DEGF	HEAT EXCHANGER
TC88-100H	62.9284	DEGF	TC89-200H	62.9284	DEGF	TC90-200H	62.9284	DEGF	HEAT EXCHANGER
TC91-100H	62.9284	DEGF	TC92-200H	62.9284	DEGF	TC93-200H	62.9284	DEGF	HEAT EXCHANGER
TC94-100H	62.9284	DEGF	TC95-200H	62.9284	DEGF	TC96-200H	62.9284	DEGF	HEAT EXCHANGER
TC97-100H	62.9284	DEGF	TC98-200H	62.9284	DEGF	TC99-200H	62.9284	DEGF	HEAT EXCHANGER
TC100-100H	62.9284	DEGF	TC101-200H	62.9284	DEGF	TC102-200H	62.9284	DEGF	HEAT EXCHANGER

AVG HEAT PIPE : TC1 THRU TC12 = 62.73°F

AVG HEAT EXCH : TC13 THRU TC 24 = 62.87°F

$$U_c = \frac{Q}{A(T_{HP} - T_{HX})}$$

$$\text{ERROR} = -0.14^\circ\text{F}$$

ORIGINAL PAGE 19
OF POOR QUALITY

VOUGHT

TABLE 8

CONTACT HEAT EXCHANGER TEST SUMMARY

TEST POINT	DATE/TIME	HEAT INPUT WATTS	DIAPHRAGM PRESS PSIG	HP-HX ΔT OF	CONTACT COND BTU/HR-FT ² -OF	REMARKS
1	26 JAN 83 11:05	503	59.0	2.58	469	
2	12:10	503	113.1	1.25	967	
3	12:45	503	203.5	0.63	1919	
4	13:30	503	306.0	0.22	5496	
5	14:02	503	201.6	0.37	3269	Decreasing diaphragm pressure
6	15:10	993	50.7	5.71	418	
7	15:30	993	99.9	3.33	717	
8	15:55	994	199.8	1.78	1343	
9	16:20	995	299.4	1.39	1721	
10	27 JAN 83 09:30	1508	50.5	9.75	372	
11	10:01	1509	99.8	5.64	643	
12	10:32	1510	199.8	3.46	1049	
13	11:04	1510	299.1	2.75	1320	

ORIGINAL PAGE 13
OF POOR QUALITY

TABLE 8

CONTACT HEAT EXCHANGER TEST SUMMARY CONT'D

TEST POINT	DATE/TIME	HEAT INPUT WATTS	DIAPHRAGM PRESS PSIG	HP-HX ΔT OF	CONTACT COND BTU/HR-FT ² -OF	REMARKS
14	11:35	1510	199.9	3.24	1120	Decreasing diaphragm pressure.
15	12:05	1509	100.7	5.23	693	Decreasing diaphragm pressure.
16	12:23	1508	50.6	9.51	381	Decreasing diaphragm pressure.
17	12:53	1991	51.0	12.68	377	Decreasing diaphragm pressure.
18	13:25	1991	100.2	7.12	672	
19	13:57	1991	199.6	4.27	1121	
20	14:27	1989	299.6	3.53	1355	
21	14:44	1986	200.2	4.24	1126	
22	15:17	997	200.3	1.99	1205	Flow = 500 lb/hr
23	15:55	998	299.5	1.68	1428	Flow = 500 lb/hr.
24	28 JAN 83 08:56	1512	50.6	8.10	449	Ambient pressure.
25	09:16	1511	100.3	5.18	701	Ambient pressure.
26	09:39	1511	199.6	3.68	987	Ambient pressure.
27	10:00	1511	299.0	3.30	1100	Ambient pressure.

ORIGINAL PAGE 15
OF POOR QUALITY

TABLE 8

CONTACT HEAT EXCHANGER TEST SUMMARY CONT'D

TEST POINT	DATE/TIME	HEAT INPUT WATTS	DIAPHRAGM PRESS PSIG	HP-HX ΔT OF	CONTACT COND BTU/HR-FT ² -OF	REMARKS
28	1 FEB 83 10:25	1504	51.1	9.11	397	Repeat TP10 with insulation blanket open at ends.
29	10:45	1504	100.0	5.20	695	Repeat TP11 with insulation blanket open at ends.
30	11:07	1505	200.0	3.05	1186	Repeat TP12 with insulation blanket open at ends.
31	11:30	1505	299.3	2.43	1489	Repeat TP13 with insulation blanket open at ends.
32	3 FEB 83 13:04	106	-14.7	46.86	5.4	Diaphragm vented to vacuum chamber during pump-down and 2.5 hrs hold @ 10 ⁻⁶ torr.
33	13:34	1499	50.6	8.87	406	
34	14:02	1498	100.1	4.90	735	
35	14:52	1498	199.6	2.61	1380	
36	15:29	1498	299.3	2.16	1667	
37	15:51	2012	301.4	2.91	1662	
38	16:11	2013	198.0	3.65	1326	Decreasing diaphragm pressure.
39	4 FEB 83 10:00	2000	299.7	3.60	1335	Ambient pressure
40	10:24	2000	200.2	4.38	1098	Ambient pressure
41	10:40	1001	99.4	5.88	818	Ambient pressure
42	10:58	2002	49.5	9.89	487	Ambient pressure
43	11:28	196	0	7.05	67	Ambient pressure, compare to TP32

ORIGINAL PAGE 13
OF POOR QUALITY

No trends were observed in the contact conductance with increasing or decreasing contact pressures or with heat load as long as the heat load resulted in measured temperature differences between the surfaces of at least 1.0°F . Test points 3, 4, and 5 had a heat input of 500 watts, resulting in small temperature differences and unreasonably high contact conductances (See Table 8). These data points are not used and all subsequent test points were conducted with a heat input of 1000 to 2000 watts. Table 9 summarizes the test data repeatability.

Figure 33 compares the test data to previous investigators. The prototype data shows a considerable improvement over the feasibility demonstration data and is somewhat higher than the results obtained by Leach (reference 1) for a bolted interface. The prototype data compares favorably with the data of Fletcher (reference 2). Apparently the surface irregularities of the feasibility demonstration unit caused by the heat exchanger tube brazing resulted in a lower contact conductance, although the results are acceptable.

A comparison of the vacuum and ambient pressure test results is shown in Figure 34. The ambient test conductance is seen to be less than the vacuum conductance at pressures above about 100 psig. This result was not expected and the data was verified by repeating a number of test points. The first 23 vacuum test points and four ambient pressure test points (24 thru 27) were conducted with the entire test article wrapped in a 10 layer aluminized mylar super insulation blanket. The blanket had a generous amount of over lapping and was secured with mylar tape. It was considered a possibility that the pressure inside the insulation "bag" was higher than the chamber pressure such that the true test conditions were not vacuum. Therefore, the insulation blanket was removed from the ends of the unit to allow the contact area to vent directly into the chamber and four vacuum test points (28 thru 31) were repeated. Contact conductances with the revised blanket configuration were slightly higher than the "bagged" configuration, but within the experimental accuracy. A theory was advanced that the ambient pressure (14.7 psia) on the diaphragm during the chamber pumpdown trapped air between the contact surfaces and thus improved the contact conductance. The test article was re-configured to vent the diaphragm to the chamber during pump down to eliminate any pressure differential between the contact surfaces. A $2\frac{1}{2}$ hour hold period at a chamber pressure of 10^{-6} torr was also incorporated before the diaphragm was pressurized. Seven additional test points were repeated (32 thru 38) with the results verifying the previous testing. The ambient test data was then repeated (test points 39 thru 43) with the results again verifying the lower than vacuum conductances.

TABLE 9

TEST DATA REPEATABILITY

O 50 PSIG DIAPHRAGM PRESSURE:			
7 TEST POINTS:	MEAN CONDUCTANCE = 403	+60 -31	BTU/HRFT ² OF
	=	+16.4% - 7.7%	
O 100 PSIG DIAPHRAGM PRESSURE:			
6 TEST POINTS:	MEAN CONDUCTANCE = 693	+42 -50	BTU/HRFT ² OF
	=	+6.1% -7.2%	
O 200 PSIG DIAPHRAGM PRESSURE:			
9 TEST POINTS:	MEAN CONDUCTANCE = 1206	+174 -157	BTU/HRFT ² OF
	=	+14.4% -13.0%	
O 300 PSIG DIAPHRAGM PRESSURE:			
7 TEST POINTS:	MEAN CONDUCTANCE = 1520	+201 -200	BTU/HRFT ² OF
	=	+13.2% -13.2%	

It should be noted that test points 32 and 43, conducted with no pressure differential between the contact surfaces at vacuum and ambient conditions respectively, yield expected results. The ambient contact conductance of 67 BTU/hr ft² °F is considerably higher than the vacuum value of 5.4 BTU/hr ft² °F.

A definitive explanation for the ambient pressure conductance being less than the vacuum conductance is not available. It can be postulated that the smooth surfaces and uniform pressure results in microscopic deformation of the contacting surfaces allowing intimate contact and high conductances under vacuum conditions, whereas in ambient pressure air trapped in the micro-voids prevents intimate contact and reduces the conductance. Further analytical investigations beyond the scope of this effort are required to confirm this theory.

Figure 35 shows the heat exchanger pressure drop test data taken at a R-21 temperature of 65°F. This pressure drop includes the manifolds, connecting tubing between the manifold and heat exchanger.

5.4 PROTOTYPE PERFORMANCE WITH CURRENT RADIATOR DESIGN

Table 10 summarizes a constructable radiator system design based on the prototype contact heat exchanger performance data and the current heat pipe radiator performance data furnished by NASA. The current heat pipe design has 6 evaporator legs each 1.6 inches in diameter and 2 ft. long for a total available contact area of 5.03 ft².

The contact heat exchanger performance has been extrapolated to the lower flow rates resulting from the six parallel evaporator legs. As indicated by Table 10, the heat exchanger conductance (hA) is the limiting heat transfer method rather than the contact conductance for the reduced flow rates. The overall heat exchanger ΔT is determining by simultaneous solution of the first radiator panel performance characteristics (see Figure 3) and the heat exchanger performance characteristics. A total of 50 radiator panels will be required as determined from Figure 2. As previously discussed, this analysis does not include the temperature drop in the heat pipe and isolates the effect of the contact heat exchanger performance on the radiator system design.

The prototype heat exchanger is seen to give excellent radiator system performance and provide a minimum radiator area. The total heat exchanger system pressure drop of 15.0 psi is quite reasonable for a 25 kW system. However, further optimization of the heat exchanger core to accommodate the reduced flow rate should yield a more efficient design.

TABLE 10

PROTOTYPE CONTACT HEAT EXCHANGER PERFORMANCE FOR A TYPICAL DESIGN

o SPACECRAFT TYPICAL DESIGN CONDITIONS

HEAT LOAD = 25 kW
TIN = 150°F, TOUT = 0°F
R-21 FLOW = 2275 LB/HR

o CURRENT HEAT PIPE RADIATOR DESIGN

6 EVAPORATOR LEGS
EACH 1.6 IN. DIAMETER, 24 IN. LONG
TOTAL EVAPORATOR AREA = 5.03 FT.²
MAXIMUM HEAT REJECTION = 1.2 kW

o RADIATOR PERFORMANCE

50 PANELS REQUIRED (FROM FIGURE 2)
MAXIMUM HEAT REJECTION = 1.075 kW

o CONTACT HEAT EXCHANGER PERFORMANCE

FLOW EACH LEG = 379.2 LB/HR
HX CONDUCTANCE = 364 BTU/HR FT² °F
CONTACT CONDUCTANCE = 1520 BTU/HR FT² °F (AT 300 psi)
OVERALL CONDUCTANCE = 294 BTU/HR FT² °F
TOTAL CONTACT AREA = 4.34 FT²
FLUID TO HEAT PIPE ΔT = 2.87°F
 ΔP = 0.30 psi
SYSTEM ΔP = 15.0 psi (50 MODULES FLOWED IN SERIES)

A smaller, lighter weight core design with a higher heat transfer coefficient should yield comparable or improved heat exchanger performance with a reduced system weight.

6.0 CONCLUSIONS AND RECOMMENDATIONS

A contact heat exchanger which provides the thermal interface between a spacecraft coolant loop and a modular constructable radiator system has been successfully developed. Efficient thermal performance has been demonstrated by testing of a feasibility demonstration unit and a prototype unit. A contact conductance of 1520 BTU/hr. ft² °F at a pressure of 300 psi was obtained in the full size prototype unit. The pressurized metal diaphragm concept is considered design ready for application to the constructable radiator system. It provides a simple direct method of retaining and releasing the heat pipe radiator panels. Each panel replacement cycle requires only 72 in.³ of 300 psi nitrogen gas (.06 lb.) for the current 6 leg evaporator heat pipe design. Due to the high contact conductances provided by the uniform diaphragm pressure, the final design may not require a 300 psi contact pressure and the expendable gas may be further reduced.

Further studies are recommended to weight optimize the heat exchanger core and incorporate a redundant coolant loop into the design. Studies are needed to determine the required opening size relative to the heat pipe size to insure ease of on-orbit assembly. Revised diaphragm designs to increase the open to closed diameter ratio need to be verified. It is also recommended that additional studies be conducted to evaluate the use of liquids for pressurization of the heat exchanger diaphragm. This could lead to a simple mechanical release/repressurization concept lending itself to electromechanical operation with EVA backup.

Numerous spacecraft thermal control system concepts require the use of efficient connectable/disconnectable thermal joints. The pressurized metal diaphragm concept appears applicable to many of these design problems. With the high conductance values available at relatively low contact pressures, weight efficient flat heat exchanger designs appear possible. New design studies are recommended to expand the use of the contact heat exchanger to replaceable electronic equipment cold plates, spacecraft to spacecraft heat transfer and heat transfer between individual coolant loops and modular add-on thermal control systems.

REFERENCES

1. Leach, J. W., "Joint Conductance Element Tests For the Self Contained Heat Rejection Module Contact Heat Exchanger", Vought Report No. T211-RP-009, 15 August 1974.
2. Fletcher, L. S., "Thermal Conductance of Gasket Materials for Spacecraft Joints", AIAA Paper No. 73-49, January 1973.

ORIGINAL PAGE IS
OF POOR QUALITY

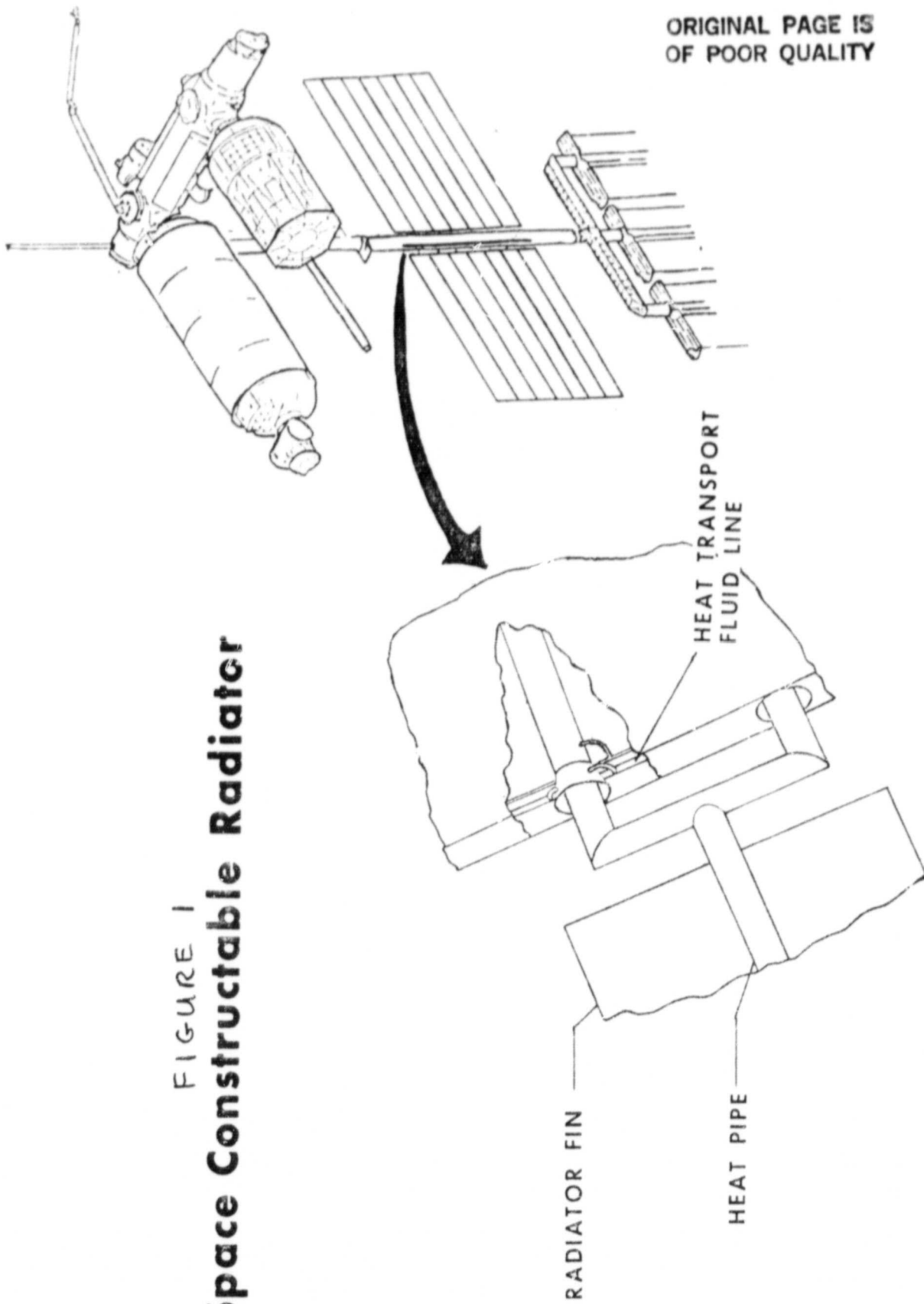


FIGURE 1
Space Constructable Radiator

FIGURE 2
EFFECT OF THERMAL INTERFACE ΔT
ON CONTRACTABLE RADIATOR SYSTEM SIZE

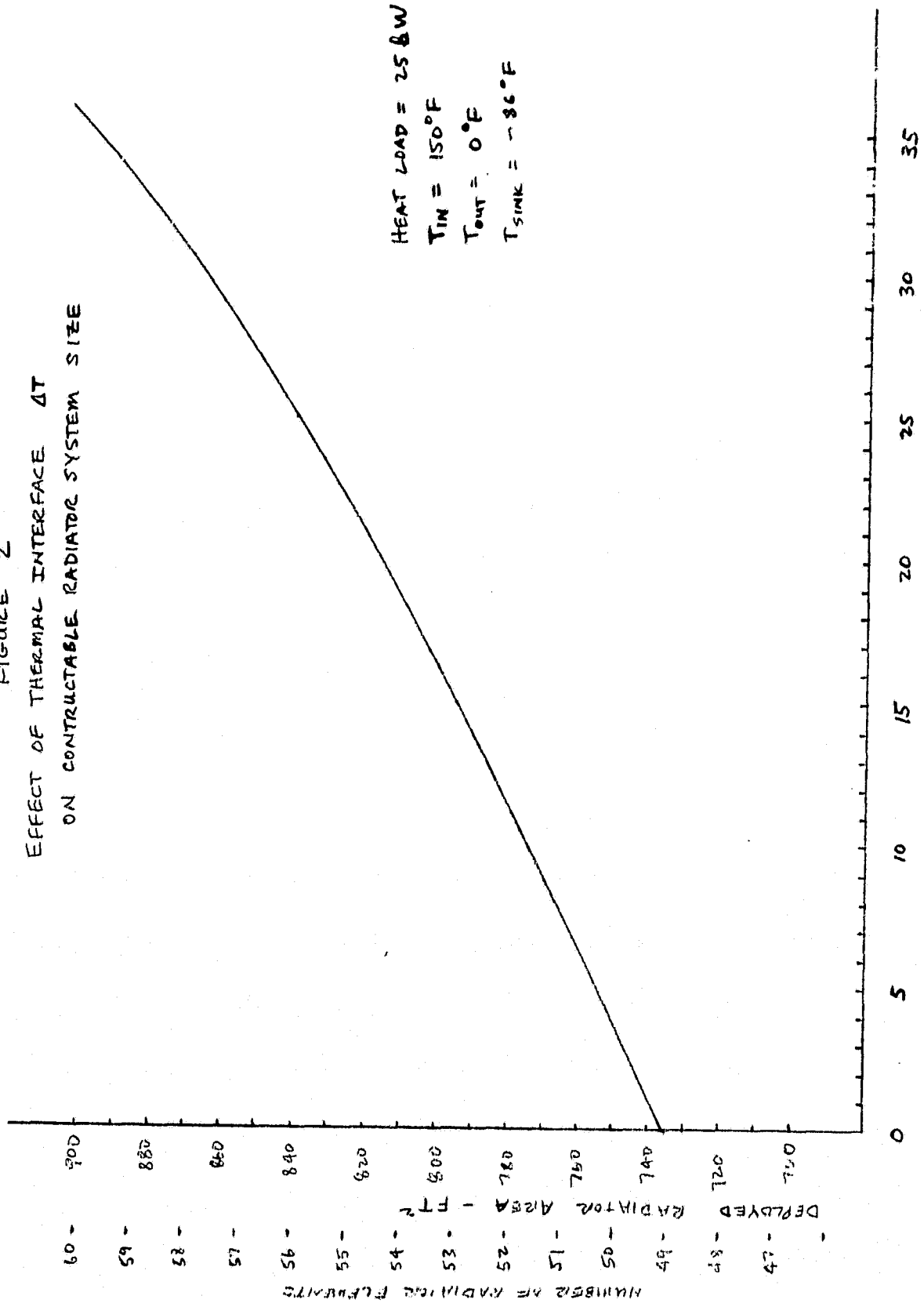
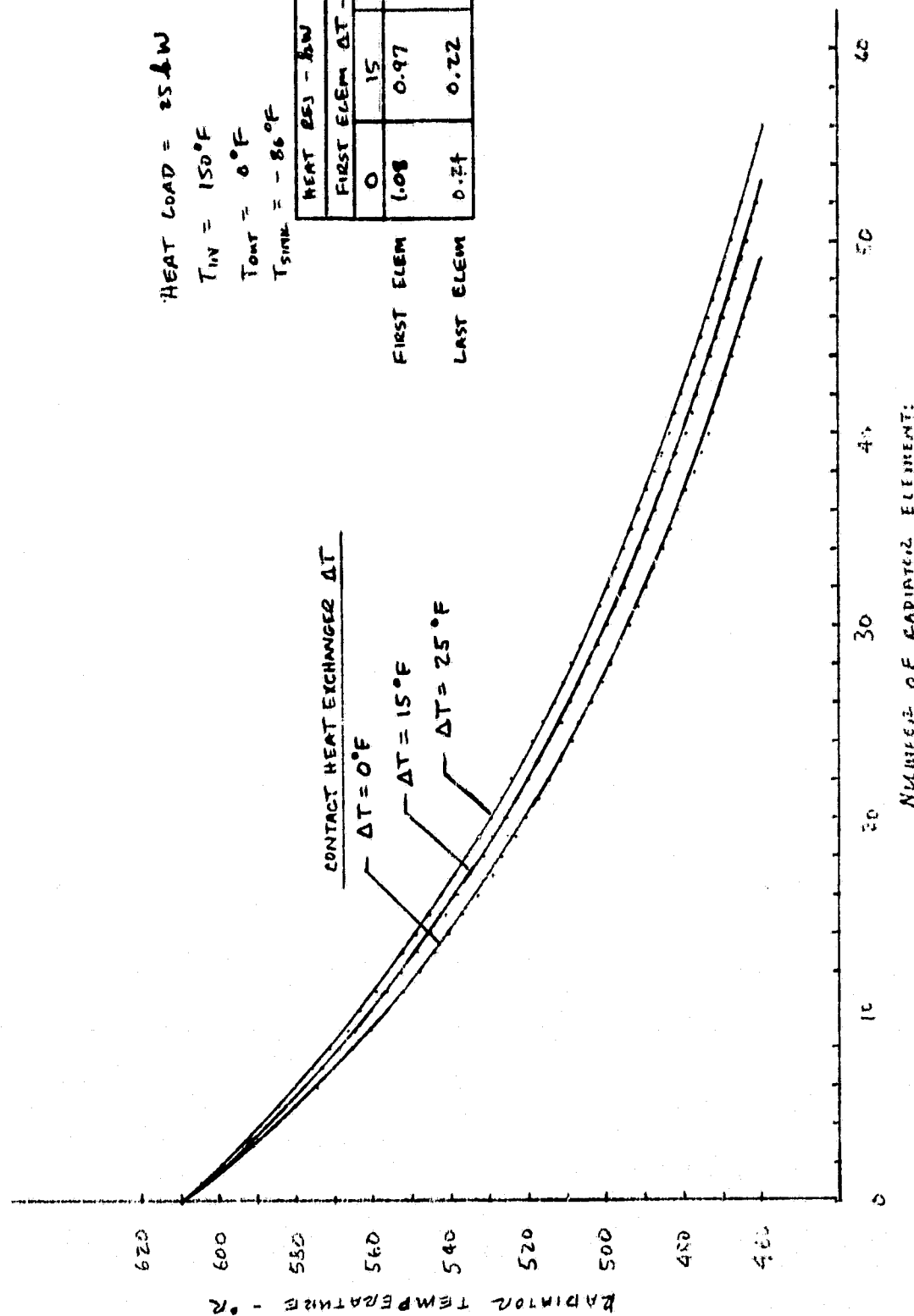
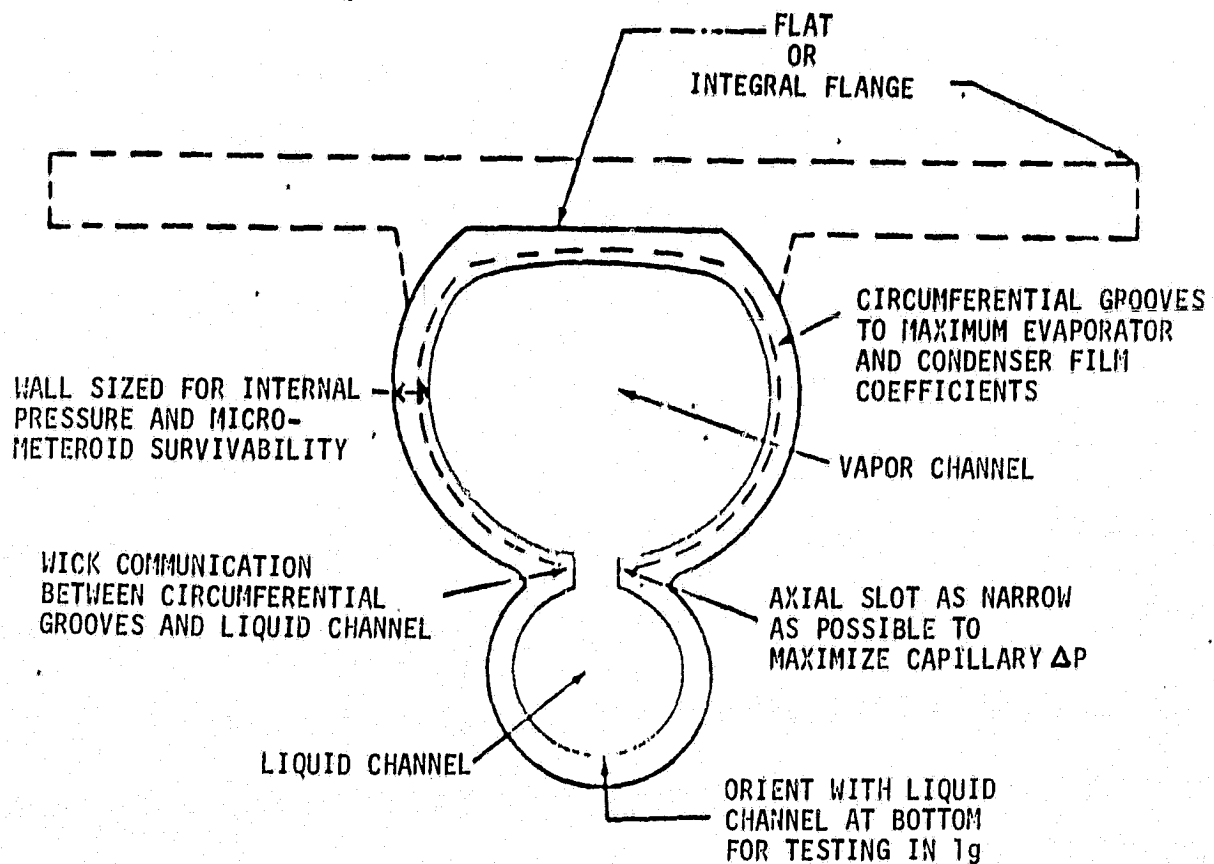


FIGURE 3
CONSTRUCTABLE RADIATOR SYSTEM TEMPERATURE PROFILE



ORIGINAL PAGE IS
OF POOR QUALITY

FIGURE 4
MONOGROOVE HEAT PIPE



ORIGINAL PAGE IS
OF POOR QUALITY

ROUND EVAPORATOR SECTION
DIAMETER - 1.21 IN O.D.
FIGURE 5 - CONCEPT 1

$h_c = 500$ (300 PSI CONTACT PRESSURE)

EVAPORATOR LENGTH FOR 150°F OVERALL
(DOES NOT INCLUDE HEAT PIPE Δ T)

ACETONE 7.3 FT
AMMONIA 3.2 FT

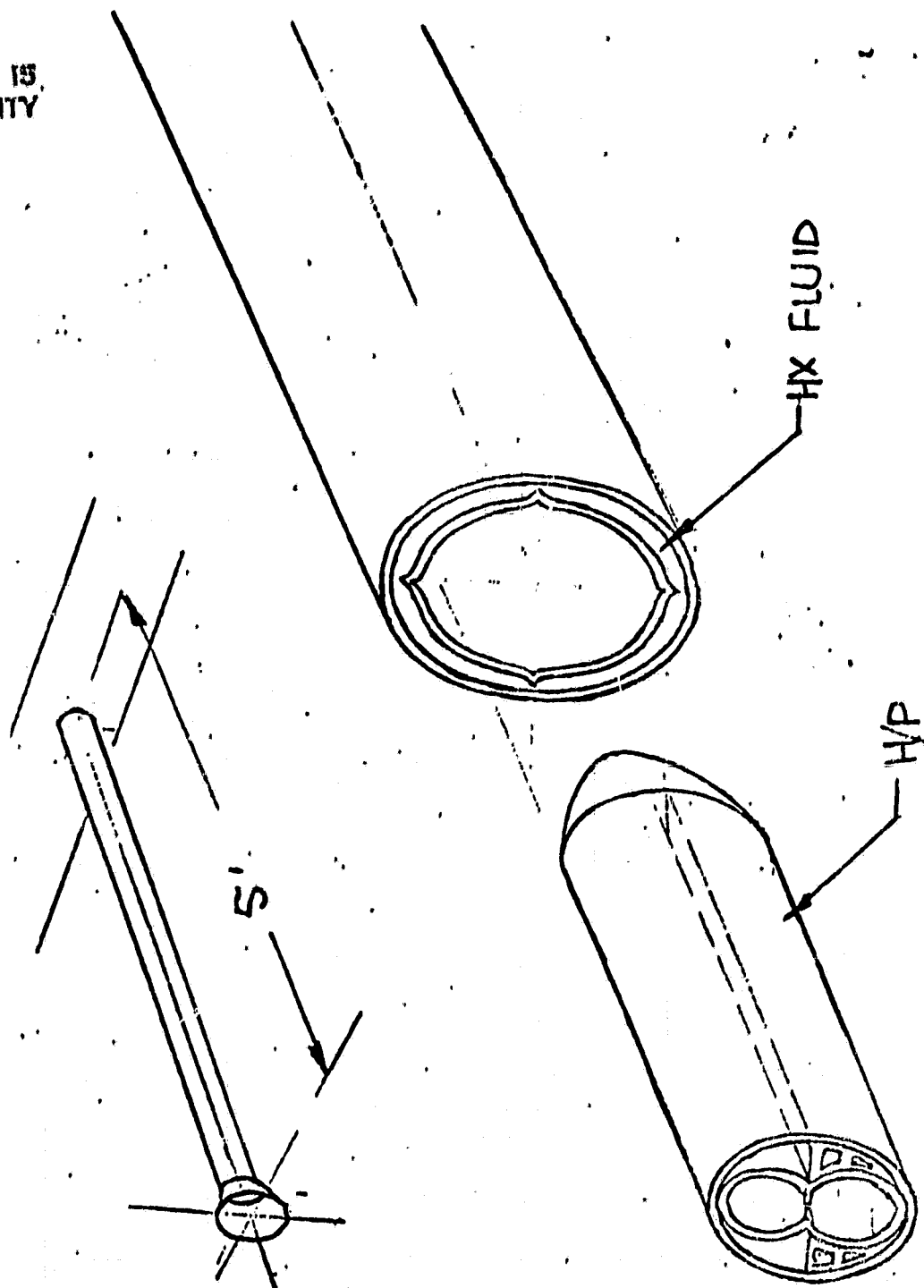
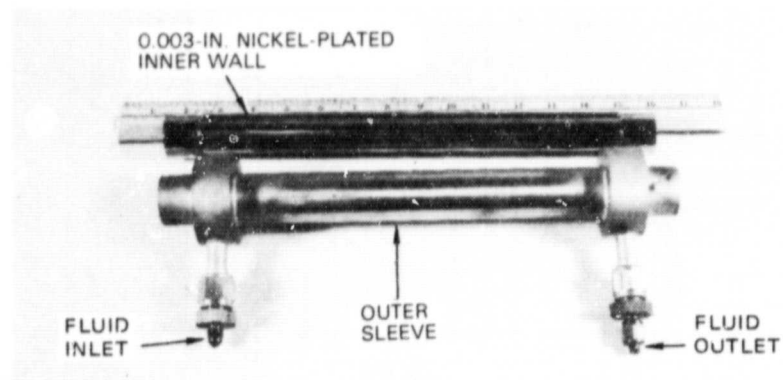
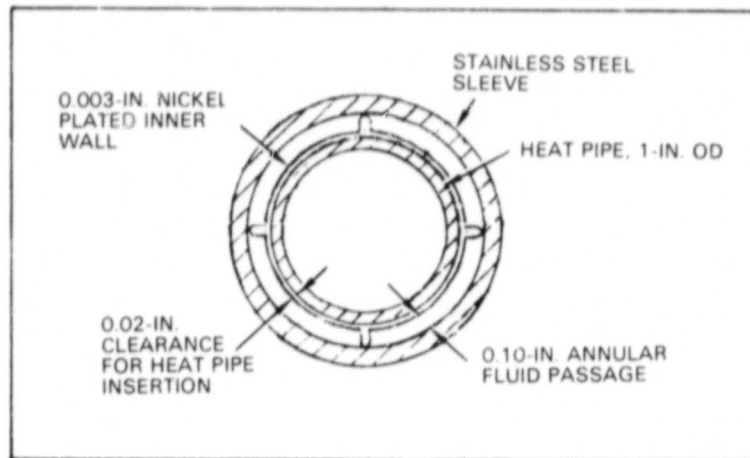


Figure 6

Fluid Pressure Clamping
Contact Heat Exchanger

ORIGINAL PAGE 13
OF POOR QUALITY

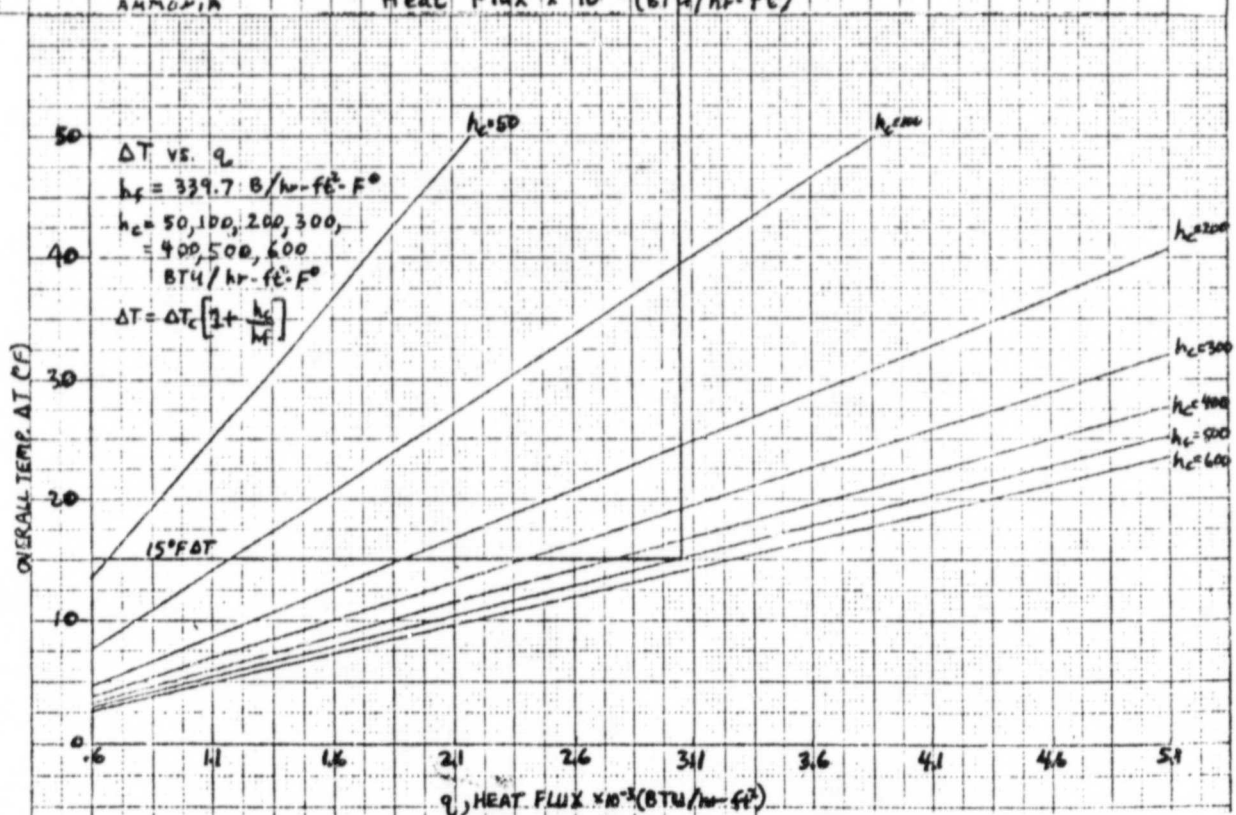
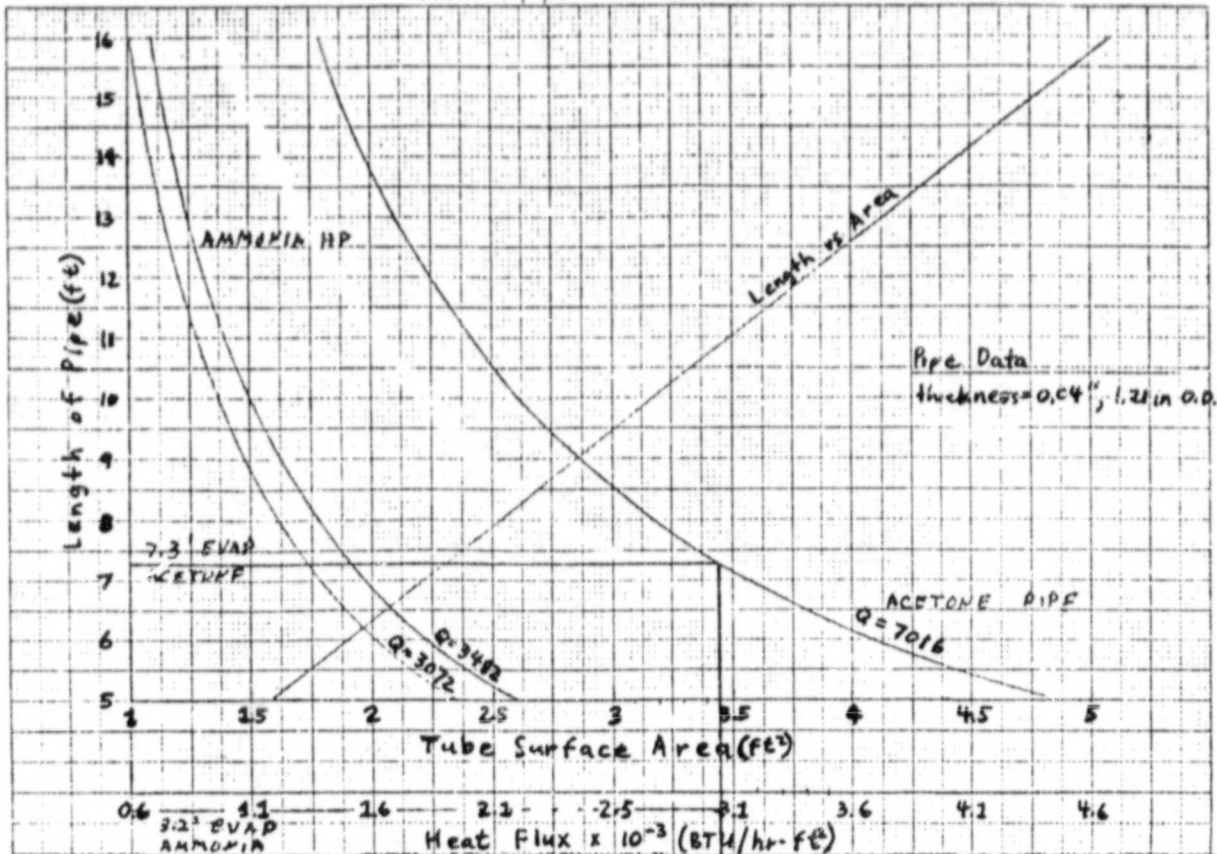


INDEPENDENTLY FUNDED
UNDER VOUGHT IR & D
RESOURCES

FIGURE 7
CONCEPT 1 - OVERALL ΔT

ORIGINAL PAGE IS
OF POOR QUALITY

360° arc pipe = 1.21 in. O.D.



VOUGHT
CORPORATION

FIGURE 8 - CONCEPT 2

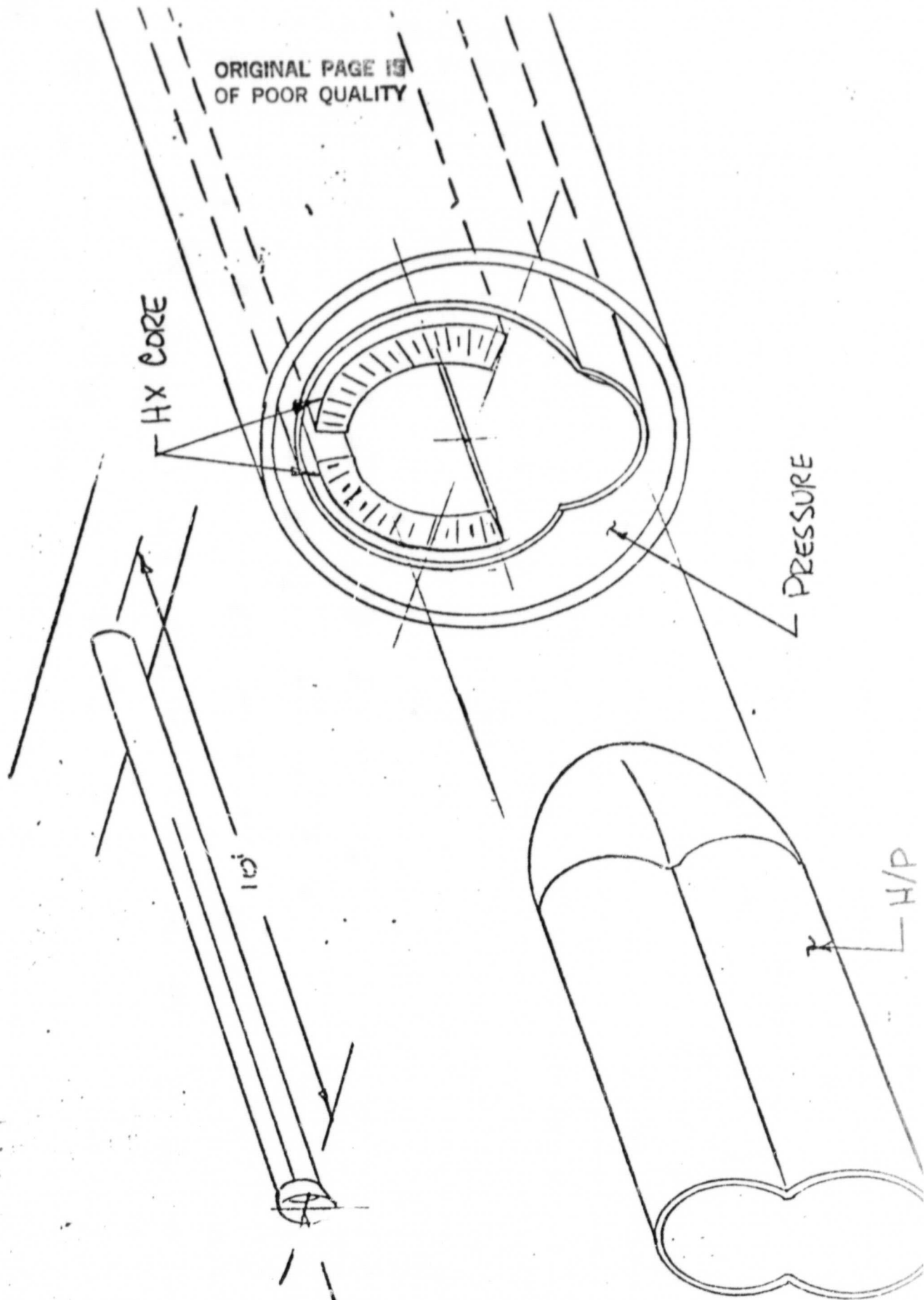
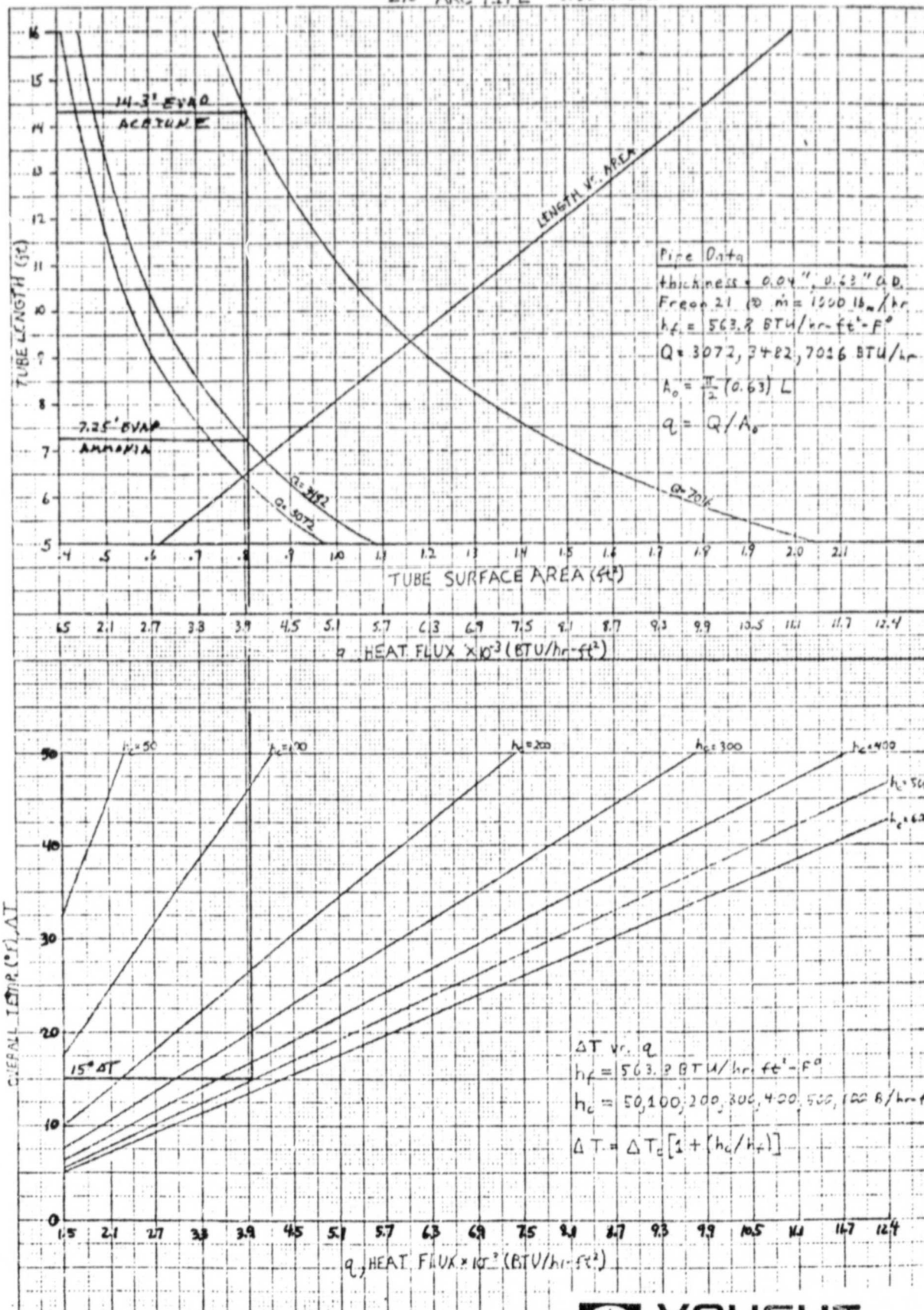


FIGURE 9
CONCEPT 2- OVERALL ΔT

ORIGINAL PAGE 18
OF POOR QUALITY

270° ARC PIPE - 0.63 in. O.D.



VOUGHT
CORPORATION

0 ASSUME 50% COPPER POWDER/KRYTOX CONDUCTIVE FLUID

COPPER CONDUCTIVITY = 220 BTU/HR FT ⁰F

FLUID CONDUCTIVITY ASSUMED = 55 BTU/HR FT ⁰F
(NO DATA AVAILABLE)

ΔT THROUGH FLUID	1.24°F	FOR ACETONE
	.62°F	FOR AMMONIA

LENGTH FOR 150°F ΔT -

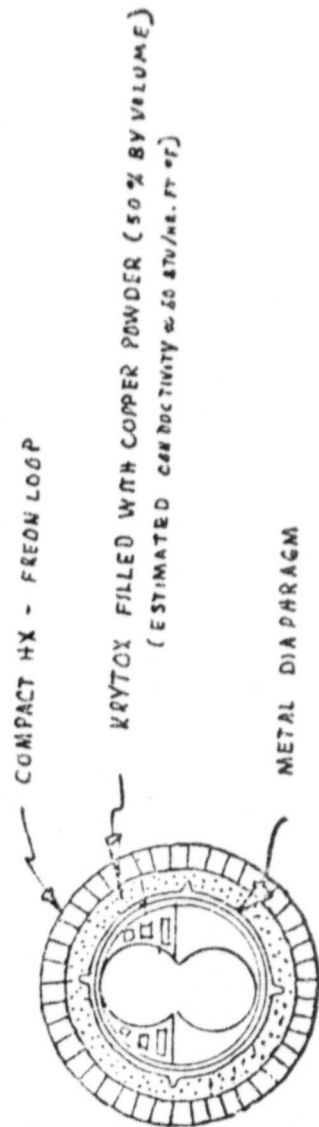


FIGURE 11 - CONCEPT 4

ORIGINAL PAGE IS
OF POOR QUALITY

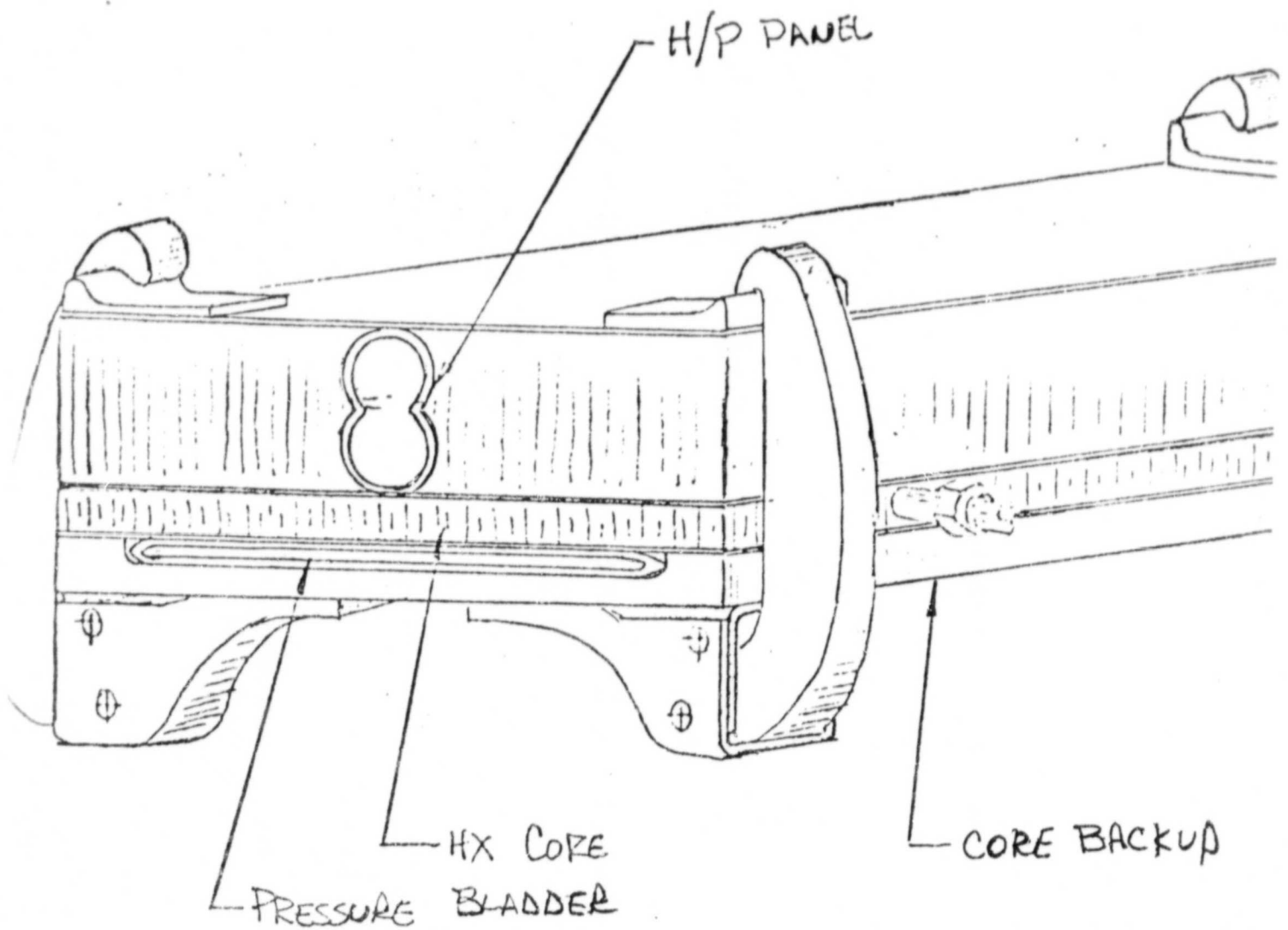
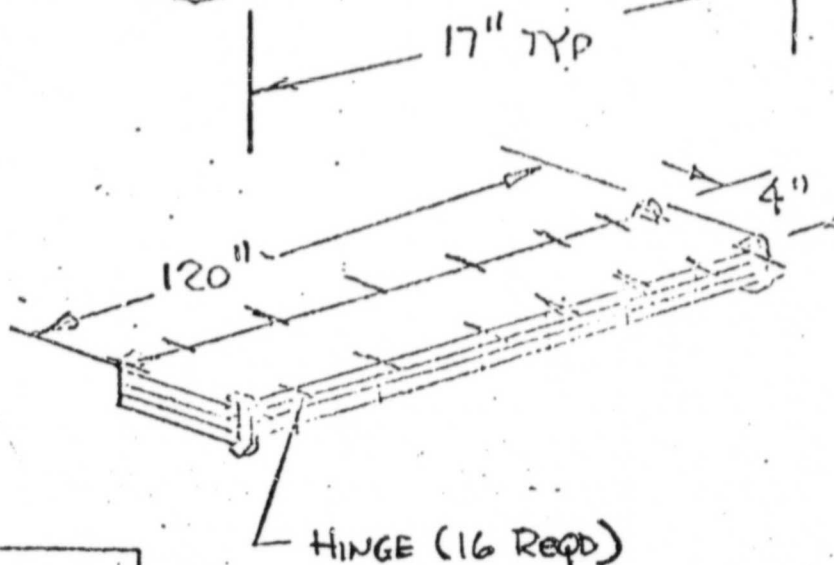
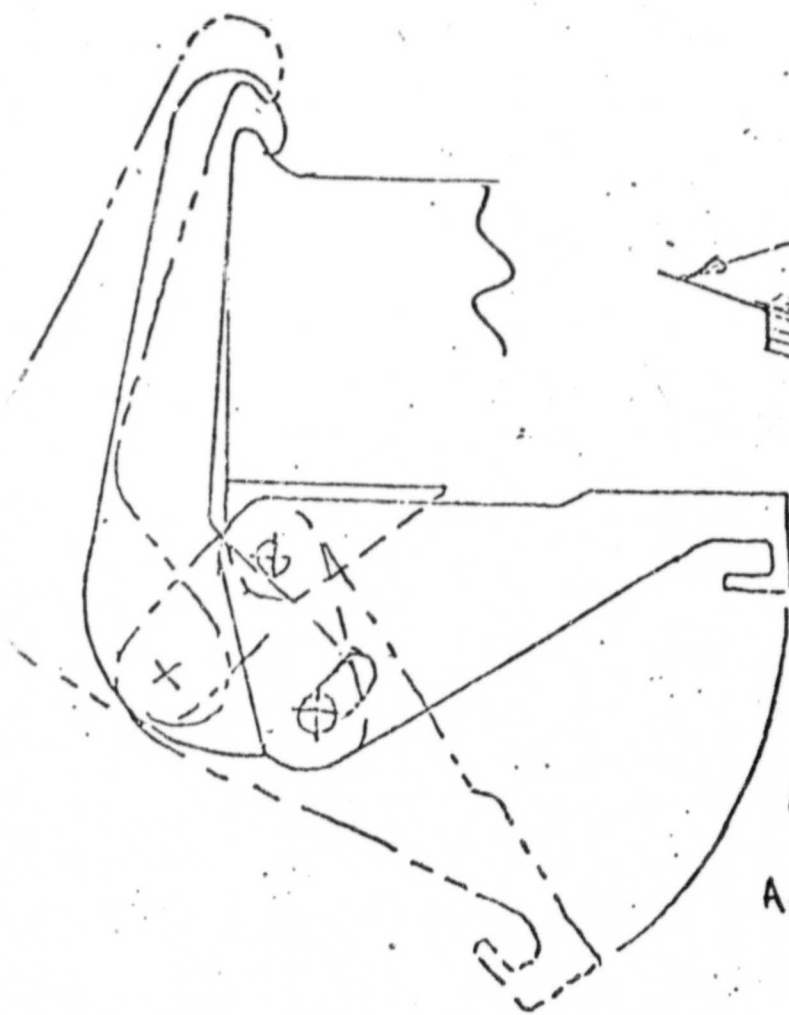
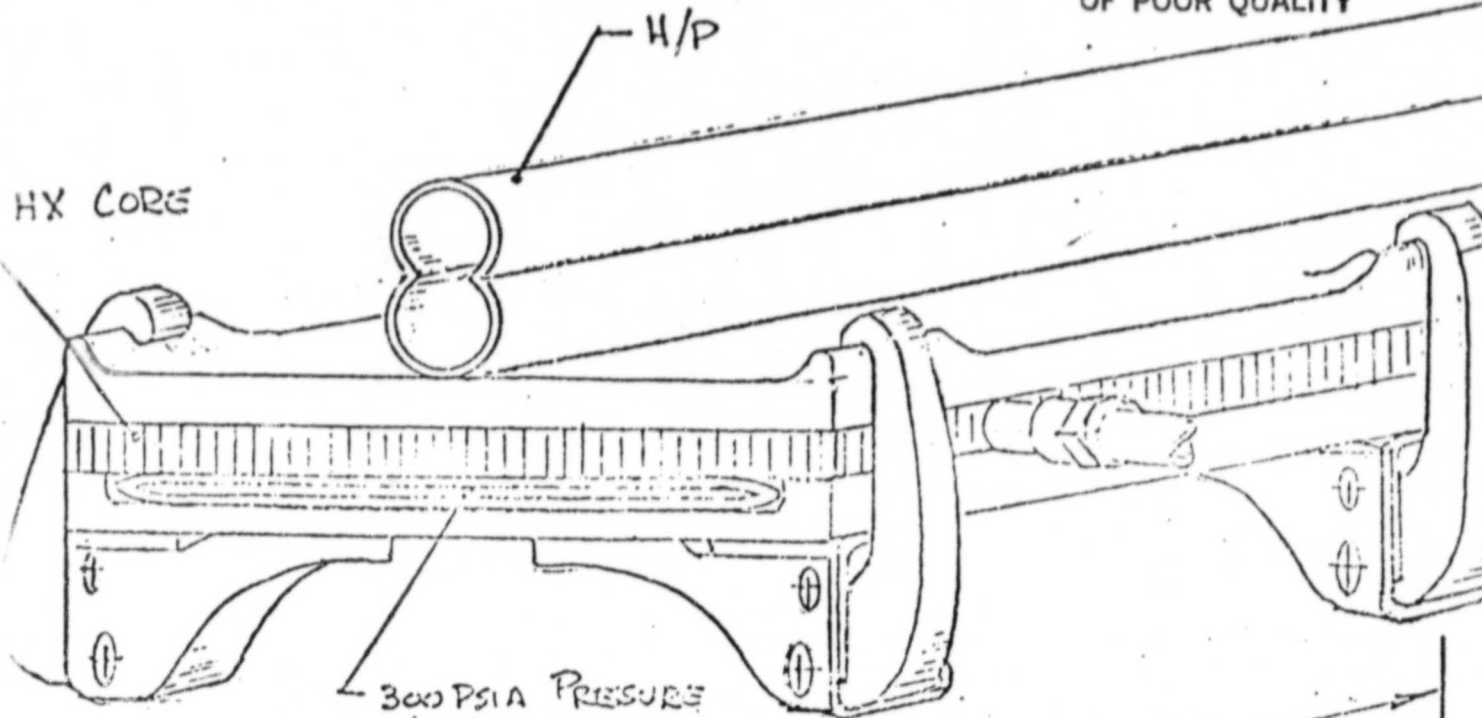


FIGURE 12 - CONCEPT 4

ORIGINAL PAGE IS
OF POOR QUALITY



$$\begin{aligned} \text{REQD } P &= 300 \text{ PSI} \\ \text{AREA} &= 120 \times 4 = 480 \text{ IN}^2 \\ \text{TOTAL LOAD} &= 300 \times 480 = 144,000 \# \\ \text{LOAD/HINGE} &= (144,000 \div 16) 1.25 = 11,250 \# \end{aligned}$$

$$F_{TU \text{ Hook}} = 40 \text{ KSI} = f_{tu} \text{ (CONSERVATIVE)}$$

$$A_{\text{Hook}} = \frac{11,212}{40,000} = .28 \text{ IN}^2$$

ORIGINAL PAGE IS
OF POOR QUALITY

FIGURE 13 - CONCEPT 5

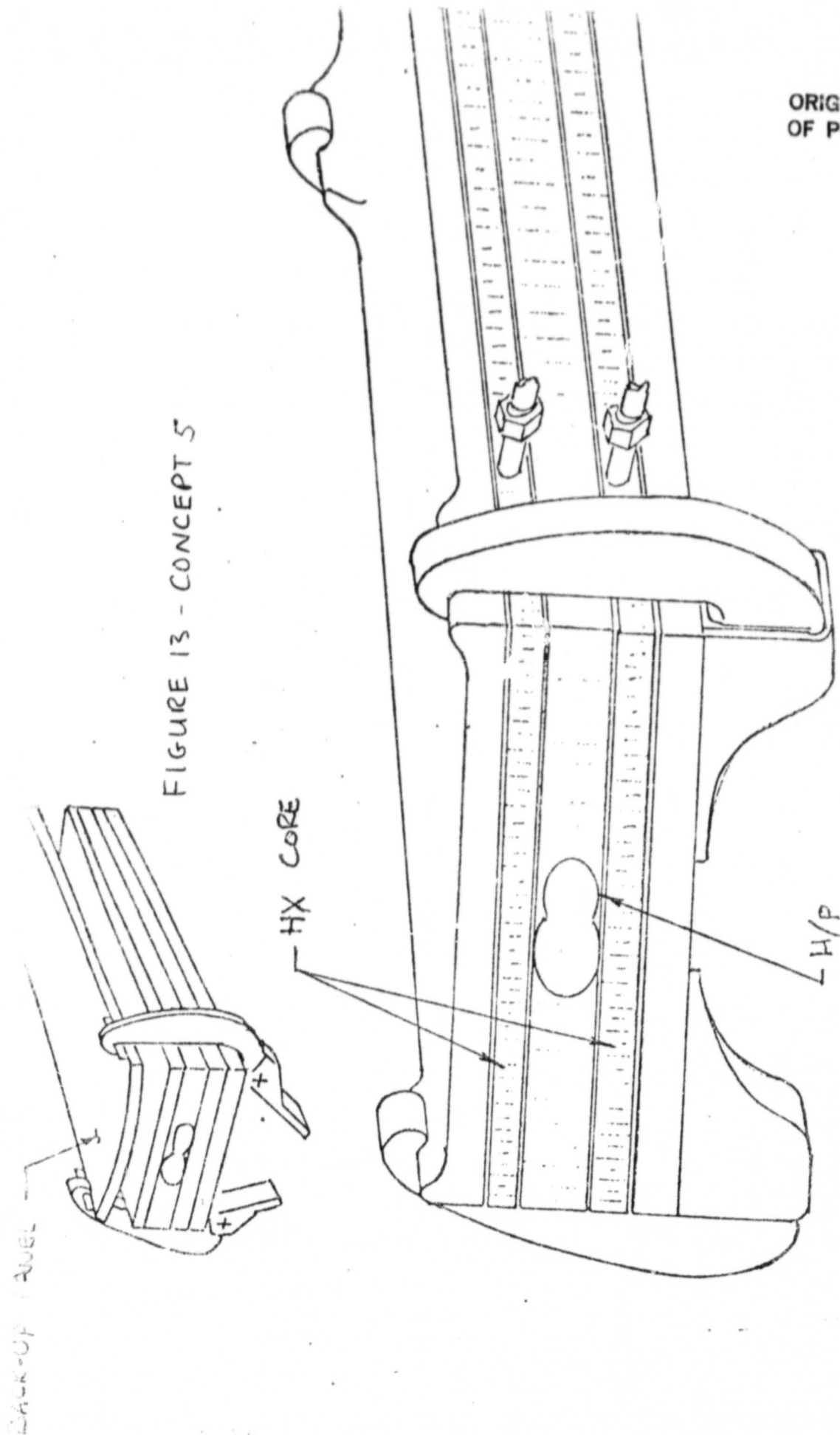


FIGURE 14 - CONCEPTS 4 AND 5
ONE SIDED HEAT INPUT

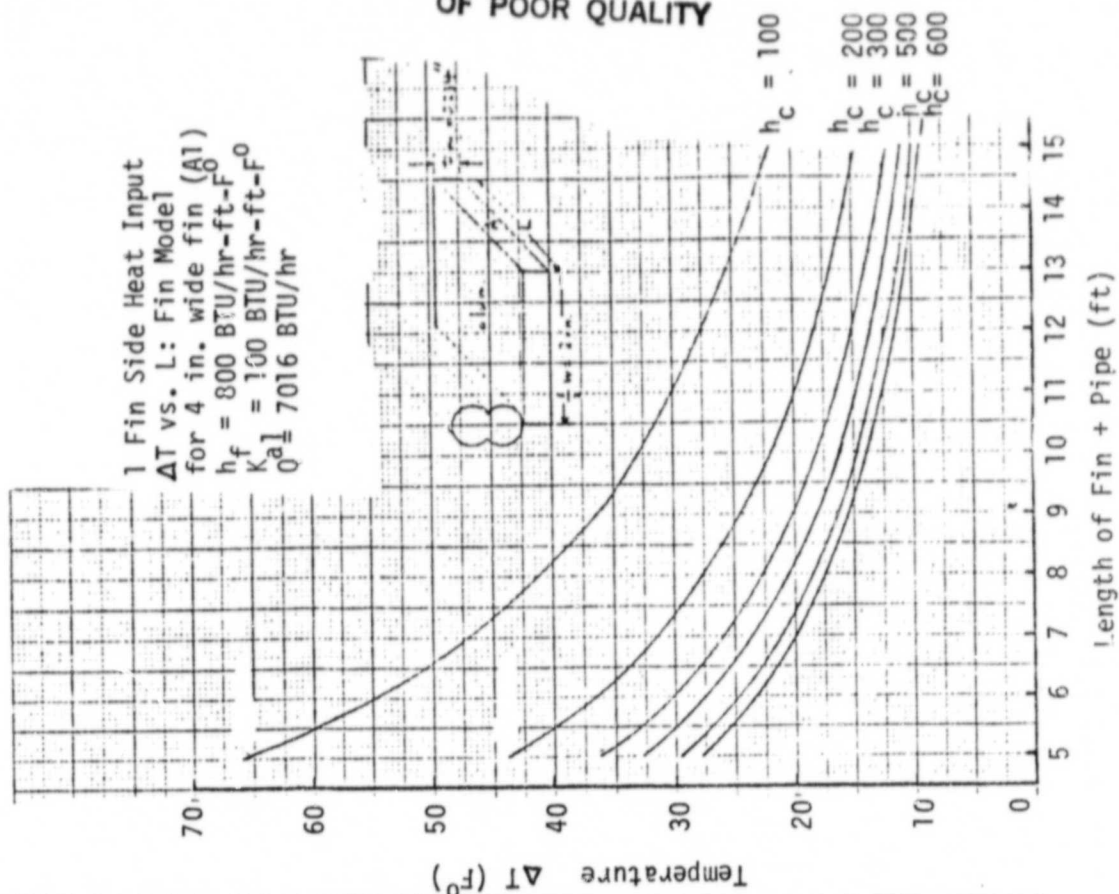
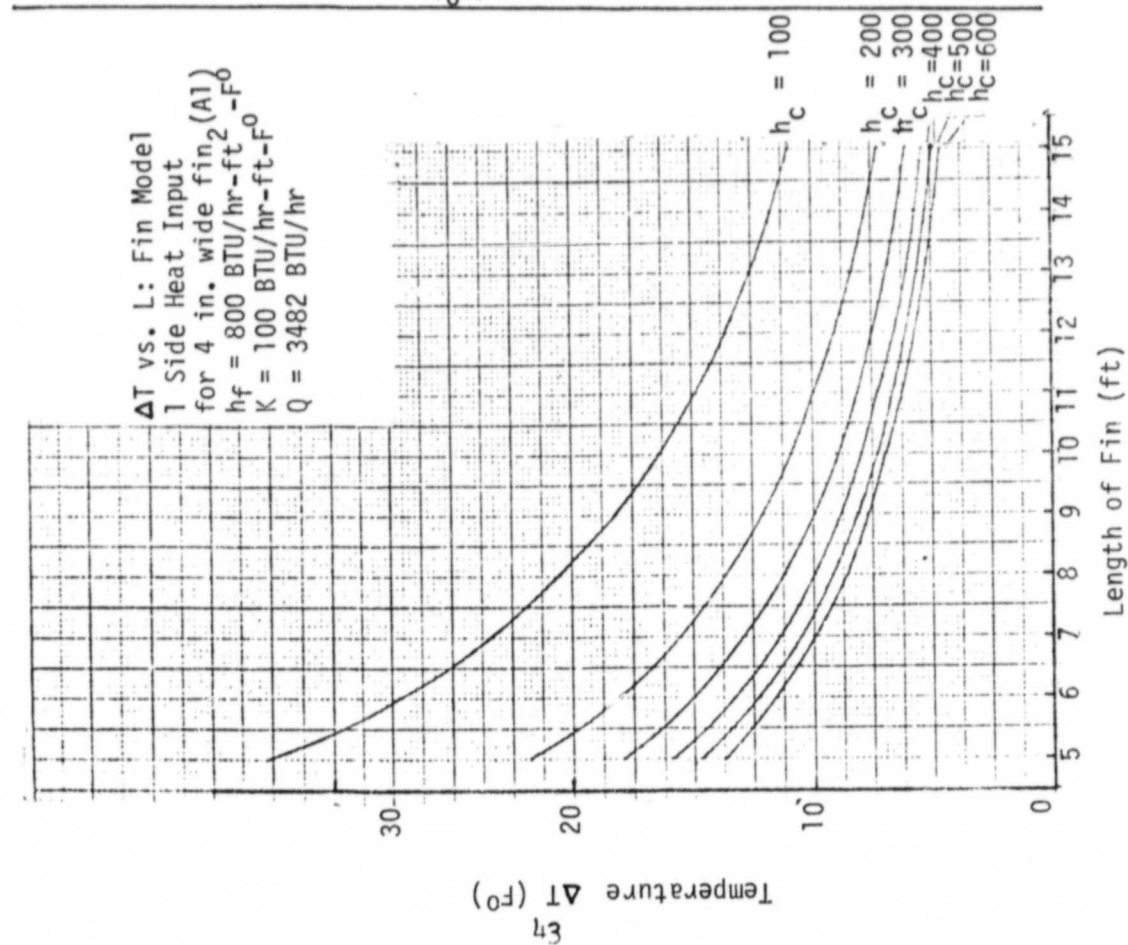


FIGURE 15 - CONCEPTS 4 AND 5
TWO SIDED HEAT INPUT

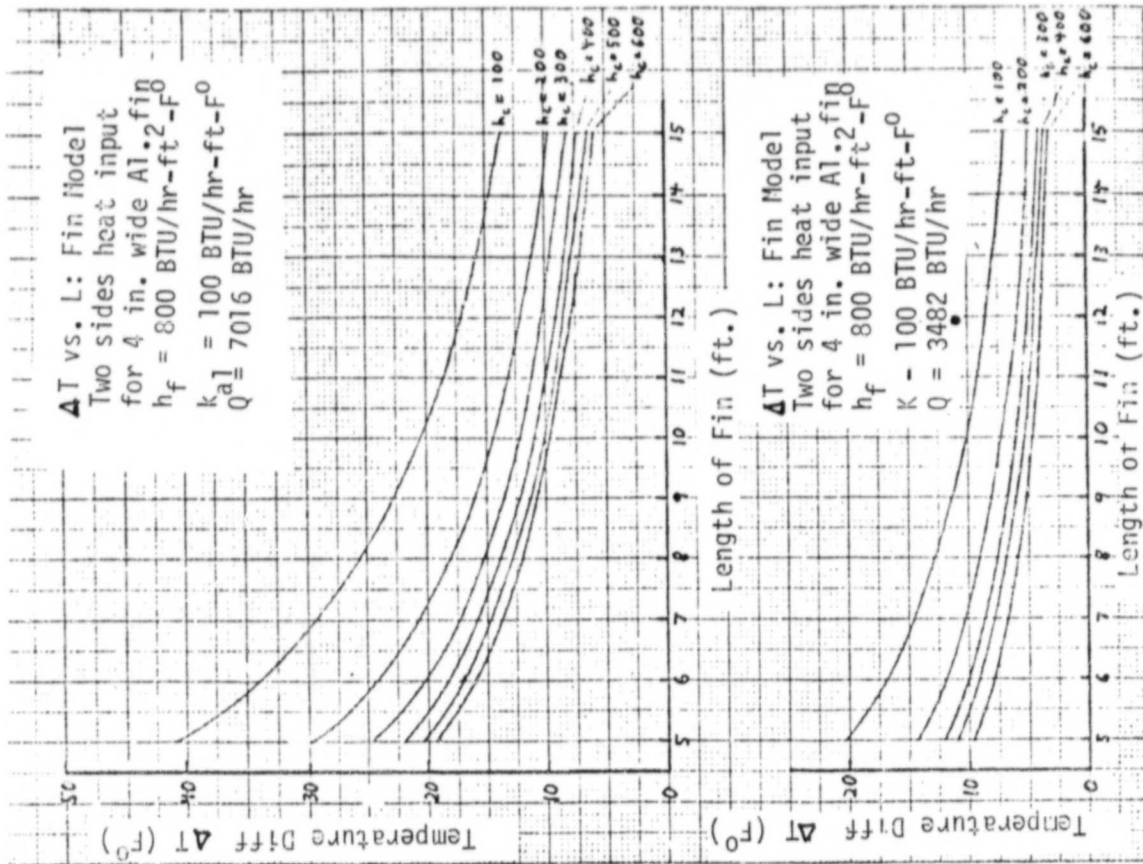
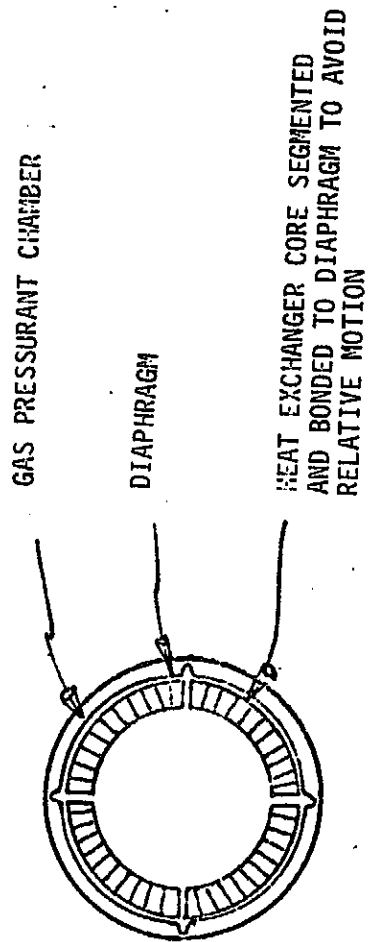


FIGURE 16 - CONCEPT 2A - COMBINING HEAT EXCHANGER
AND FLEXIBLE DIAPHRAGM



ORIGINAL PAGE IS
OF POOR QUALITY

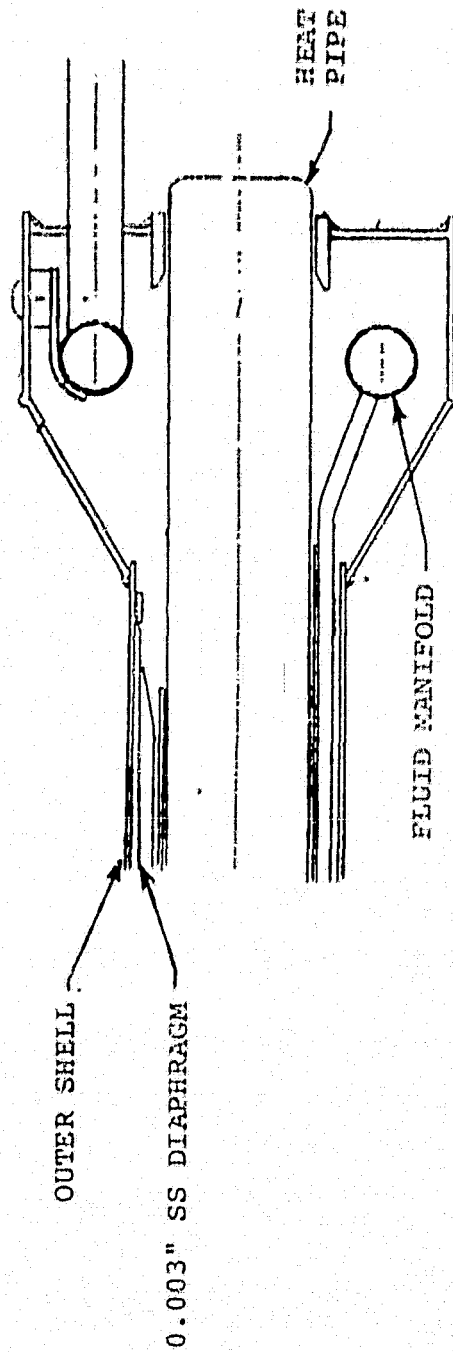
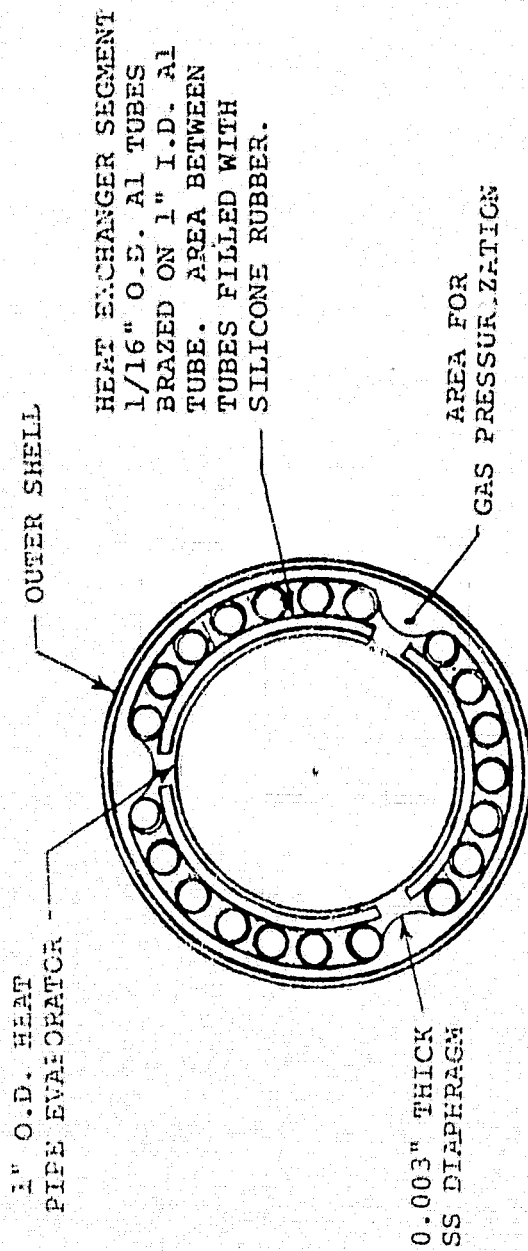
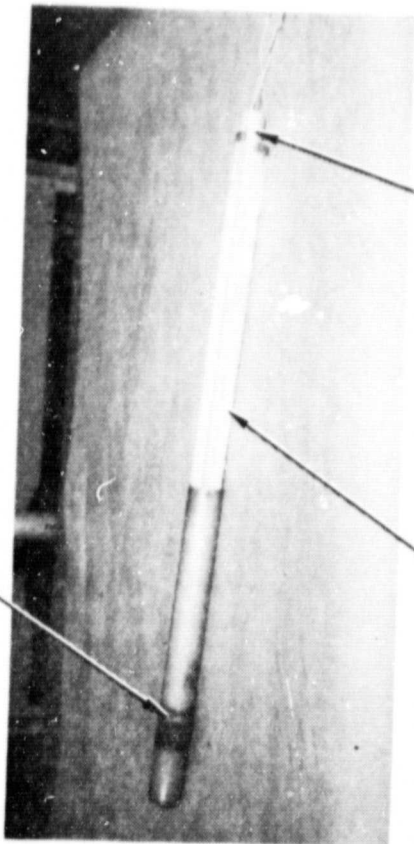


FIGURE 17
SKETCH OF SELECTED CONCEPT HEAT EXCHANGER CROSS SECTION

DIAPHRAGM ASSEMBLY

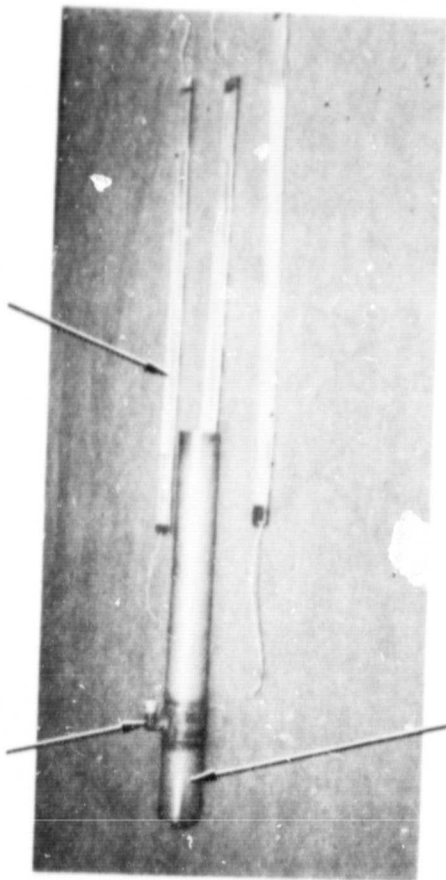


HEAT EXCHANGER
ELEMENTS

SIMULATED
HEAT PIPE

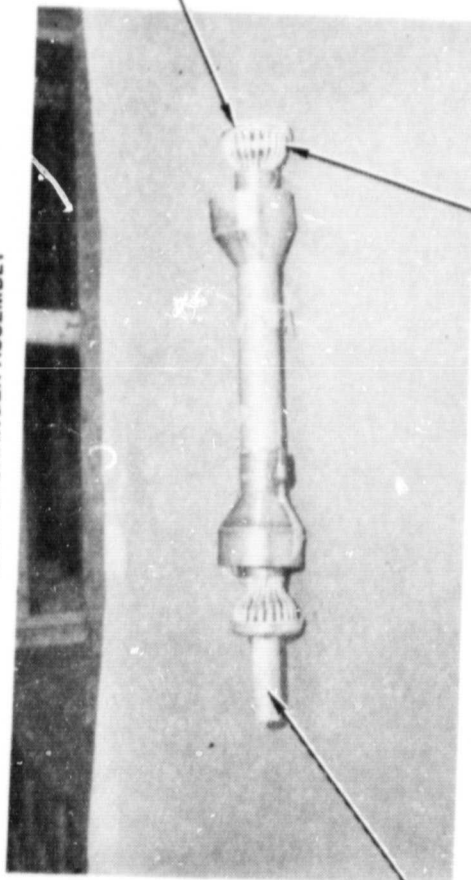
GAS PRESSURIZATION
FITTING

HEAT EXCHANGER
ELEMENTS



DIAPHRAGM ASSEMBLY

HEAT EXCHANGER ASSEMBLY



FLUID MANIFOLD

HEAT EXCHANGER
ELEMENT TUBES

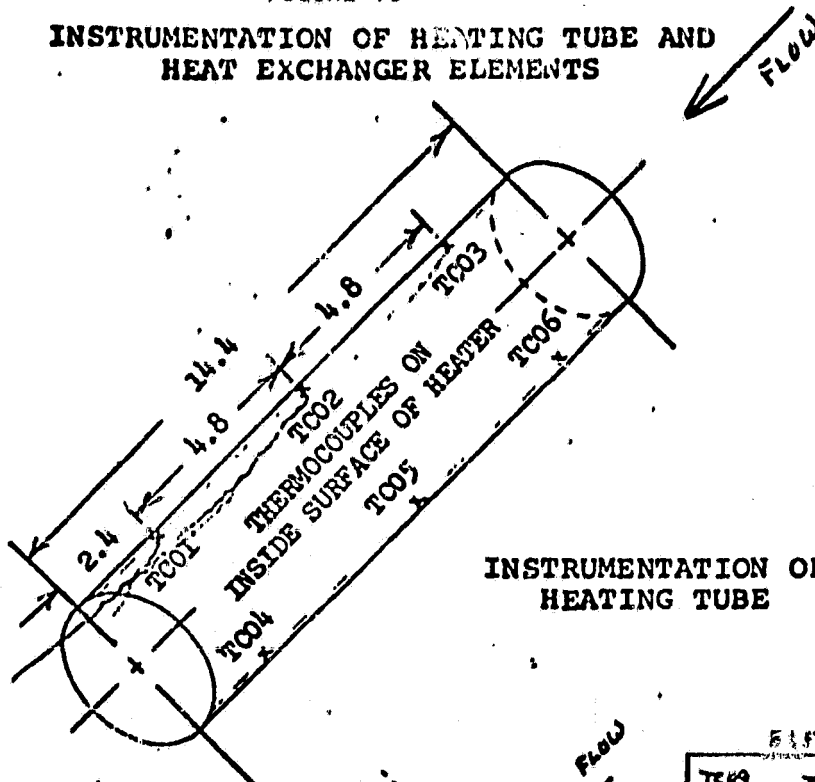
SIMULATED HEAT PIPE

ORIGINAL PAGE IS
OF POOR QUALITY

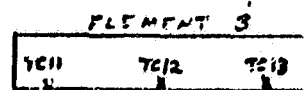
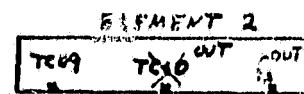
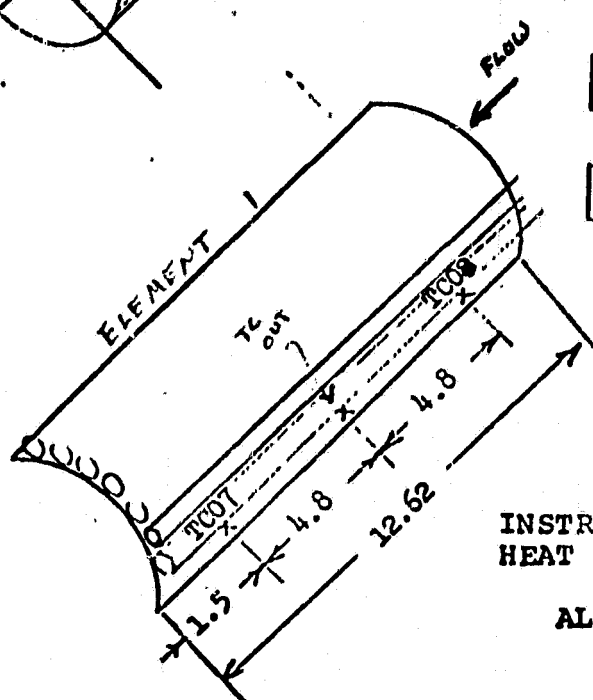
B2-2768-2

Figure 13 Photographs of Feasibility Demonstration Test Article Contact Heat Exchanger

FIGURE 19
INSTRUMENTATION OF HEATING TUBE AND
HEAT EXCHANGER ELEMENTS



INSTRUMENTATION OF
HEATING TUBE



INSTRUMENTATION OF EACH
HEAT EXCHANGER ELEMENT
(3 ELEMENTS)
ALSO TC10 - TC15

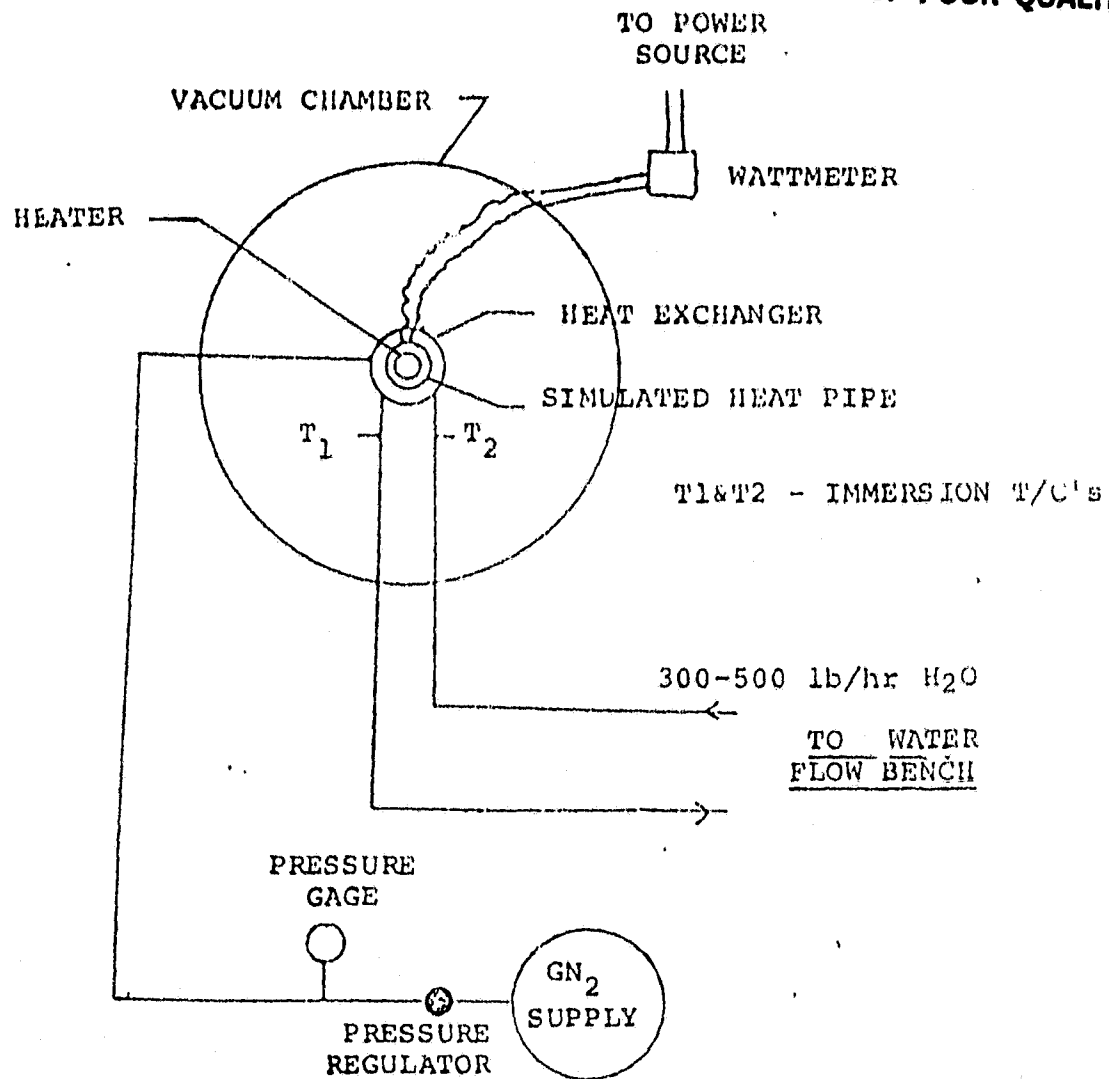


FIGURE 20

THERMAL VACUUM TEST SETUP

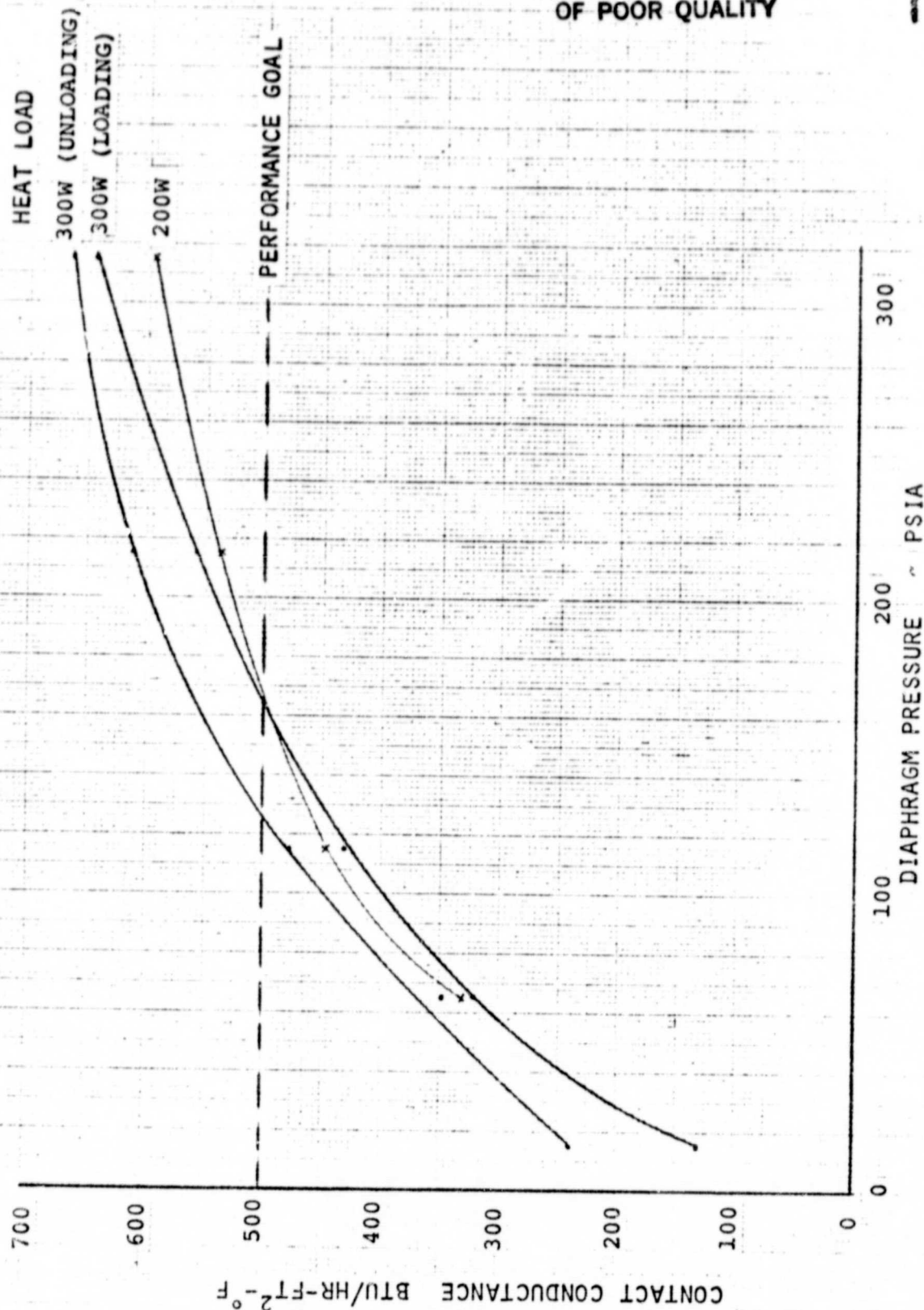
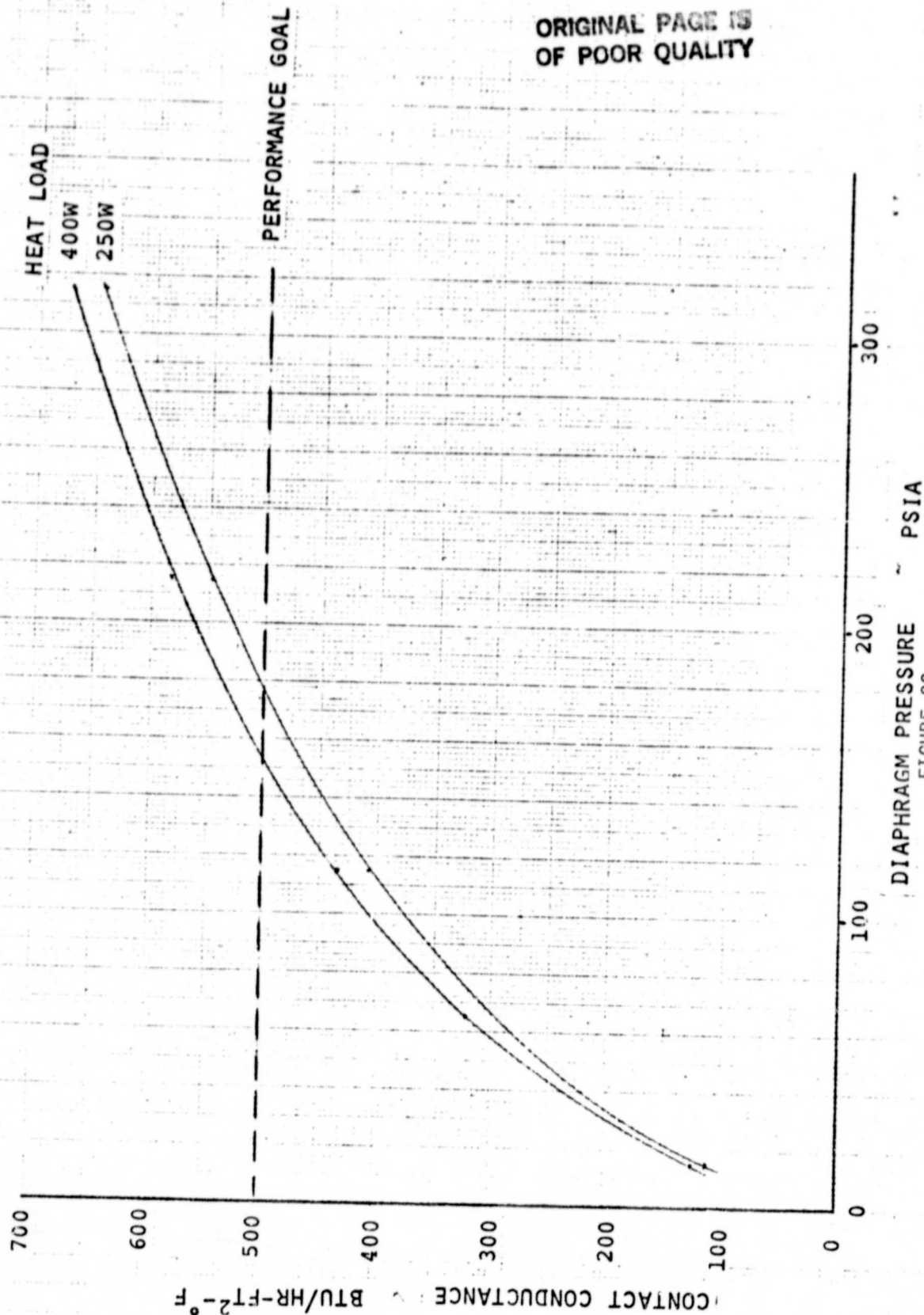


FIGURE 21
TEST RESULTS - CONTACT CONDUCTANCE VS DIAPHRAGM PRESSURE
FOR TWO HEAT LOADS



TEST RESULTS - CONTACT CONDUCTANCE VS DIAPHRAGM PRESSURE
 FIGURE 22
 FOR TWO HEAT LOADS

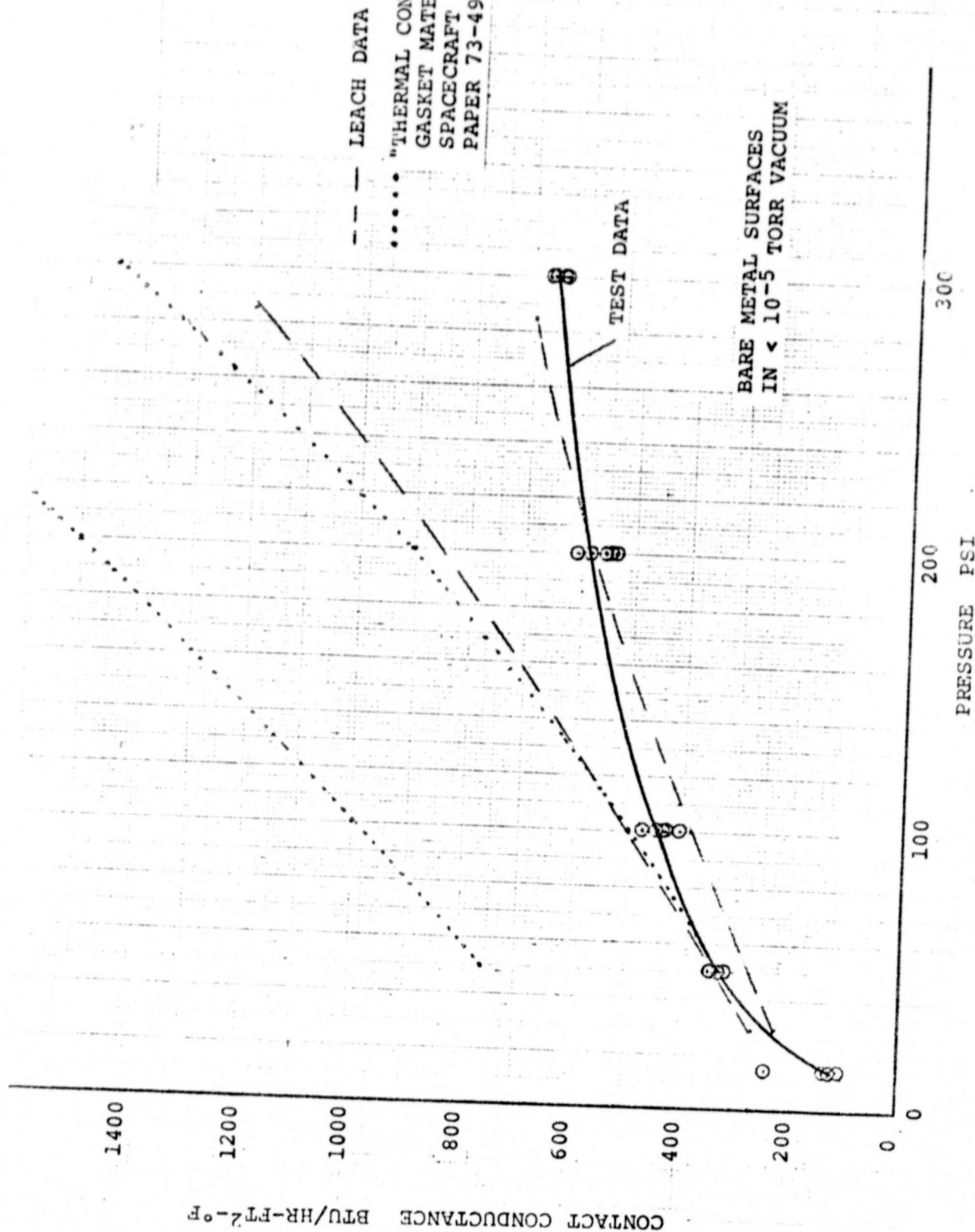
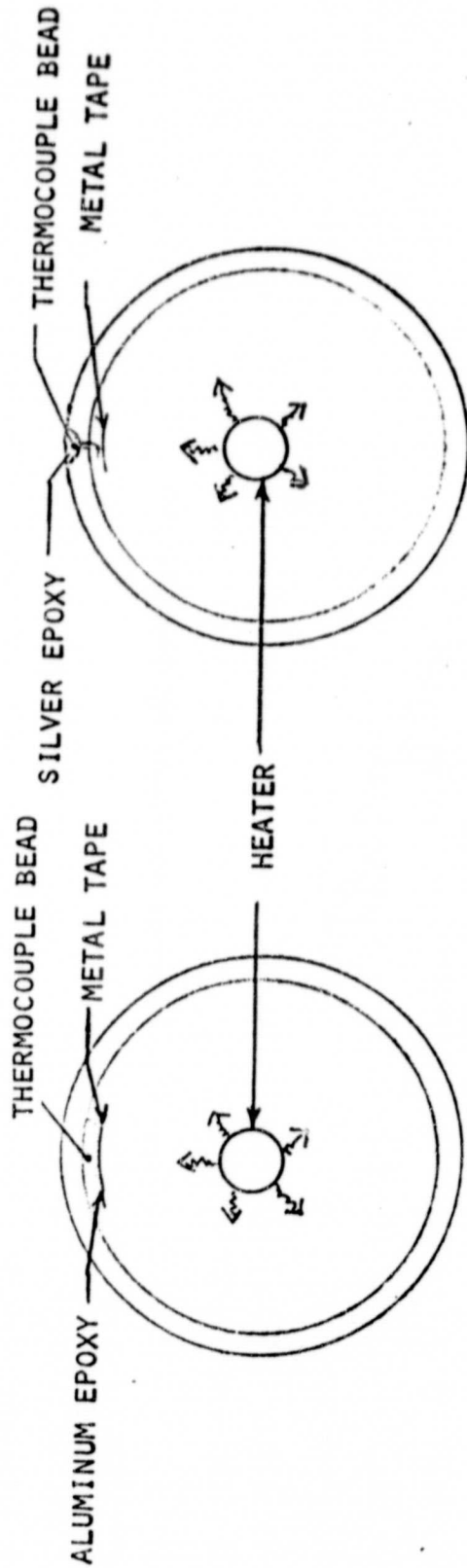


FIGURE 23 CONSTRUCTABLE INTERFACE CONTACT CONDUCTANCE COMPARISON WITH PREVIOUS DATA

ORIGINAL PAGE IS
OF POOR QUALITY



INITIAL THERMOCOUPLE INSTALLATION

FINAL THERMOCOUPLE INSTALLATION

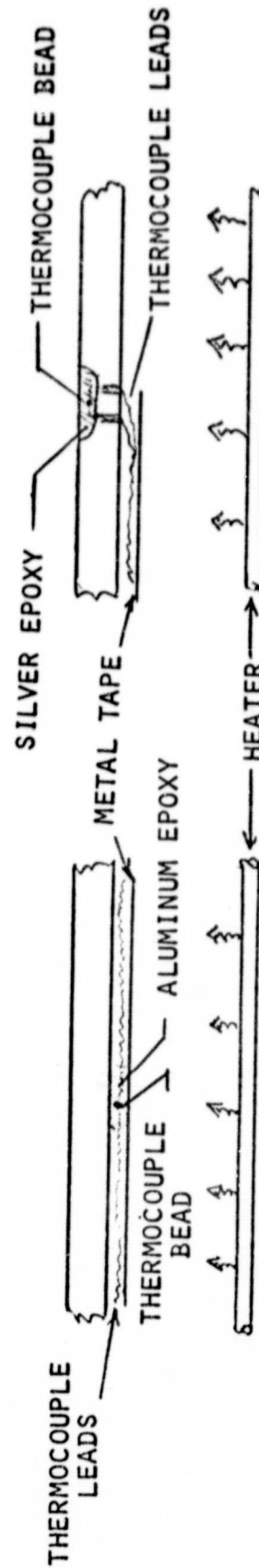


FIGURE 24
SIMULATED HEAT PIPE INSTRUMENTATION

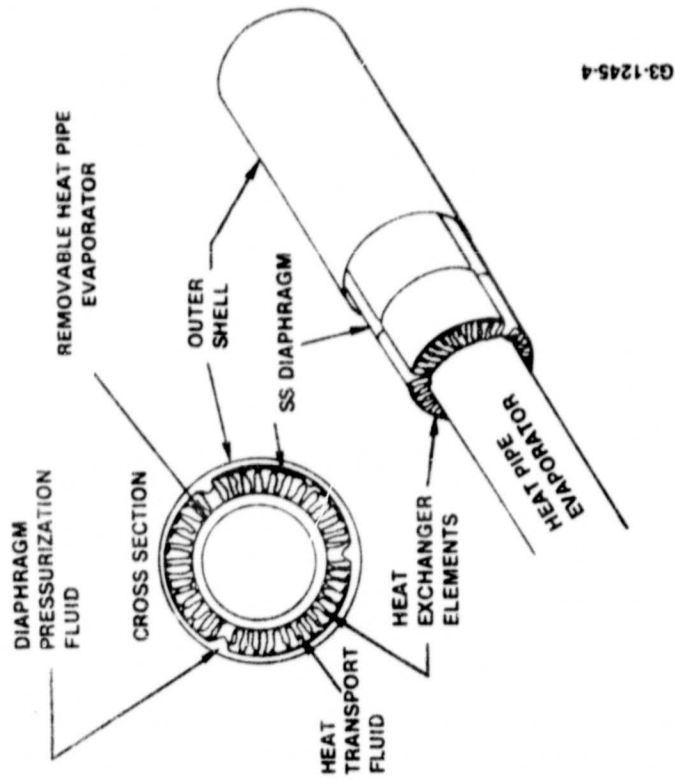


Figure 25 - Prototype Heat Exchanger Cross Section

FIGURE 26
PROTOTYPE CONTACT HEAT EXCHANGER
OVERALL VIEW

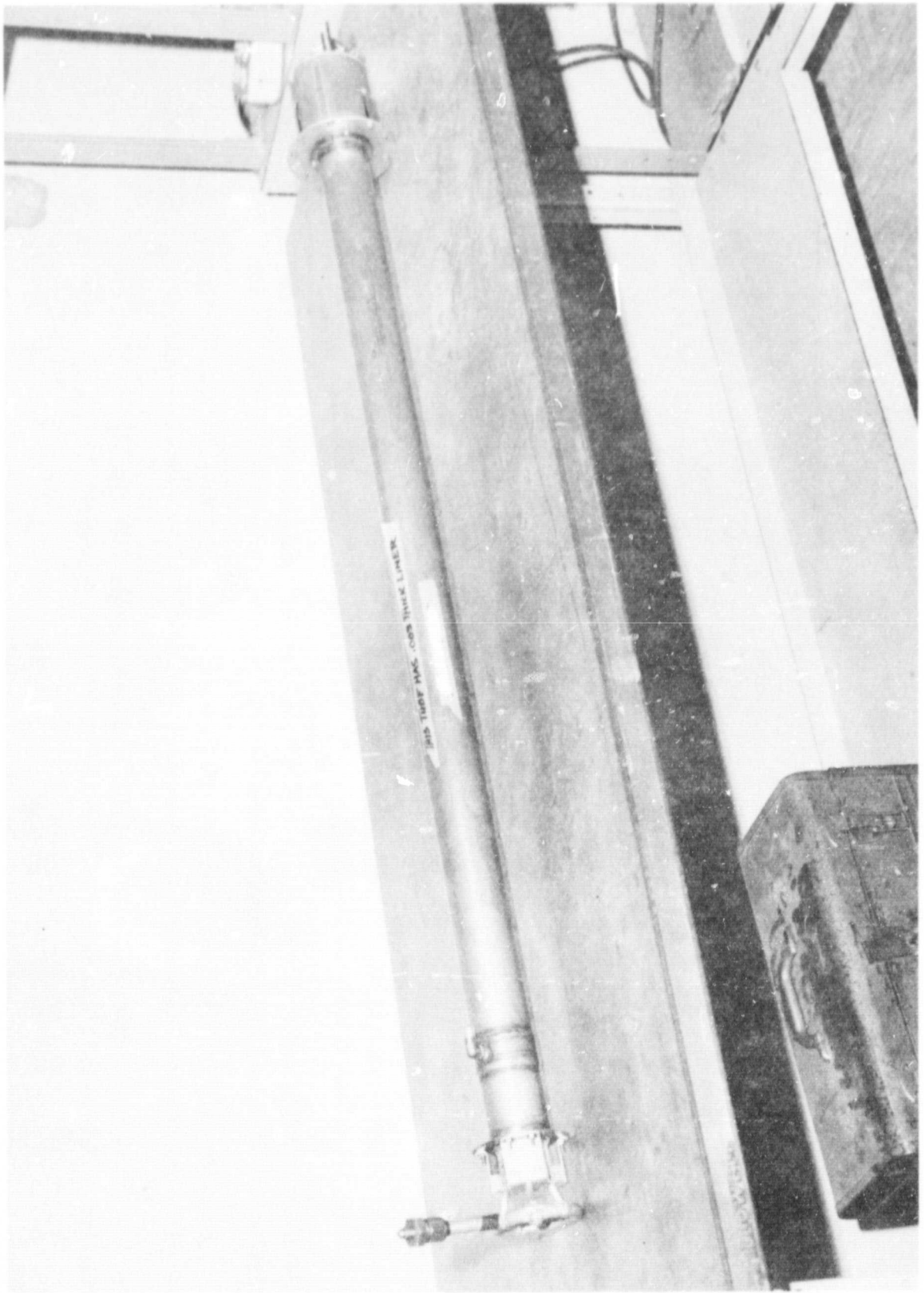


FIGURE 27
PROTOTYPE CONTACT HEAT EXCHANGER
MANIFOLD ASSEMBLY

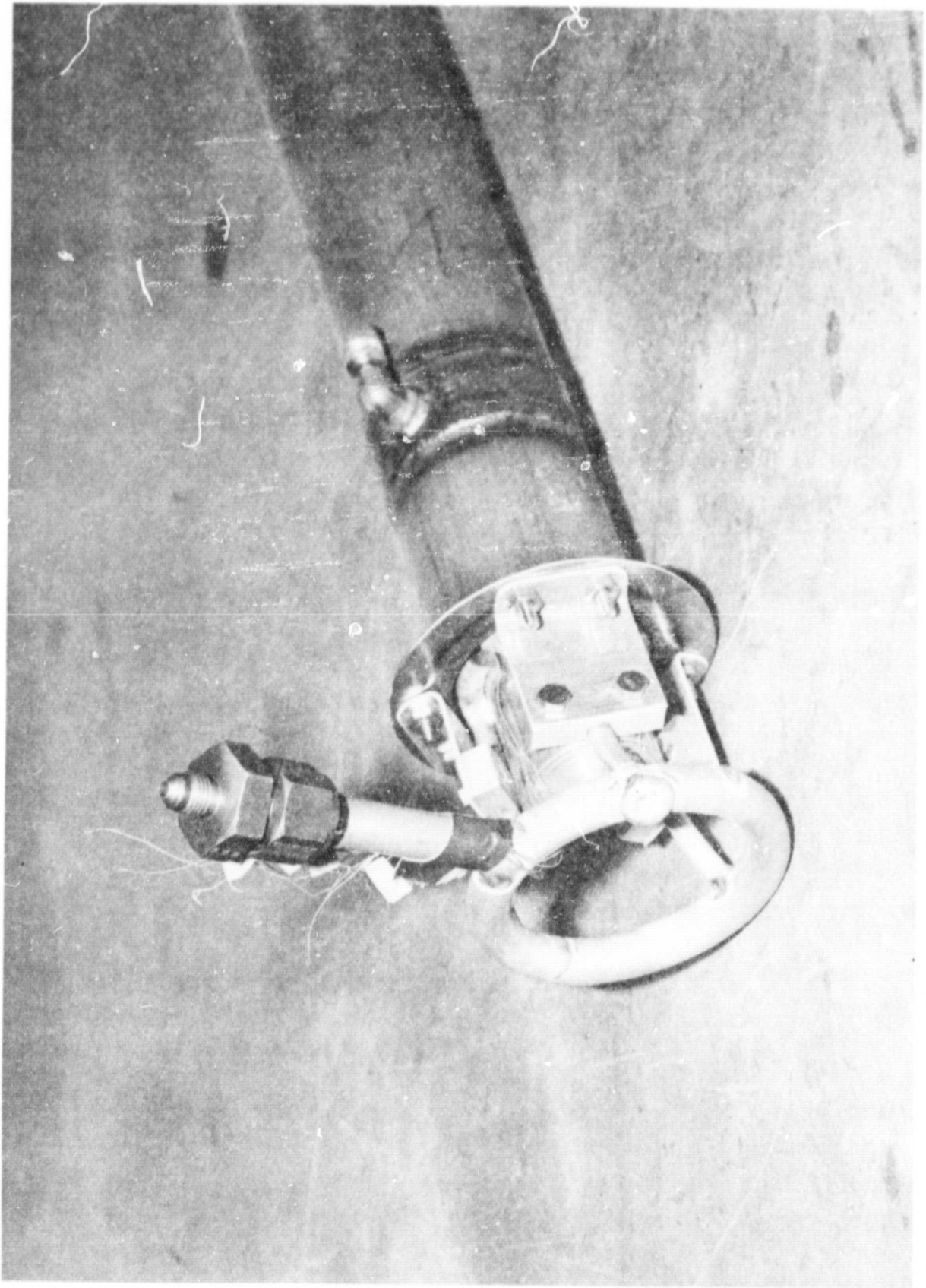


FIGURE 28
PROTOTYPE CONTACT HEAT EXCHANGER
INSERTION END VIEW

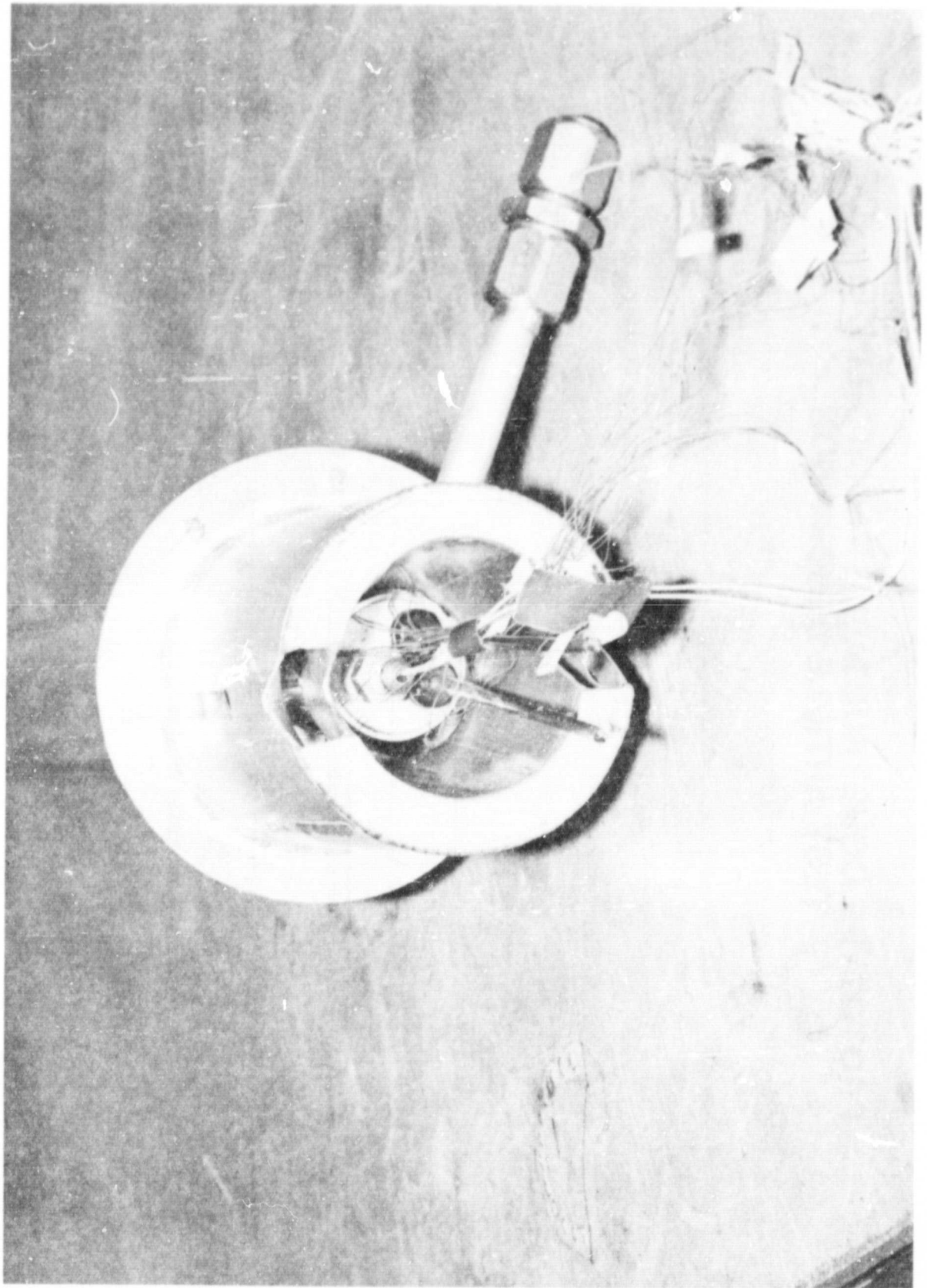
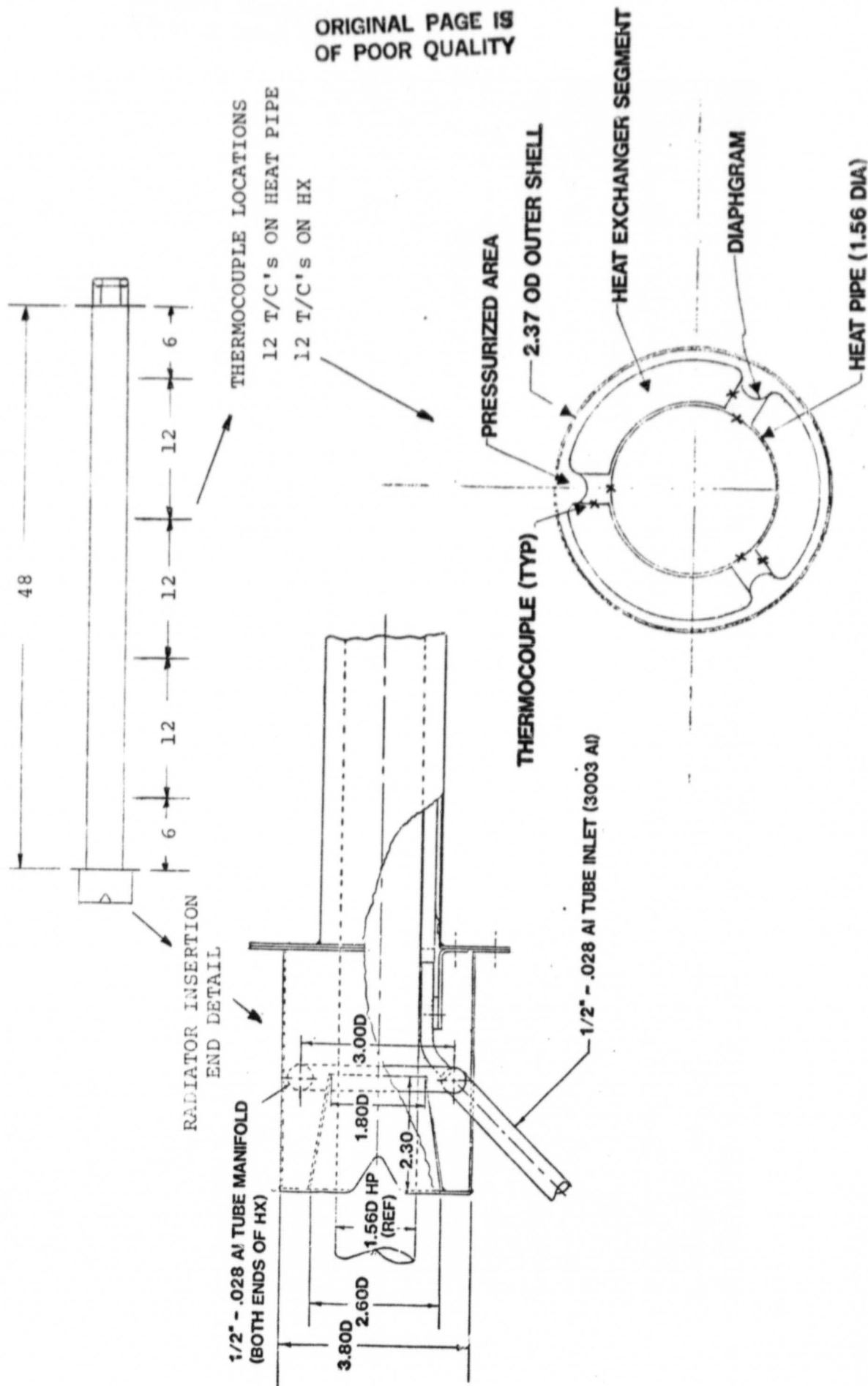


FIGURE 29

PROTOTYPE CONSTRUCTABLE RADIATOR INTERFACE TEST ARTICLE DESCRIPTION



ORIGINAL PAGE IS
OF POOR QUALITY

FIGURE 30
TEST DATA REDUCTION EXAMPLE

TP 13

POWER = 1509.63 WATTS

FLOW = 774.5 LB/HR

DIAPHRAGM PRESS = 299.12 PSIG

$$\text{CONTACT AREA} = 48 [\pi (1.57) - 3 (2.23)]$$

$$= 203.9 \text{ IN}^2$$

$$= 1.42 \text{ FT}^2$$

$$U_{\text{CONTACT}} = \frac{Q}{A \Delta T}$$

$$= \frac{1509.63 (3.413)}{1.42 (2.75)}$$

$$= 1319.81 \text{ BTU/HR FT}^2 \text{ } ^\circ\text{F}$$

ORIGINAL PAGE IS
OF POOR QUALITY

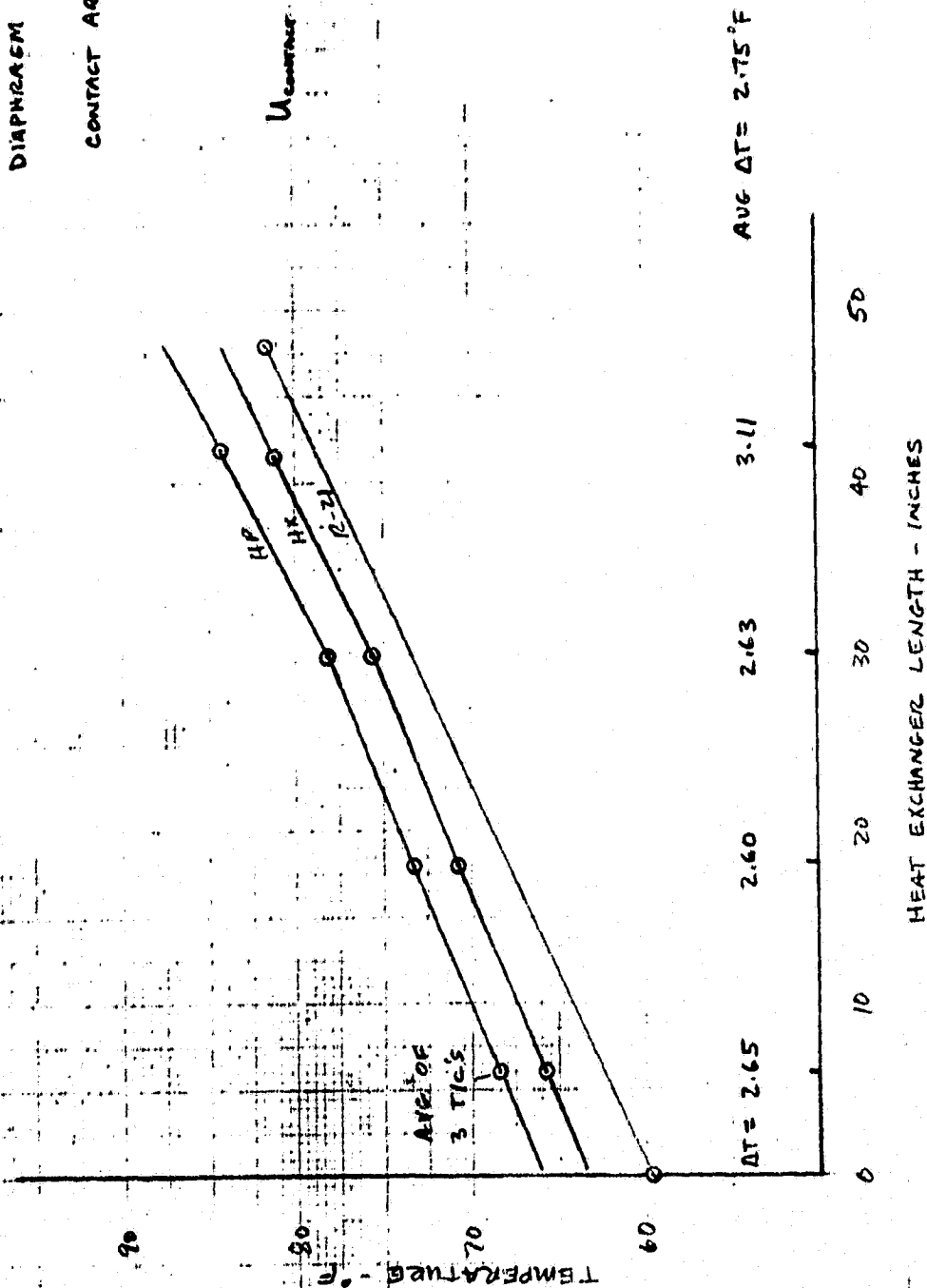


FIGURE 31
PROTOTYPE CONSTRUCTABLE RADIATOR INTERFACE
OVERALL CONDUCTANCE

CALCULATED FROM AVG FLUID TEMP $\left(\frac{T_{IN} + T_{OUT}}{2} \right)$
AND AVG HEAT PIPE TEMP (12 TIC'S)

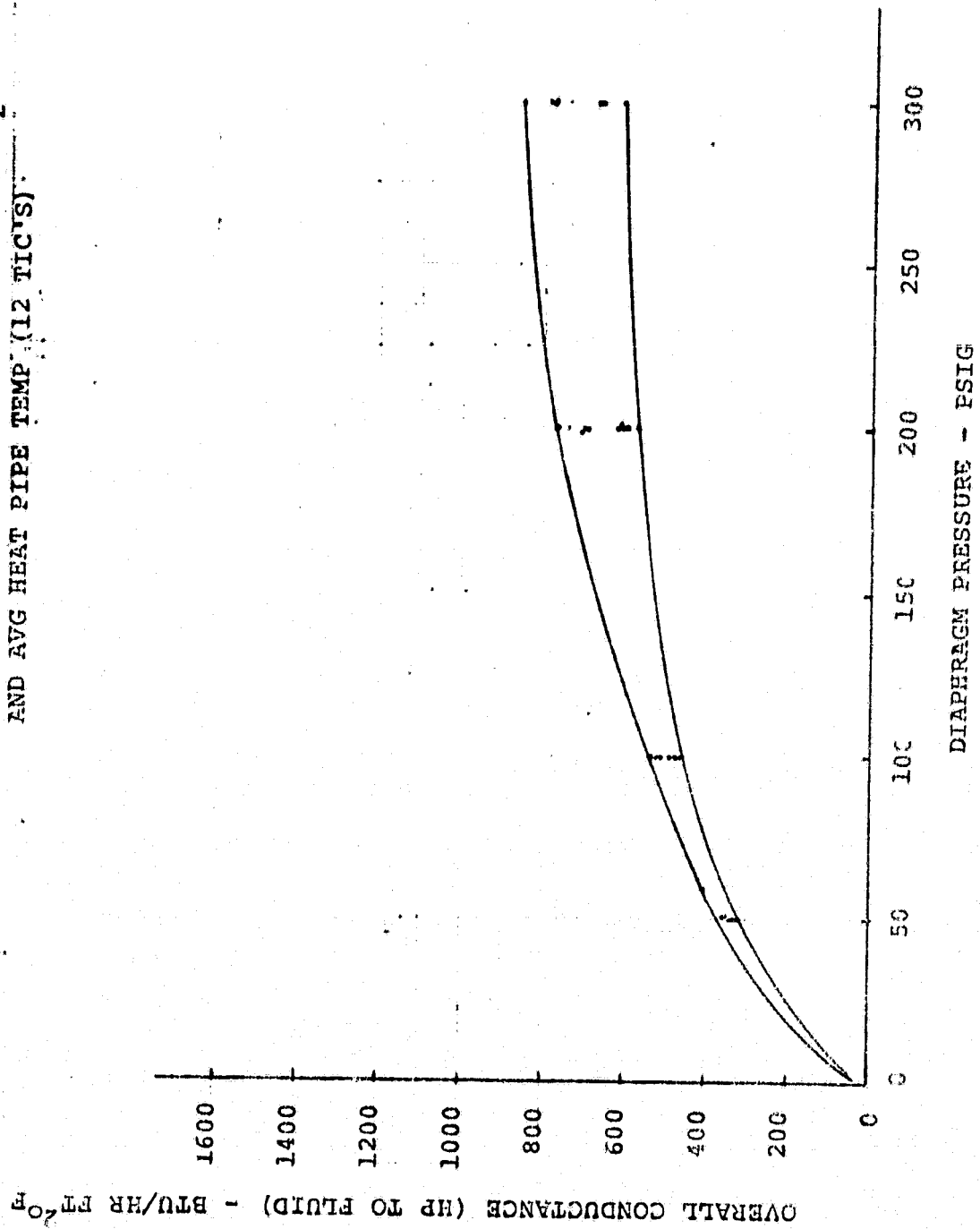
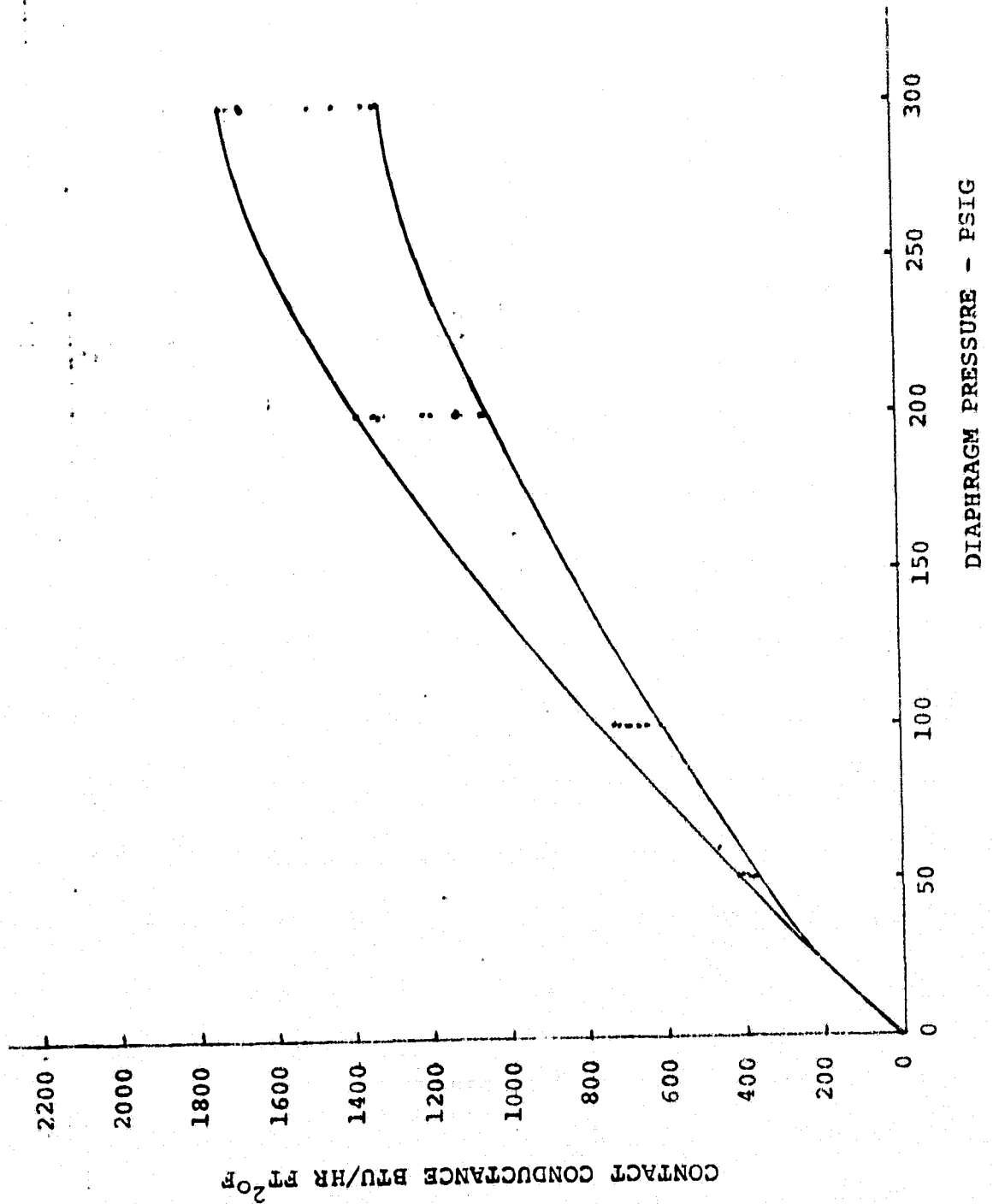


FIGURE 32
PROTOTYPE CONSTRUCTABLE RADIATOR INTERFACE
CONTACT CONDUCTANCE



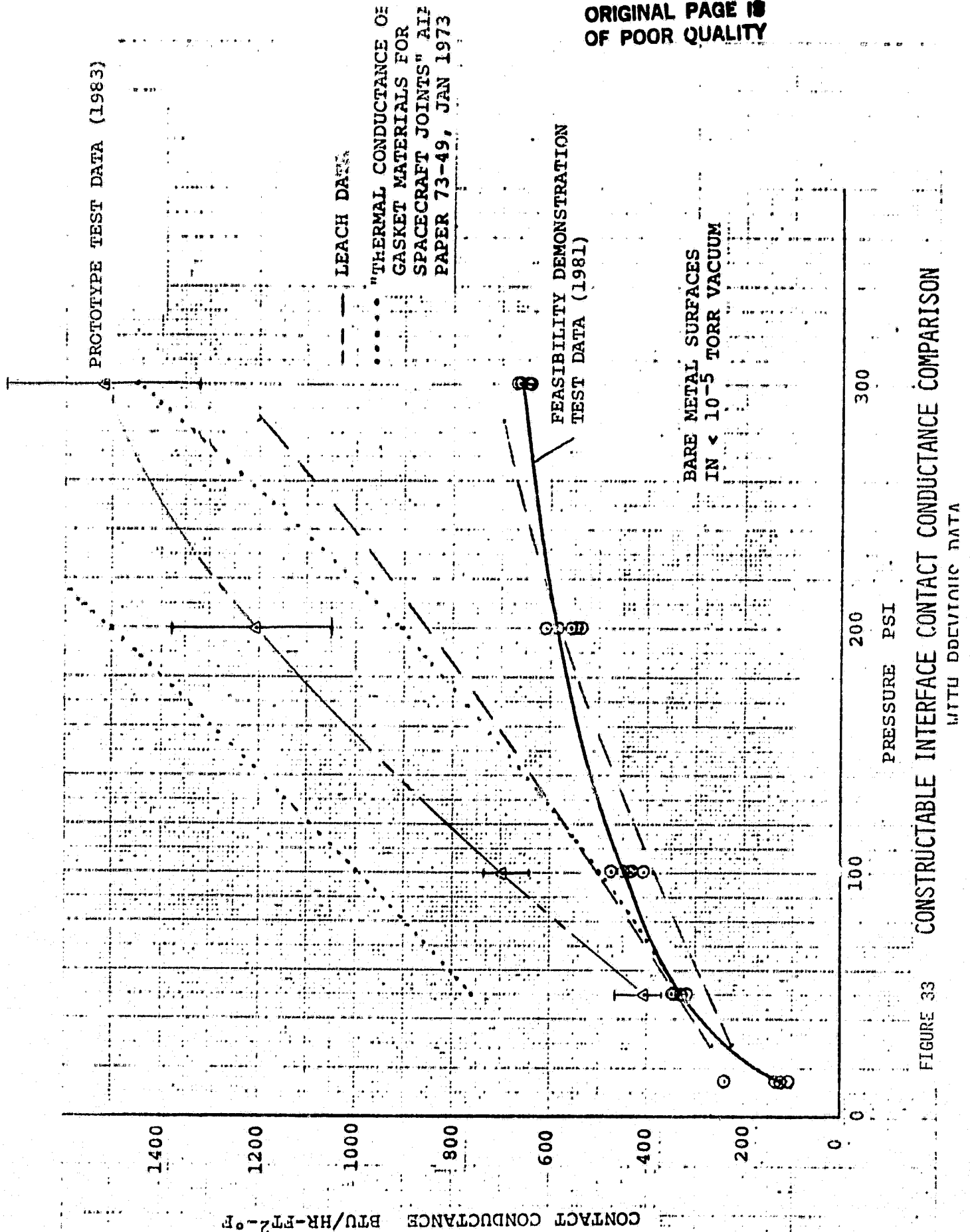
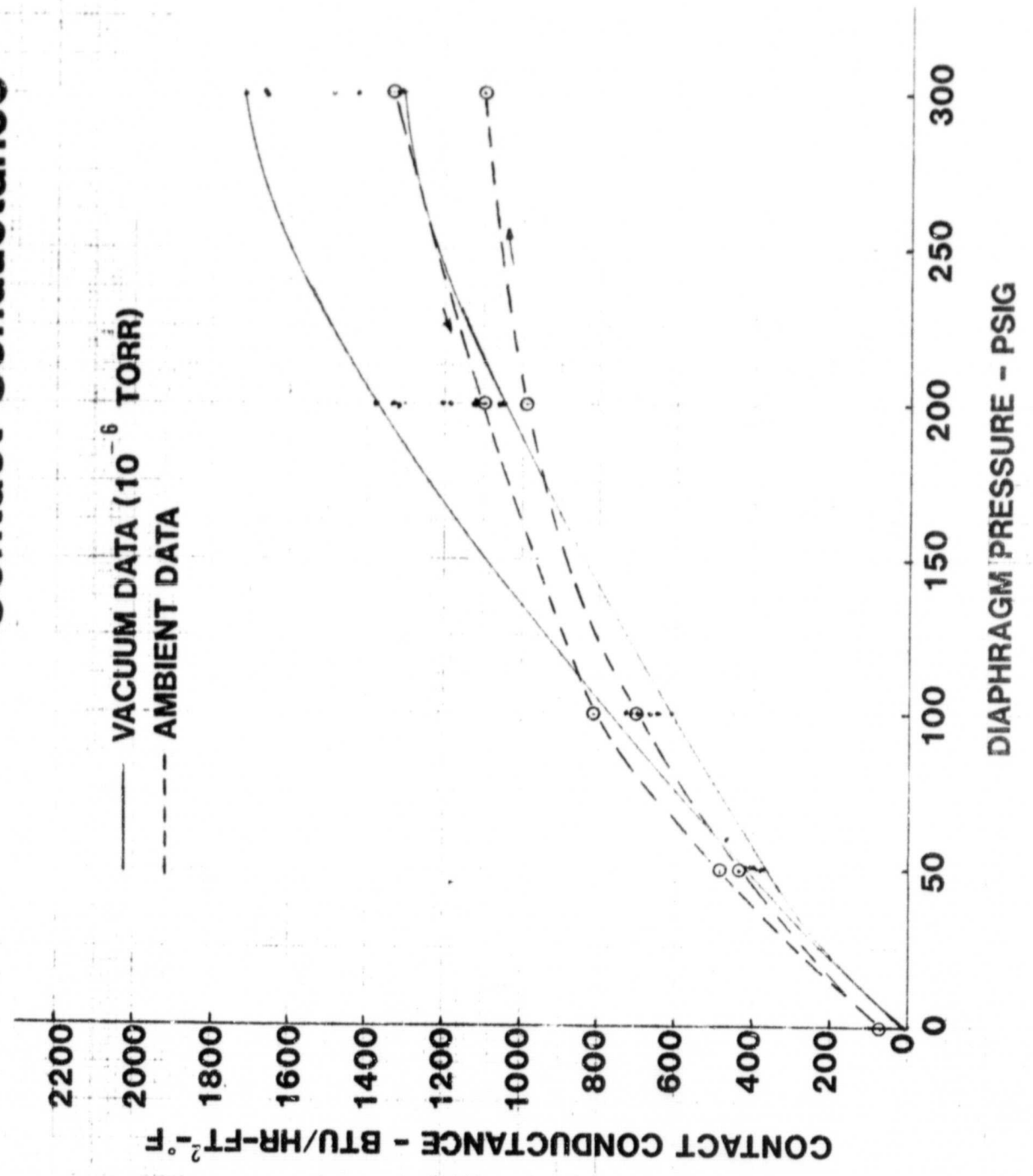


FIGURE 33

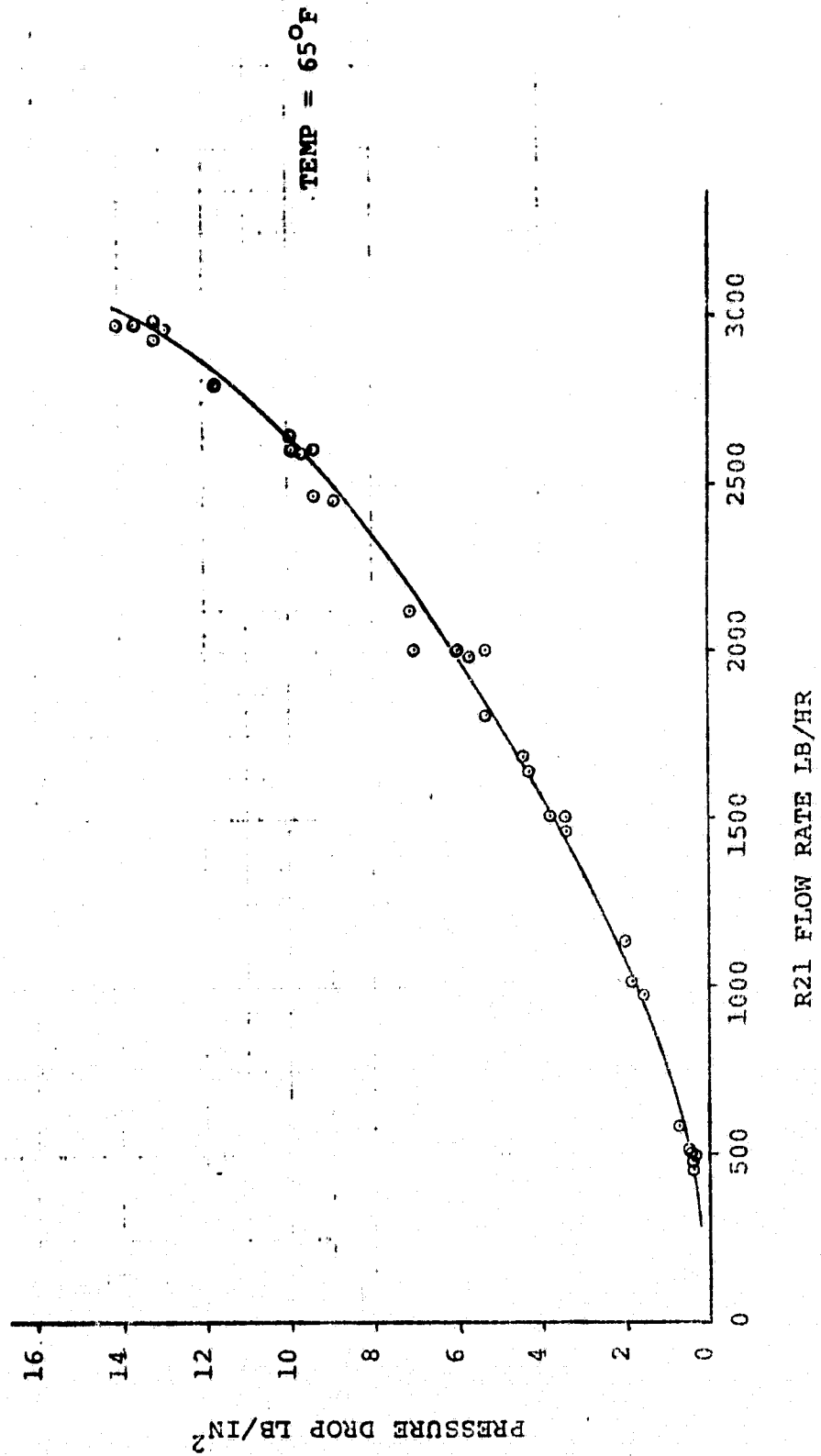
Comparison of Vacuum and Ambient Pressure Contact Conductance

FIGURE 34



ORIGINAL PAGE 19
OF POOR QUALITY

FIGURE 35
PROTOTYPE CONSTRUCTABLE RADIATOR INTERFACE
HEAT EXCHANGER PRESSURE DROP



APPENDIX A

FLUID PRESSURE CLAMPING CONTACT

HEAT EXCHANGER TEST

ORIGINAL PAGE IS
OF POOR QUALITY

- QUICK LOOK REPORT -

FLUID PRESSURE CLAMPING CONTACT HEAT EXCHANGER TEST
FOR
MODULAR HEAT PIPE RADIATOR.

REPORT NO. 2-30320/9R-52119

7 May 1979

PREPARED BY:

D. D. Stalmach
D. D. Stalmach

REVIEWED BY:

J. A. Oren
J. A. Oren

APPROVED BY:

R. L. Cox
R. L. Cox

INTRODUCTION

This Quick Look Report describes the results of thermal vacuum and ambient tests conducted on the contact heat exchanger for a replaceable concentric heat pipe radiator panel. The tests were conducted on the IR&D task "Heat Pipe Radiator Test and Analysis". The tests were performed on 27 and 30 April, 1979, in the Vought Space Environment Simulation Chamber.

The test article consisted of (1) a heat pipe radiator panel, and (2) a contact heat exchanger manifold to interface the heat pipe panel with a pumped fluid loop. The heat pipe panel consists of a 6-ft. long by 1-inch diameter concentric aluminum/ammonia/aluminum/propane heat pipe adhesively bonded into a 4.5 ft. x 1.1 ft. x 0.5 in. honeycomb panel. Fabrication and thermal vacuum performance of the heat pipe panel has been previously reported.

The contact heat exchanger consists of a cylindrical sleeve, 1.04" I.D. x 12" long, which slides over the evaporator section of the heat pipe. The sleeve, illustrated in Figures 1 and 2, is made up of concentric inner and outer walls, separated by a 0.1" annular fluid passageway. The inner wall is an axially convoluted nickel diaphragm, 0.003" thick, which deforms slightly under fluid pressure and clamps against the heat pipe. The nickel wall is made by nickel plating a mandrel that has been cast from a low melting point alloy. After plating, the mandrel is melted out leaving the nickel shell. The outer wall is stainless steel tubing, with fluid inlet and outlet collector weldments. The nickel inner wall is silver soldered into the outer steel tube.

The unique advantage of this design is the ability to easily install or remove the heat pipe from the heat exchanger assembly. At the same time a high contact conductance may be obtained to minimize the contact temperature drop. This high contact conductance is obtained because of the uniformly high contact pressure possible with this design and does not require precise matching of the heat exchanger to the heat pipe. The flexibility of the thin nickel-plated heat exchanger surface allows it to conform to any waviness or other irregularities of the heat pipe outer wall. The 0.02 inch radial clearance provided between the unpressurized heat exchanger wall and the heat pipe allows for tolerances in the heat pipe diameter as well as easy insertion and removal of the heat pipe.

The current series of tests was run to obtain experimental data for the contact thermal performance both in vacuum and in air.

TEST SETUP

The thermal vacuum test was conducted in Vought's 12 foot vacuum chamber. Liquid nitrogen wall temperatures were maintained throughout the vacuum test. Freon 21 was used as the heat transport fluid. Immersion thermocouples were used to measure the Freon inlet and outlet temperatures. These thermocouples were wired in a delta arrangement to allow accurate measurement of the fluid temperature drop. Pressure transducers in the fluid loop allowed measurement of the pressure drop through the manifold and heat exchanger assembly.

Prior to installation in the vacuum chamber, the heat exchanger was slid onto the evaporator section of the heat pipe and leak tested with helium up to a pressure of 350 psig. No leaks were detected. Verification of a high contact pressure was made by trying to slide the pressurized heat exchanger off of the heat pipe. At a gas pressure of 10 psig the heat exchanger was already clamped tight enough that it could not be moved by hand. Releasing the gas pressure allowed the heat exchanger to easily slide off of the heat pipe.

RESULTS AND ANALYSIS

Tests points were taken at fluid flow rates ranging from 320 to 3000 lb/hr and inlet temperatures of 33°F to 69°F during the vacuum test and 120°F to 126°F during the ambient test. The results of the vacuum test are presented in Table 1(a). The heat rejected was determined from the measured fluid temperature drop and checked with a radiation heat balance. The overall heat transfer coefficient per unit area, U , was calculated knowing the amount of rejected heat and the measured temperature difference between the Freon and the adiabatic region of the heat pipe. This value of U includes the fluid heat transfer coefficient, the contact conductance, and the evaporative heat transfer coefficient of the heat pipe. Since the value of the contact conductance, h_c , was the only unknown it could be calculated with the following equation,

$$h_c = \frac{1}{A_c} \left[\frac{1}{\frac{1}{UA} - \left[\frac{1}{(hA)_f} + \frac{1}{(hA)_e} \right]} \right]$$

where A is area and the subscripts f and e refer to the fluid and the heat pipe evaporator respectively. The calculated value of contact conductance was 580 BTU/hr-ft²-°F. This value is slightly lower than the value $h_c = 740$ BTU/hr-ft²-°F reported for aluminum-to-aluminum at the same contact pressure (Ref. 1).

This difference may be explained by the fact that the heat pipe evaporator was not machined to a smooth finish. Scotch Brite was used to smooth the heat pipe evaporator and many small scratches were visible.

Following the thermal vacuum test an ambient test was conducted in order to obtain a correlation between the contact conductance in a vacuum and in an air atmosphere. The test setup was the same as for the vacuum test. The results of this test are presented in Table 1(b). The calculated contact conductance for the heat exchanger in air was 1980 BTU/hr-ft²-°F. The ratio of the contact conductances in air and in vacuum is $1980/580 = 3.4$. This compares well with the 3.2 value of this ratio reported for stainless steel at a contact pressure of 450 psi (Reference 2).

REFERENCES

- (1) "Joint Conductance Element Tests for the Self Contained Heat Rejection Module Contact Heat Exchanger", Vought Report No. T211-RP-009, August 1974.
- (2) J. F. Cassidy and H. Mark, "Thermal Contact Resistance Measurements at Ambient Pressures of One Atmosphere to 3×10^{-12} mm Hg and Comparison With Theoretical Predictions", AIAA Paper No. 69-629, June 1969.

APPENDIX B

PROTOTYPE CONTACT HEAT EXCHANGER

TEST DATA

ORIGINAL PAGE IS
OF POOR QUALITY

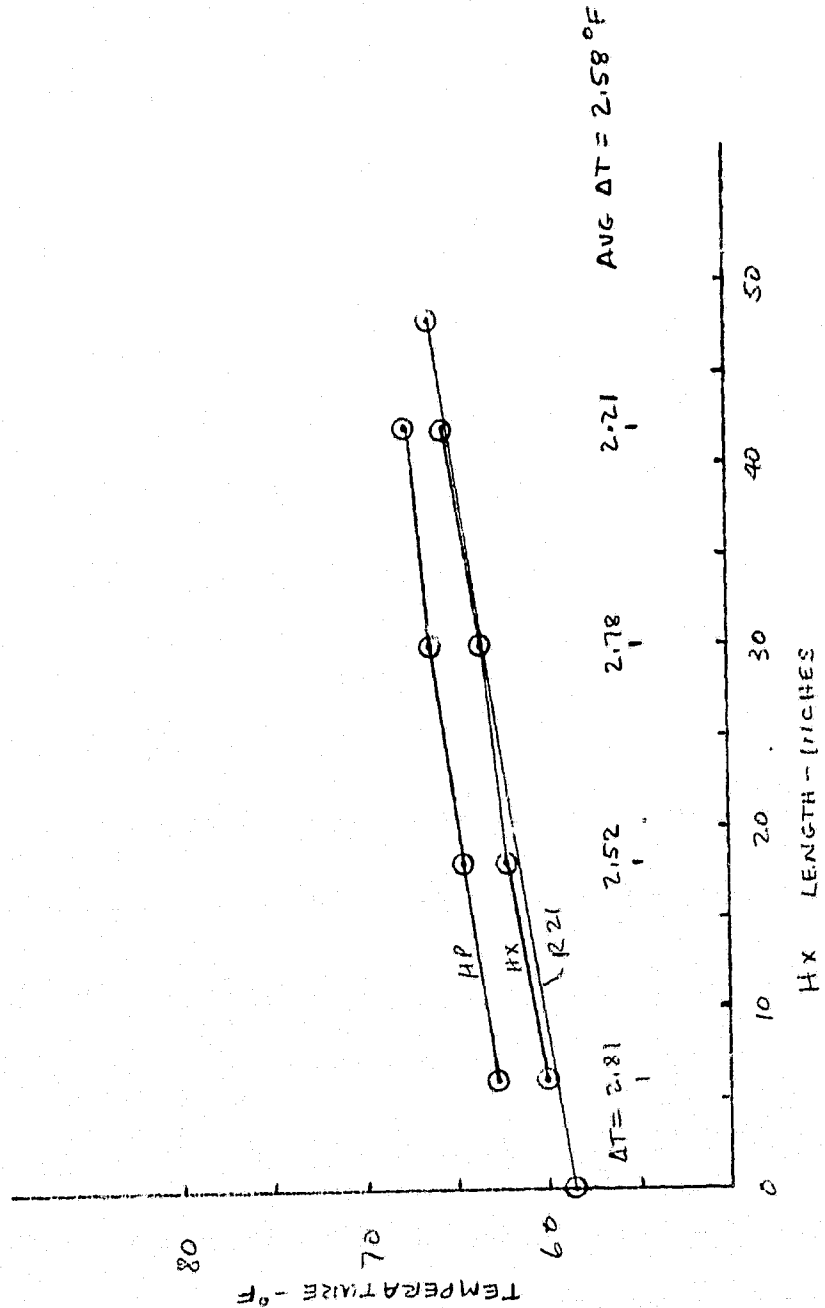
TP 1:

$$P = 503.55 \text{ WATTS}$$

$$\dot{W} = 992.171 \text{ LB/HR}$$

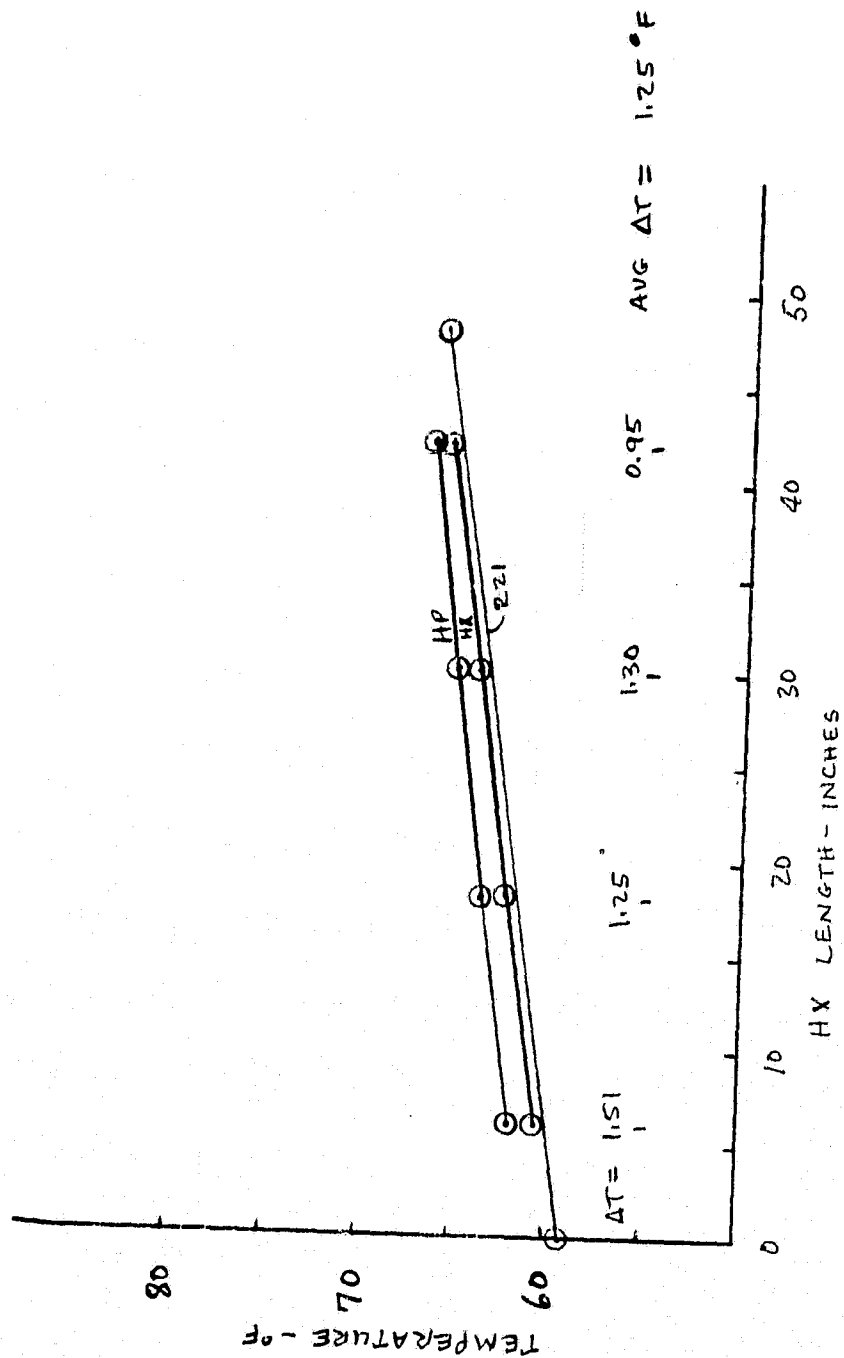
$$P.D = 59.0214 \text{ P=18}$$

$$U_{AVG} = 468.72 \text{ BTU/HR FT}^2 \text{ OF}$$



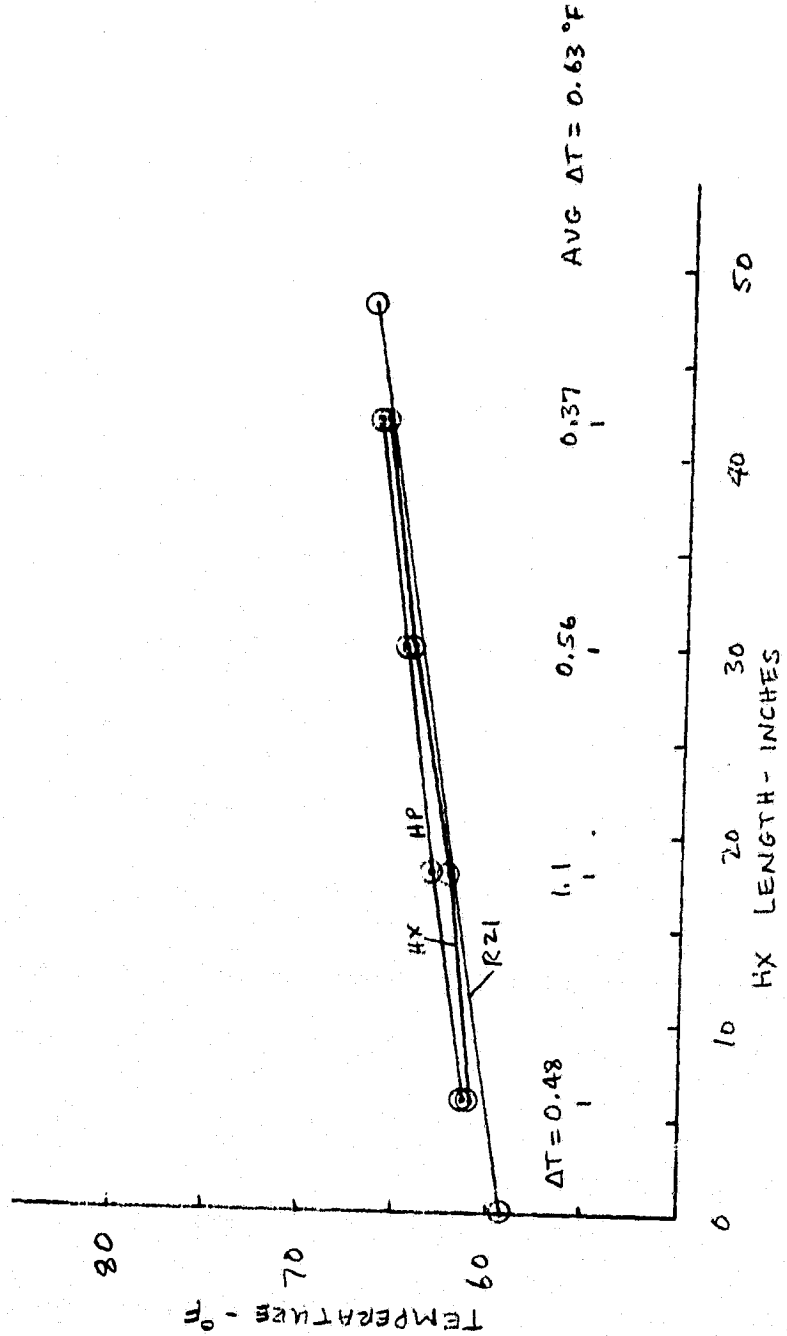
ORIGINAL PAGE IS
OF POOR QUALITY

TP 2
 $P = 502.958$ watts
 $\dot{m} = 1018.33$ lb/hr
 $P.D. = 113.112$ psig
 $U_{AVG} = 967.29$ BTU/HR FT² °F



ORIGINAL PAGE IS
OF POOR QUALITY

TP 3
 $P = 502.88$ watts
 $\dot{m} = 980.617$ lb/hr
 $P.D. = 203.519$ psig
 $U_{AVG} = 1918.93$ BTU/HRT²°F



ORIGINAL PAGE 19
OF POOR QUALITY

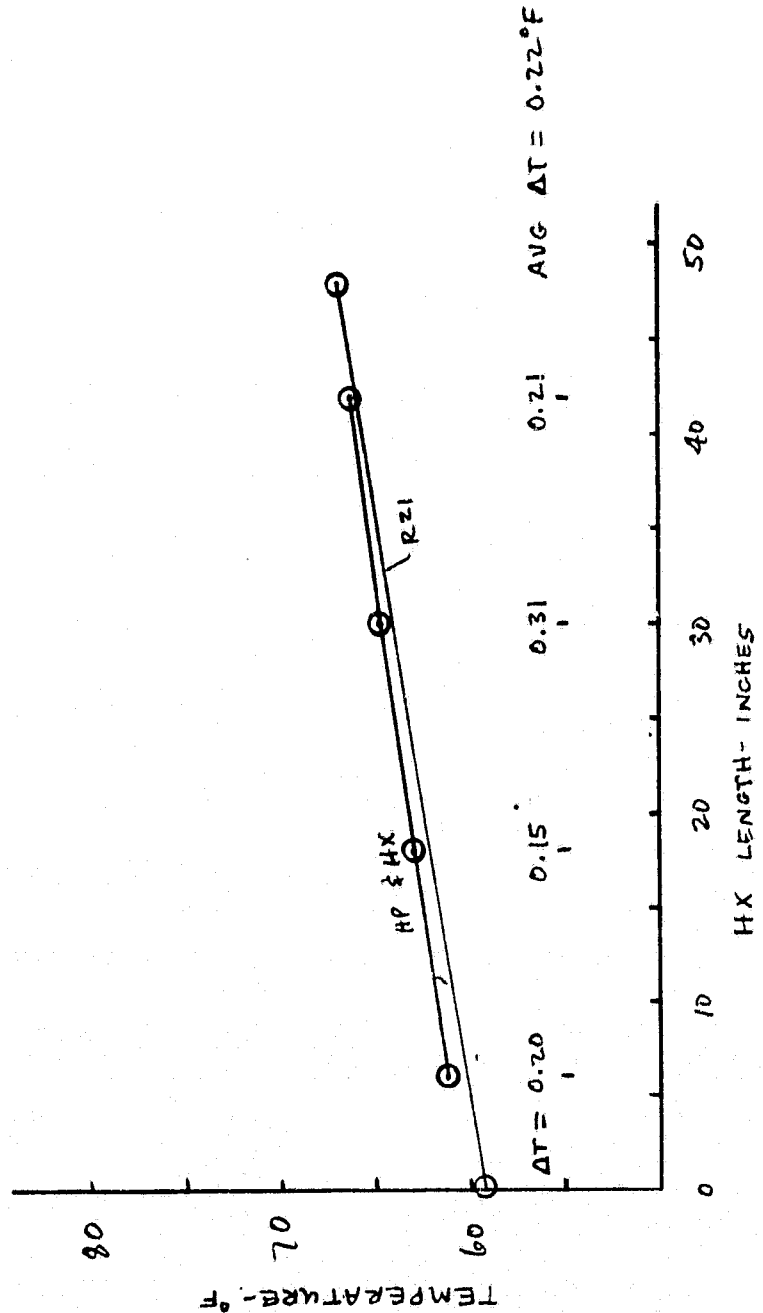
TP 4

$P = 502.943$ WATTS

$\dot{W} = 997.411$ LB/MR

P.D. 305.956 PSIG

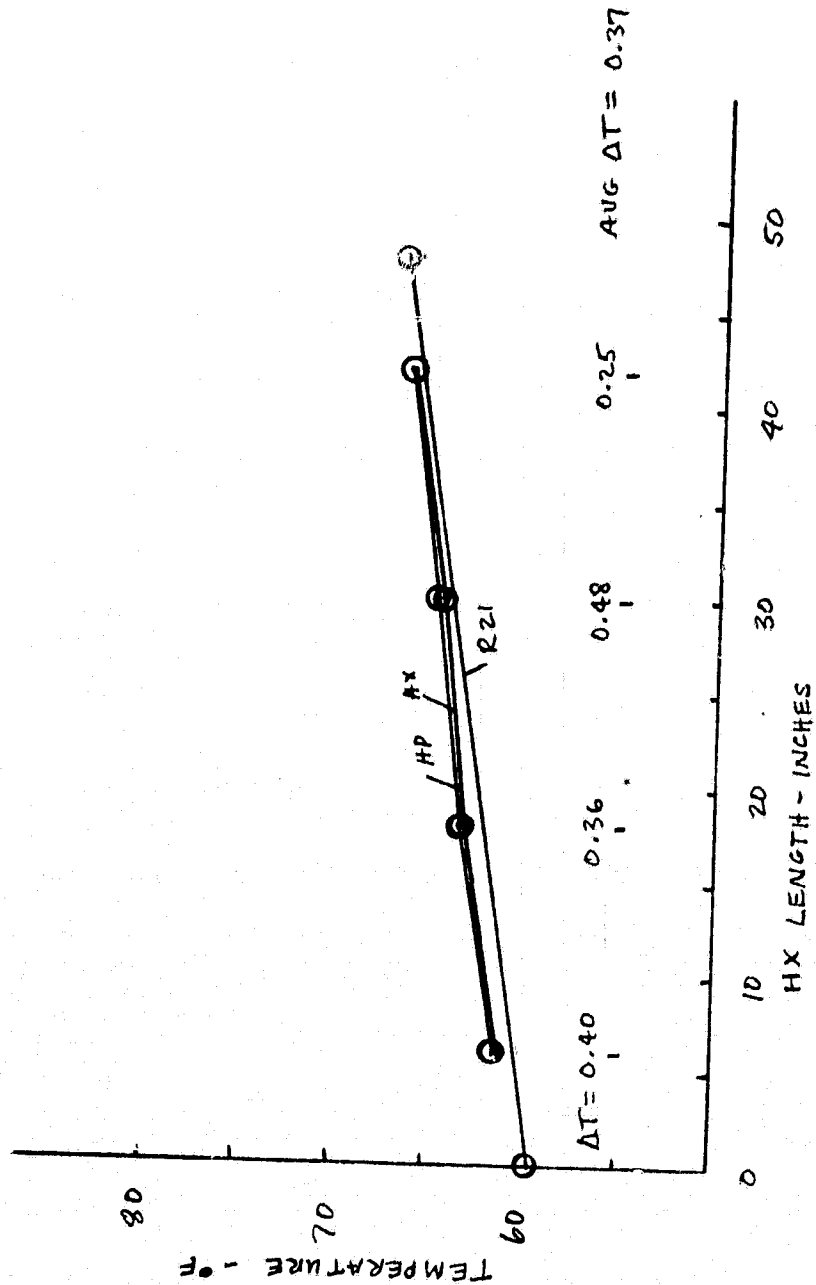
$U_{AVE} = 5495.79$ BTU/HR FT² °F



ORIGINAL PAGE IS
OF POOR QUALITY

TP 5

$P = 503.081$ WATTS
 $\dot{W} = 982.869$ LB/Hr
 $P.D. = 201.584$ PSIG
 $U_{avg} = 3268.67$ BTU/HrFt²°F



ORIGINAL PAGE IS
OF POOR QUALITY

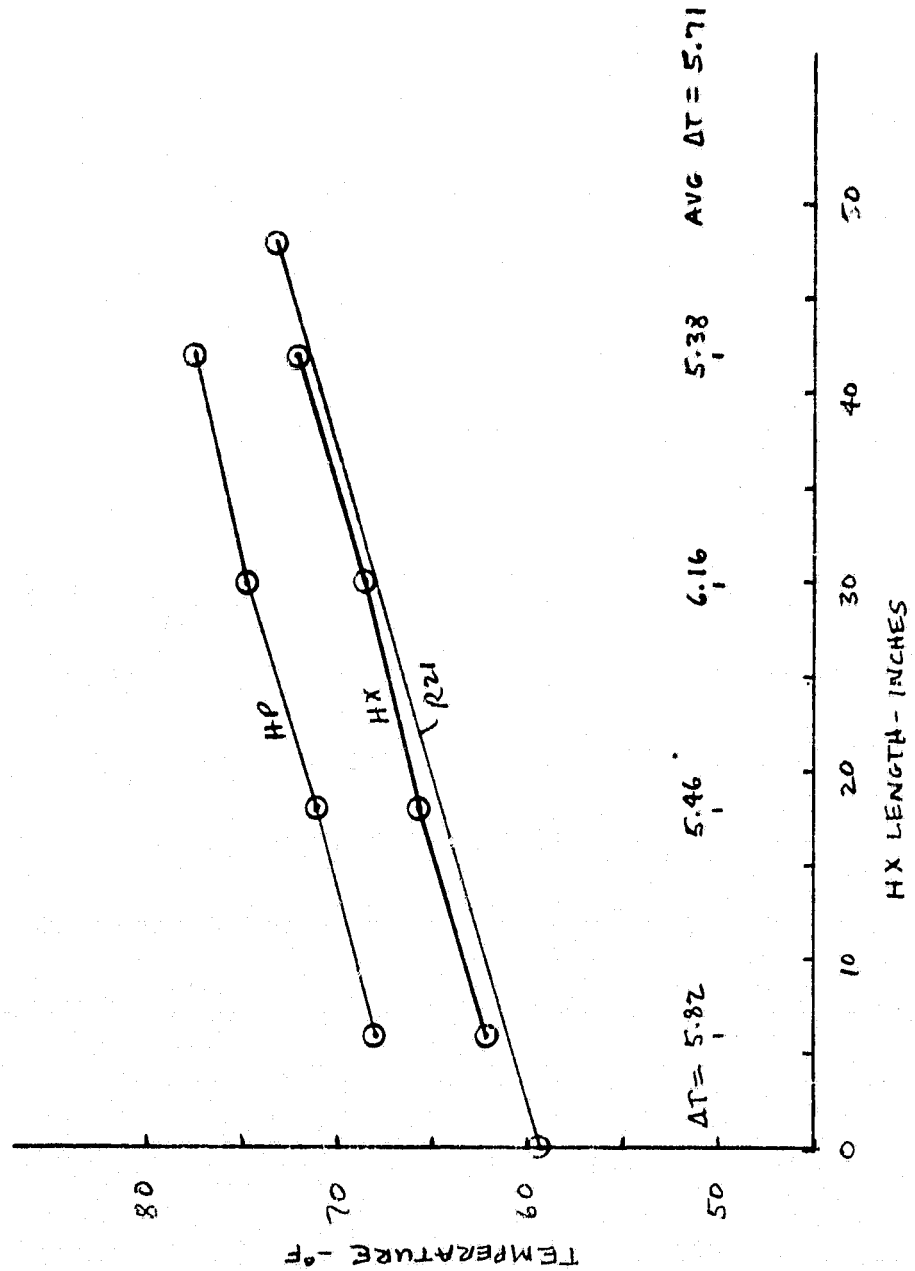
TP 6

$P = 993.111$ WATTS

$\dot{W} = 990.632$ LB/HR

P.D. = 50.7482 PSIG

$U_{AVG} = 418.12$ BTU/HR FT² °F



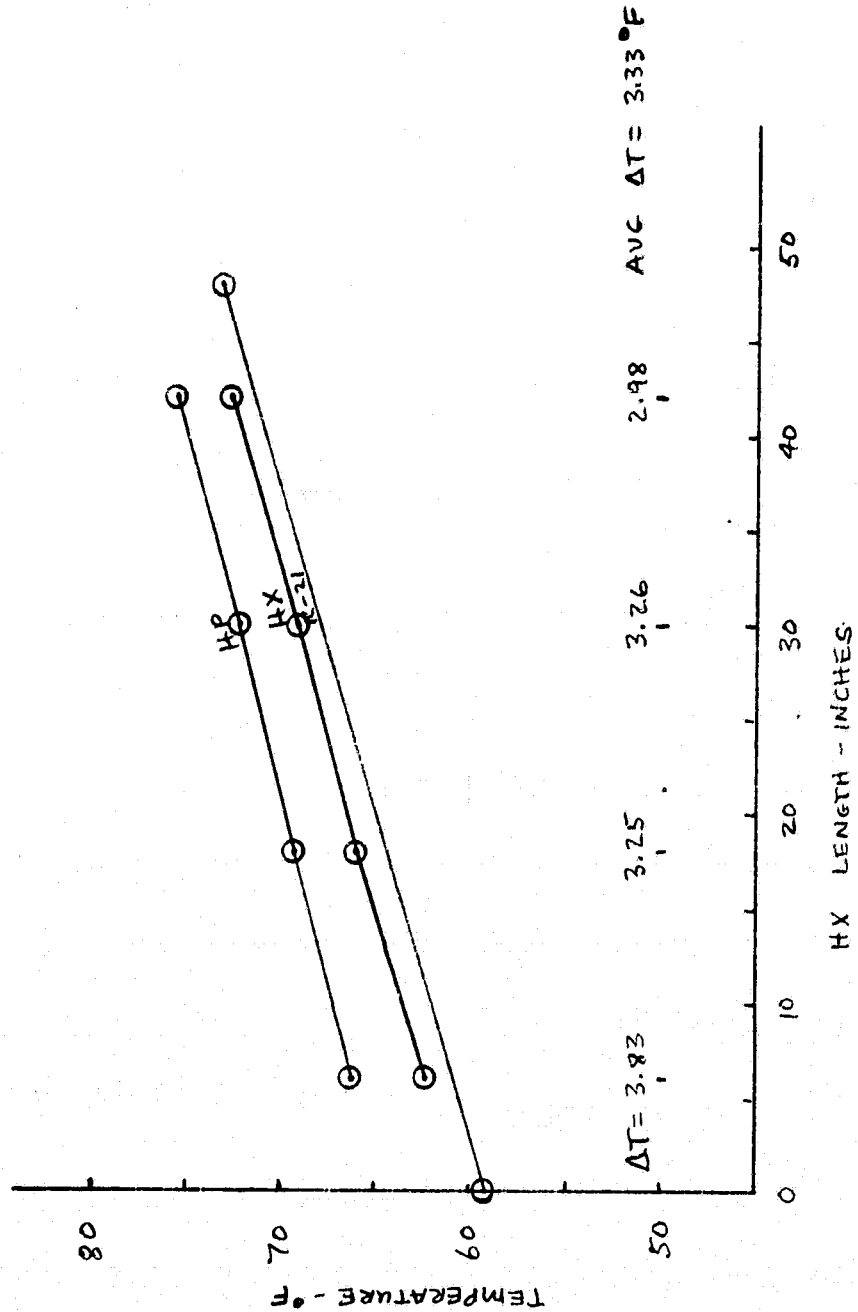
TP 7

$P = 993.461$ WATTS

$\dot{w} = 1020.49$ LB/HR

P.D. = 99.88 PSIG

$U_{AVG} = 717.20$ BTU/HR FT² °F



ORIGINAL PAGE IS
OF POOR QUALITY

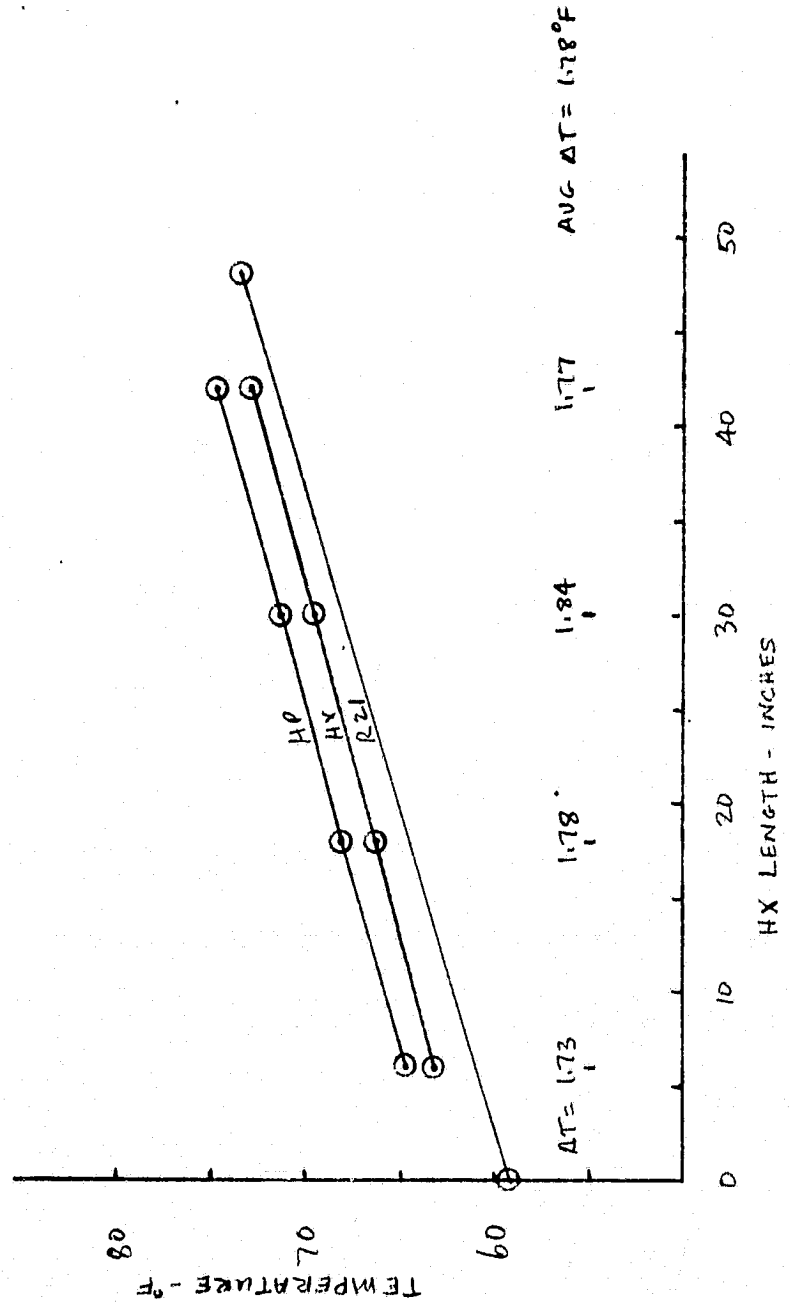
TP 8

$P = 994.032 \text{ WATTS}$

$\dot{W} = 1007.56 \text{ lb/hr}$

$P.D. = 199.822 \text{ psig}$

$U_{AVE} = 1342.5 \text{ BTU/hr ft}^2 \text{ } ^\circ\text{F}$



ORIGINAL PAGE IS
OF POOR QUALITY

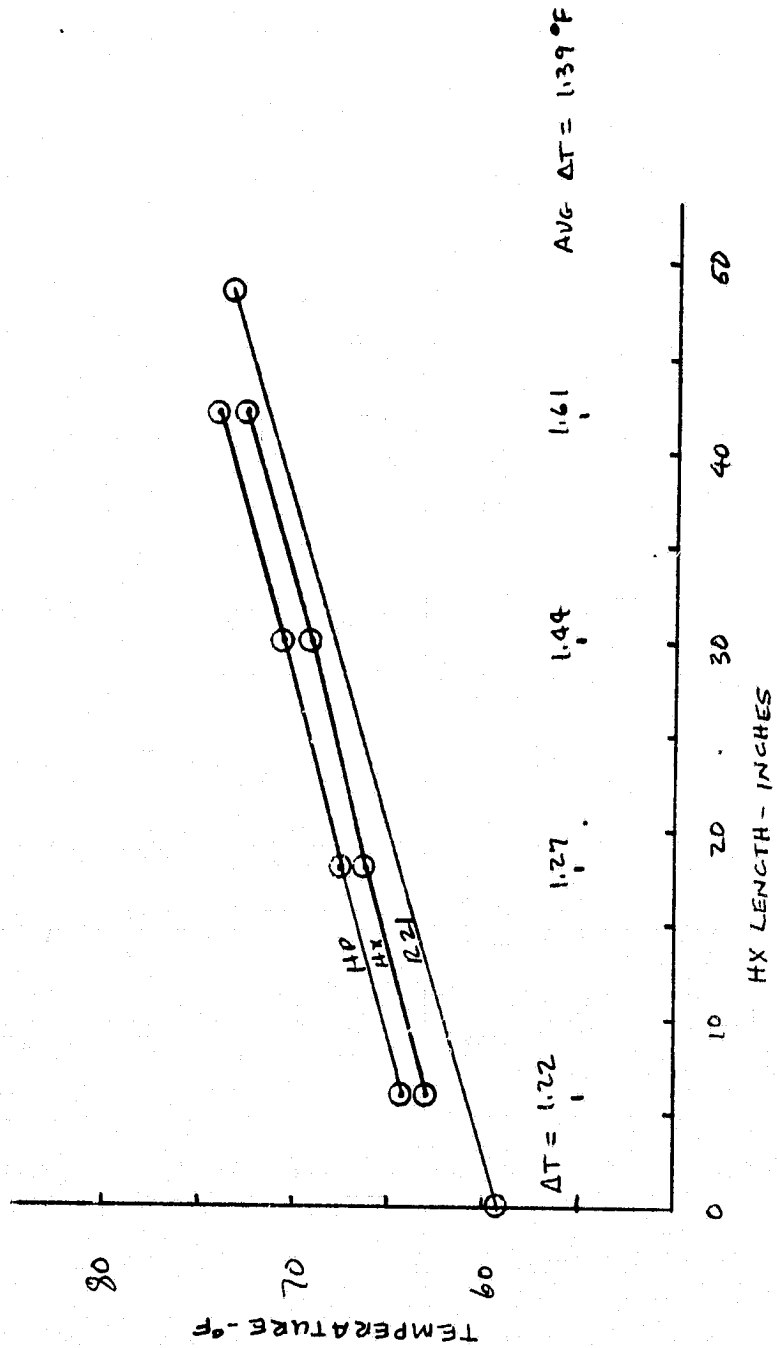
TP 9

$P = 994.869$ WATTS

$\dot{m} = 991.677$ LB/HR

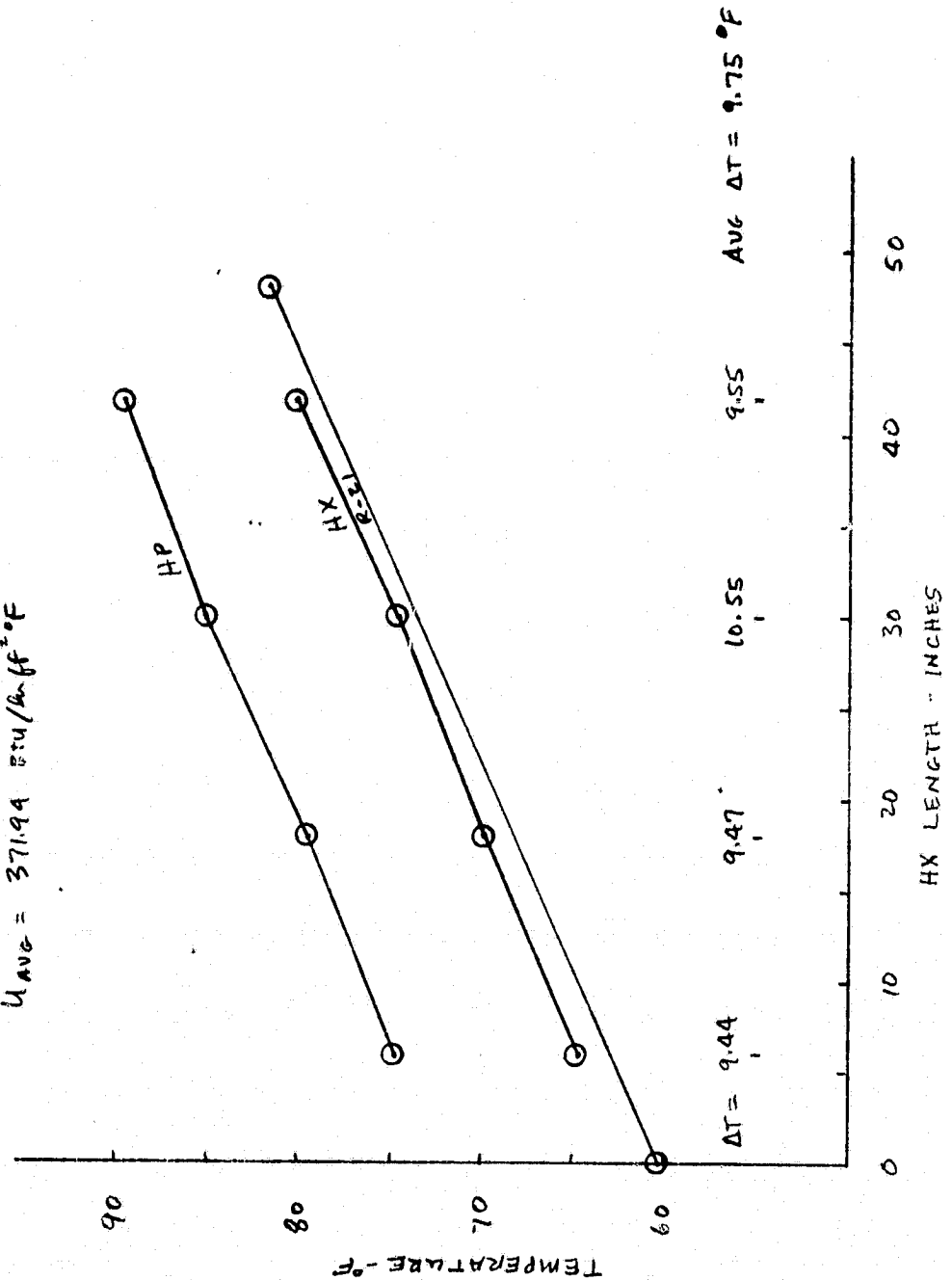
P.D. = 299.414 PSIG

$U_{avg} = 1720.52$ BTU/HR FT² °F



ORIGINAL PAGE IS
OF POOR QUALITY

TP 10
 $P = 1508.48 \text{ watts}$
 $\dot{m} = 985.6 \text{ lb/hr.}$
 $P.D. = 50.5 \text{ psig}$
 $U_{AVE} = 371.94 \text{ BTU/hr.ft}^2\text{.}^\circ\text{F}$



ORIGINAL PAGE IS
OF POOR QUALITY

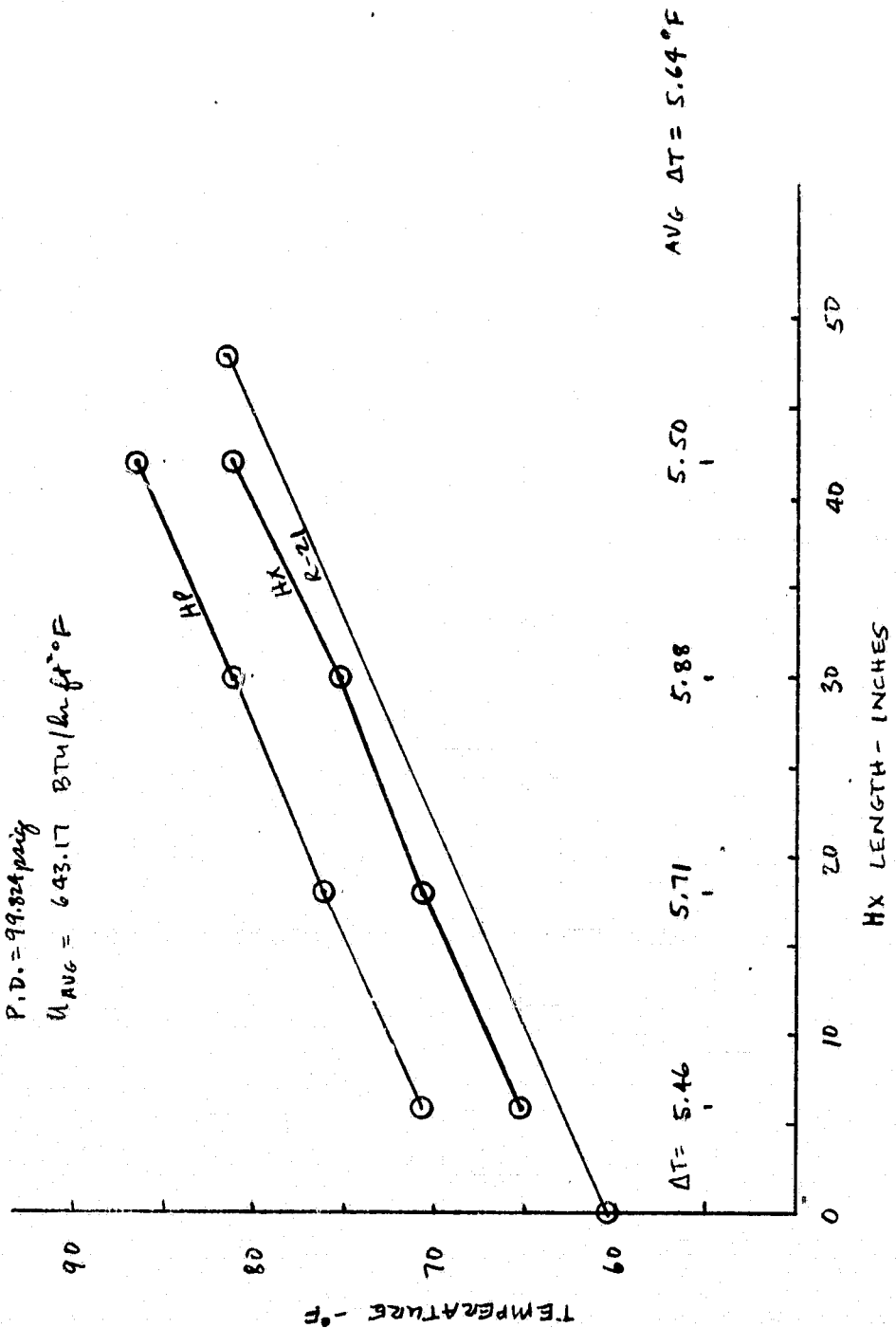
TP 11:

$P = 1508.94$ watts

$\dot{m} = 976.905$ lb/lb.

$P.D. = 99.824$ psig

$u_{AVG} = 643.17$ BTU/lb ft² °F



ORIGINAL PAGE 19
OF POOR QUALITY

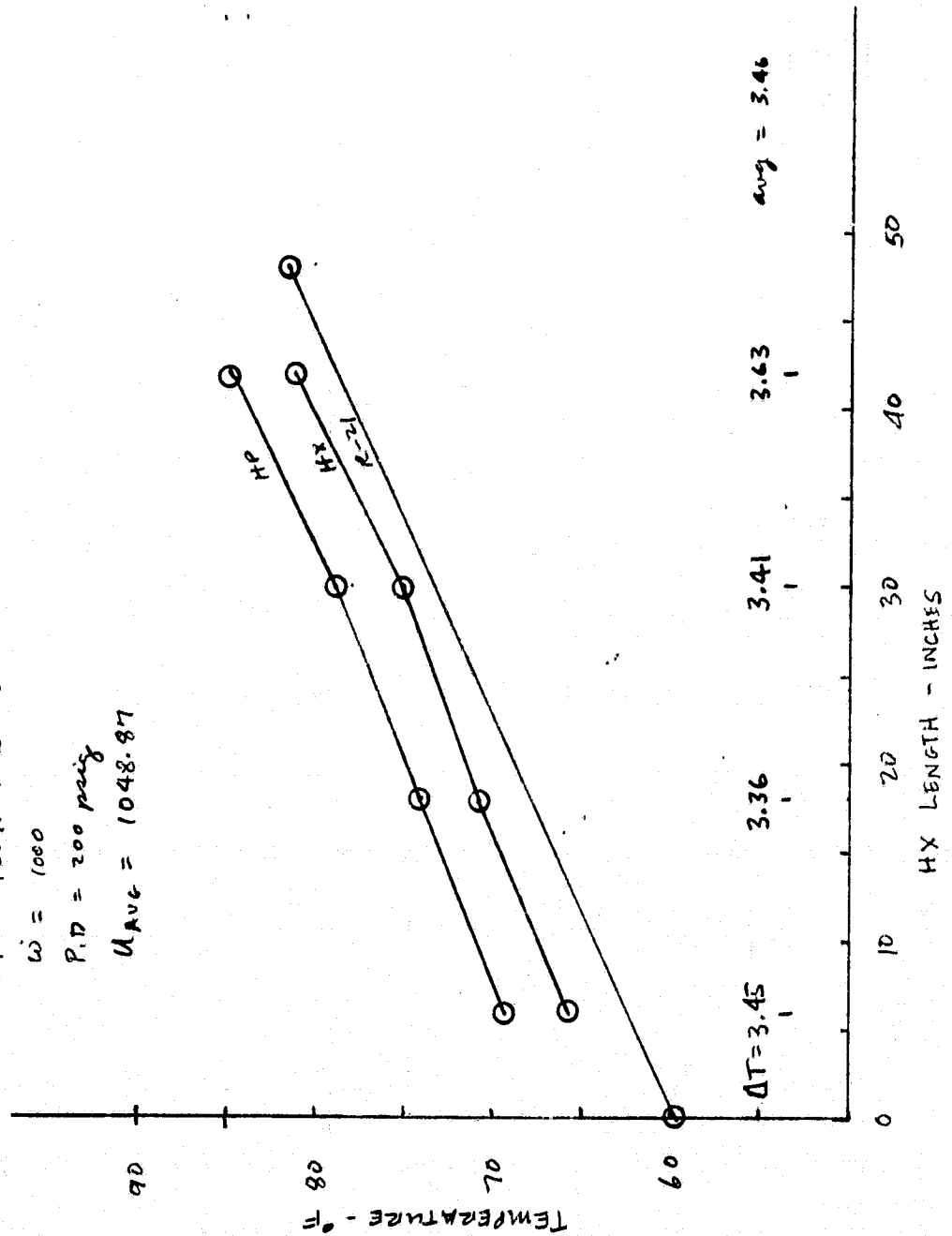
TP 12

$P = 1509.61 \text{ watts}$

$\dot{m} = 1000$

$P.D. = 200 \text{ psig}$

$U_{AVE} = 1048.87$



$$U_{AVE} = \frac{1509.61 (2.000)}{3.46} = 1048.87$$

$U_{AVE} =$

$avg = 3.46$

3.63

3.41

3.36

3.45

$\Delta T = 3.45$

TEST DATA REDUCTION EXAMPLE

TP 13

POWER = 1509.63 WATTS

FLOW = 774.5 LB/HR

DIAPHRAGM PRESS = 299.12 PSIG

$$\text{CONTACT AREA} = 48 [\pi (1.57) - 3 (2.25)]$$

$$= 203.9 \text{ IN}^2$$

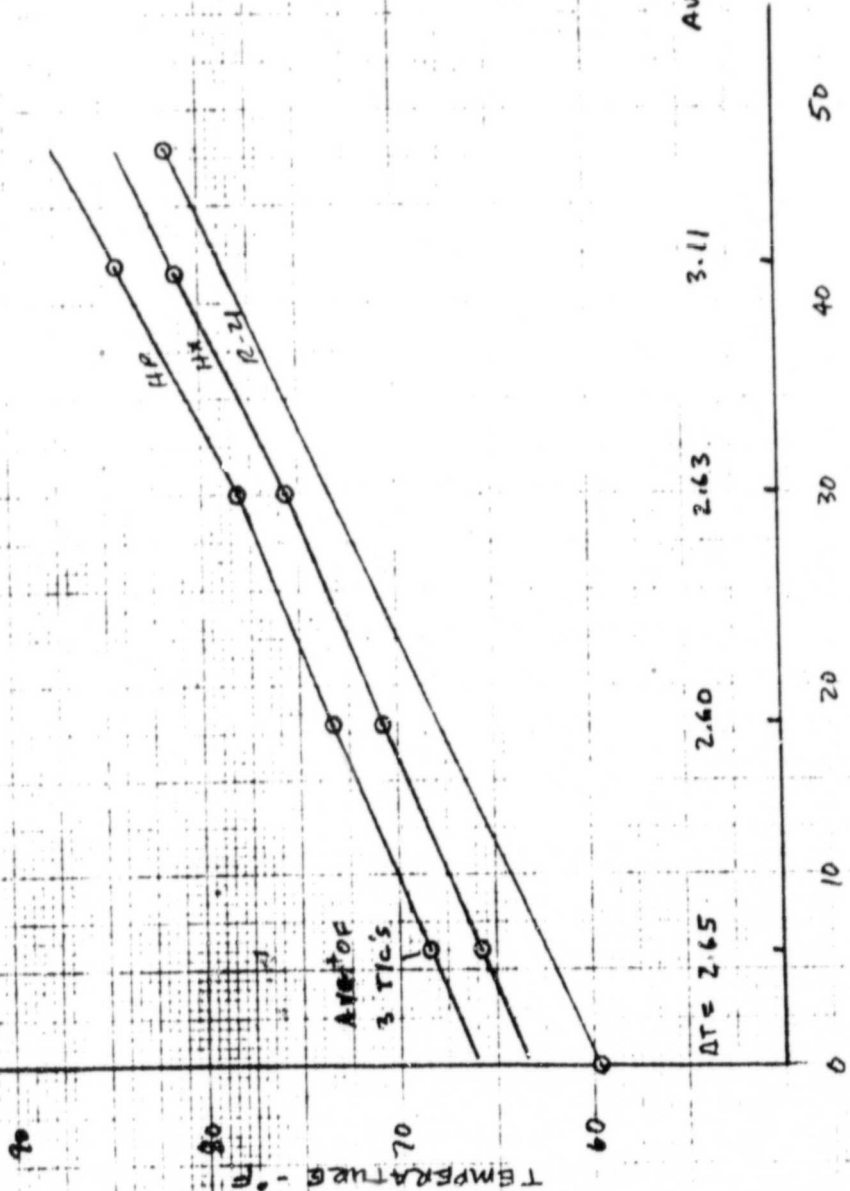
$$= 1.42 \text{ FT}^2$$

$$U_{\text{CONTACT}} = \frac{Q}{A \Delta T}$$

$$= \frac{1509.63 (3.413)}{1.42 (2.75)}$$

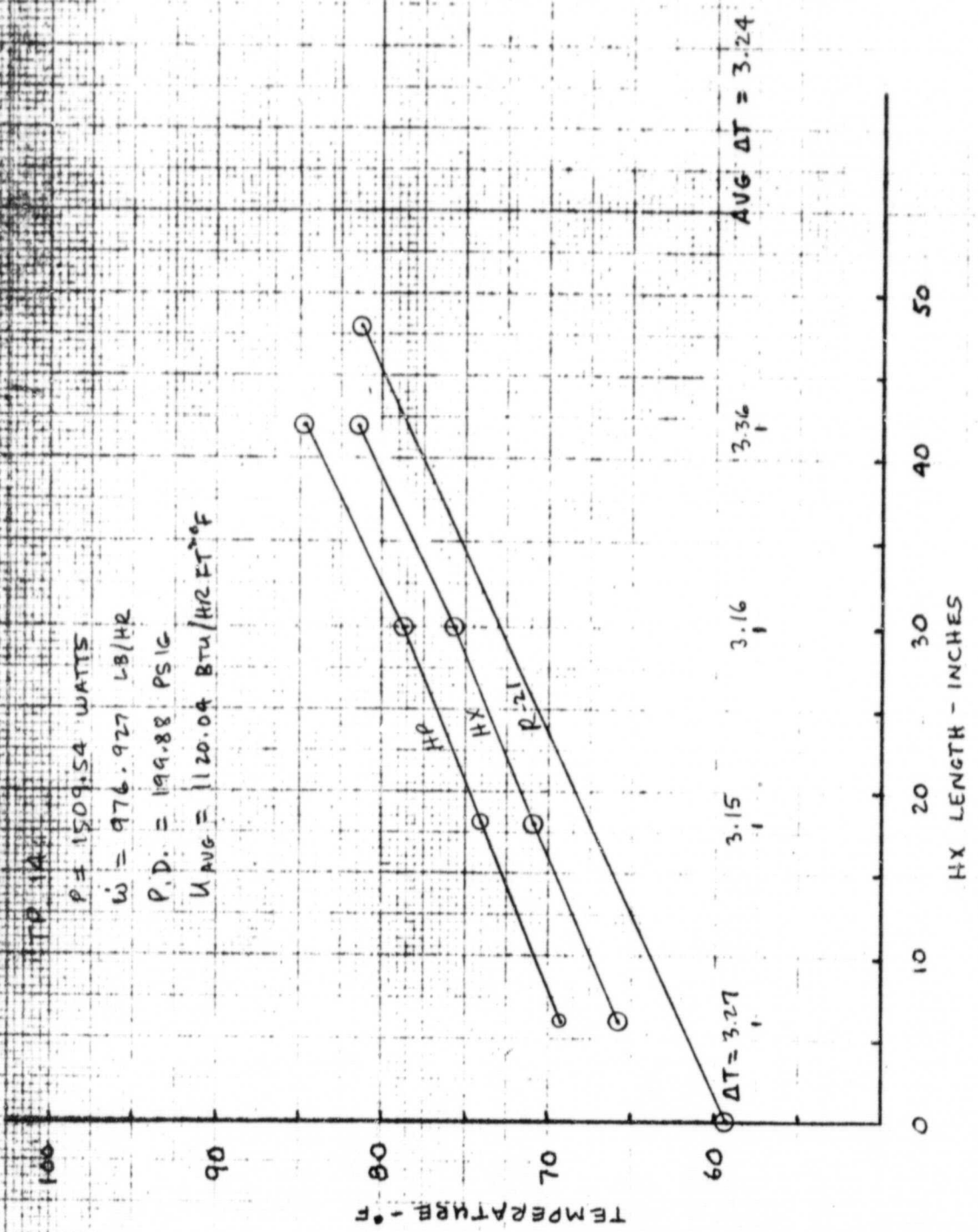
$$= 1319.81 \text{ BTU/HR FT}^2 \text{ } ^\circ\text{F}$$

ORIGINAL PAGE 19
OF POOR QUALITY

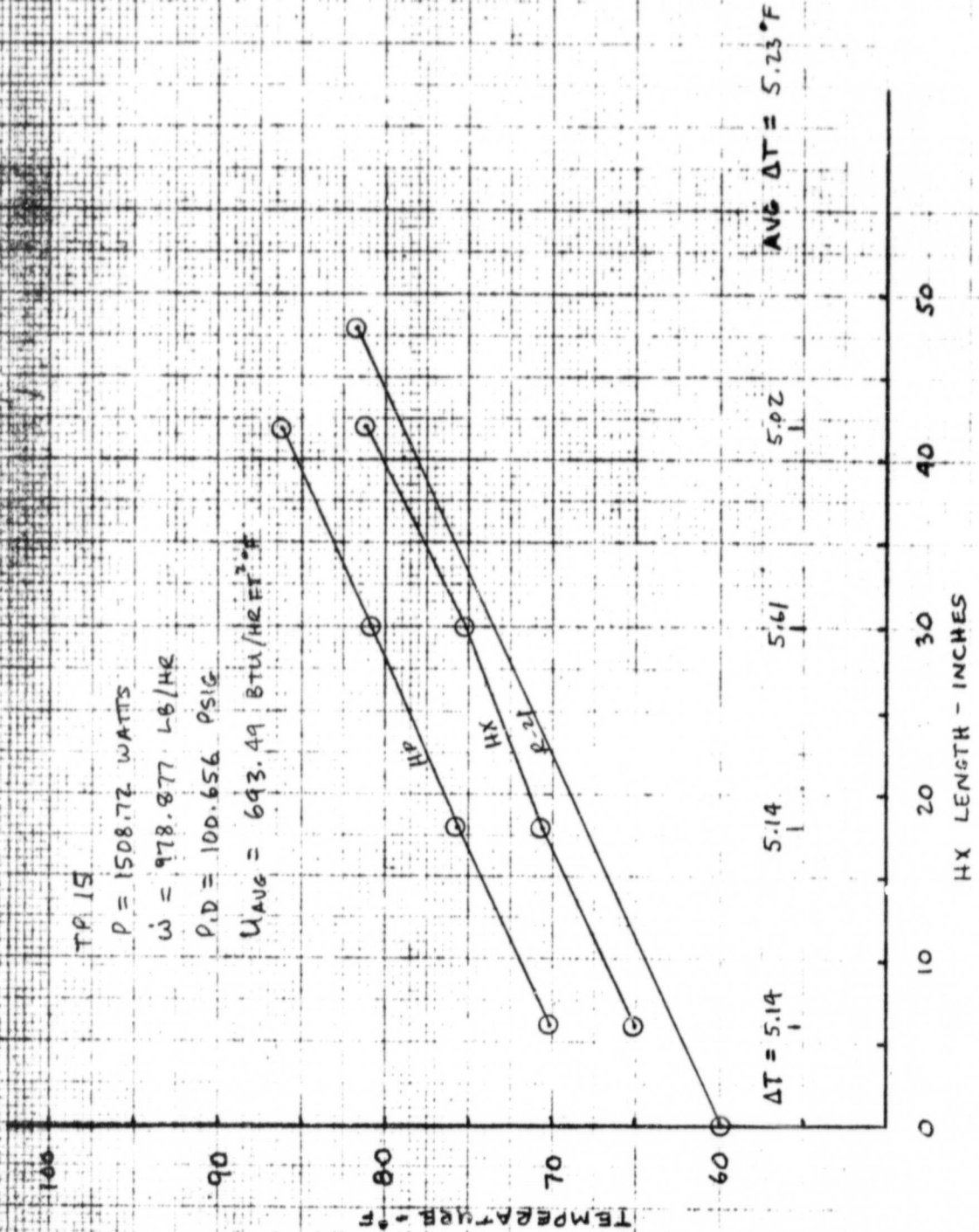


VOUGHT

$P = 1509.54 \text{ WATTS}$
 $\dot{W} = 976.927 \text{ LB/HR}$
 $P.D. = 199.88 \text{ PSIG}$
 $U_{\text{AVG}} = 1120.09 \text{ BTU/HR FT}^2 \text{ } ^\circ\text{F}$

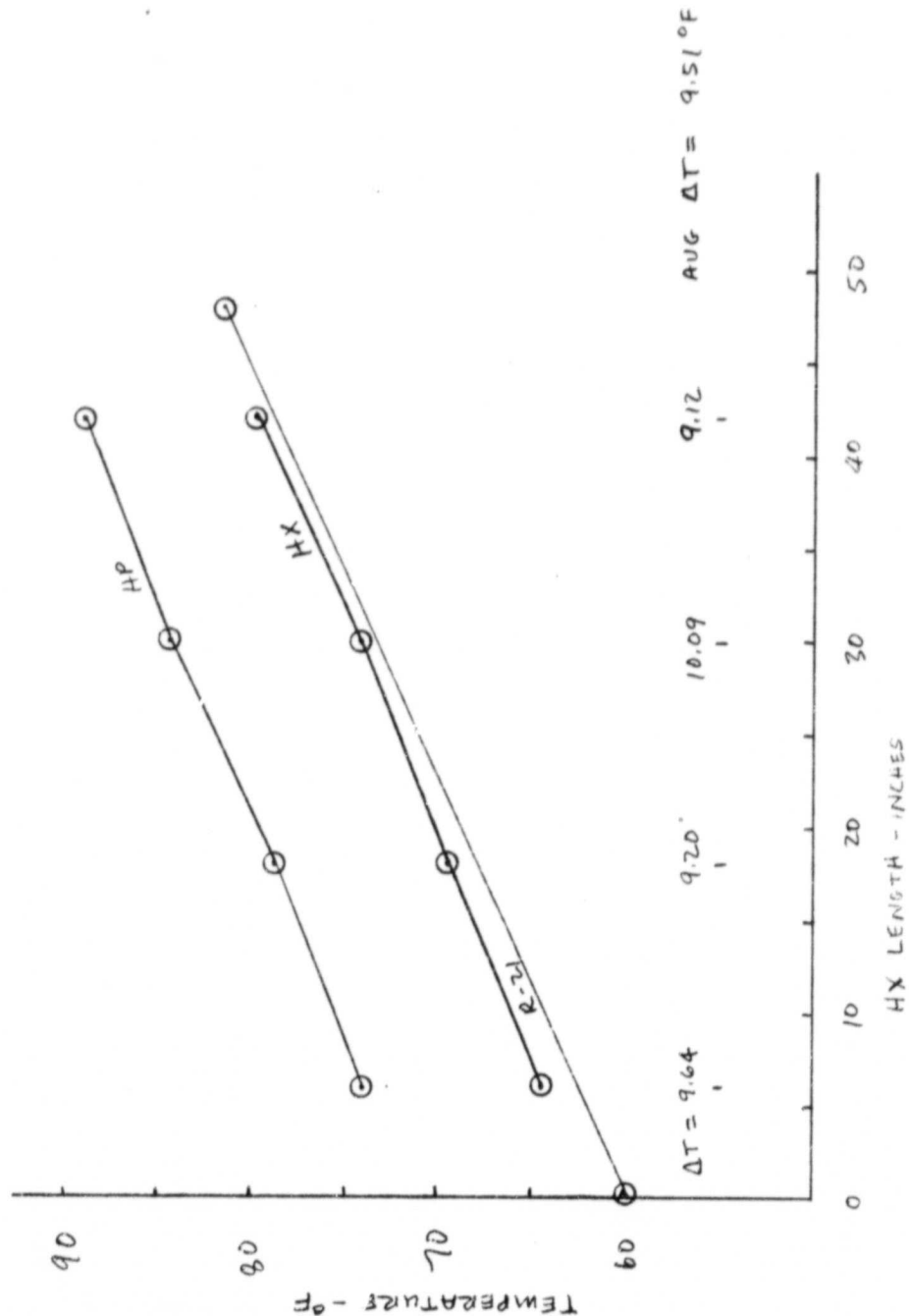


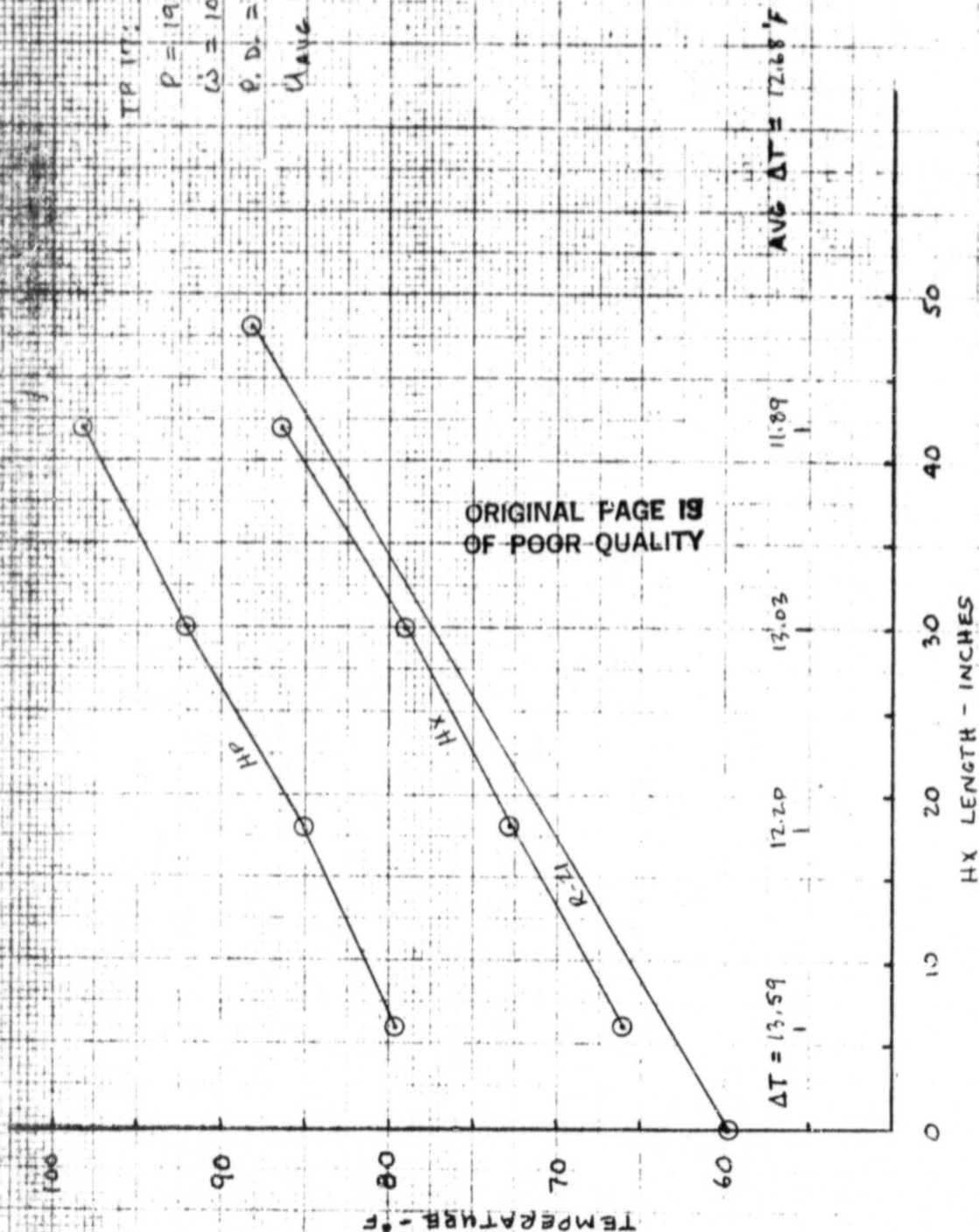
ORIGINAL PAGE IS
OF POOR QUALITY



ORIGINAL PAGE IS
OF POOR QUALITY

TP 16
 $P = 1508.08$ watts
 $\dot{m} = 993.767$ lb/hr
 $P.D. = 50.5914$ psig
 $U_{avg} = 381.22$ BTU/hr ft² °F





ORIGINAL PAGE 19
OF POOR QUALITY

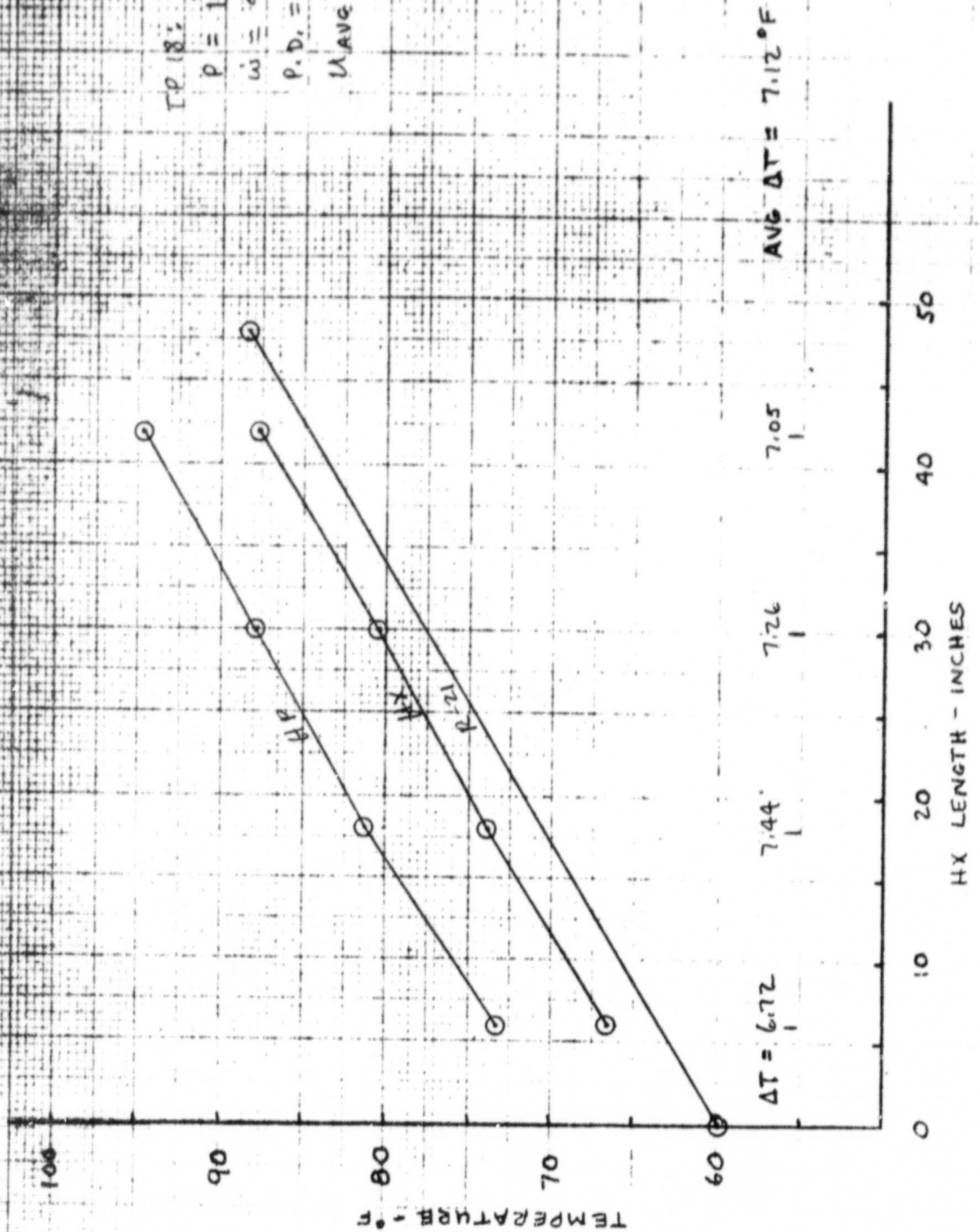
TP 18:

$P = 1991.19$ WATTS

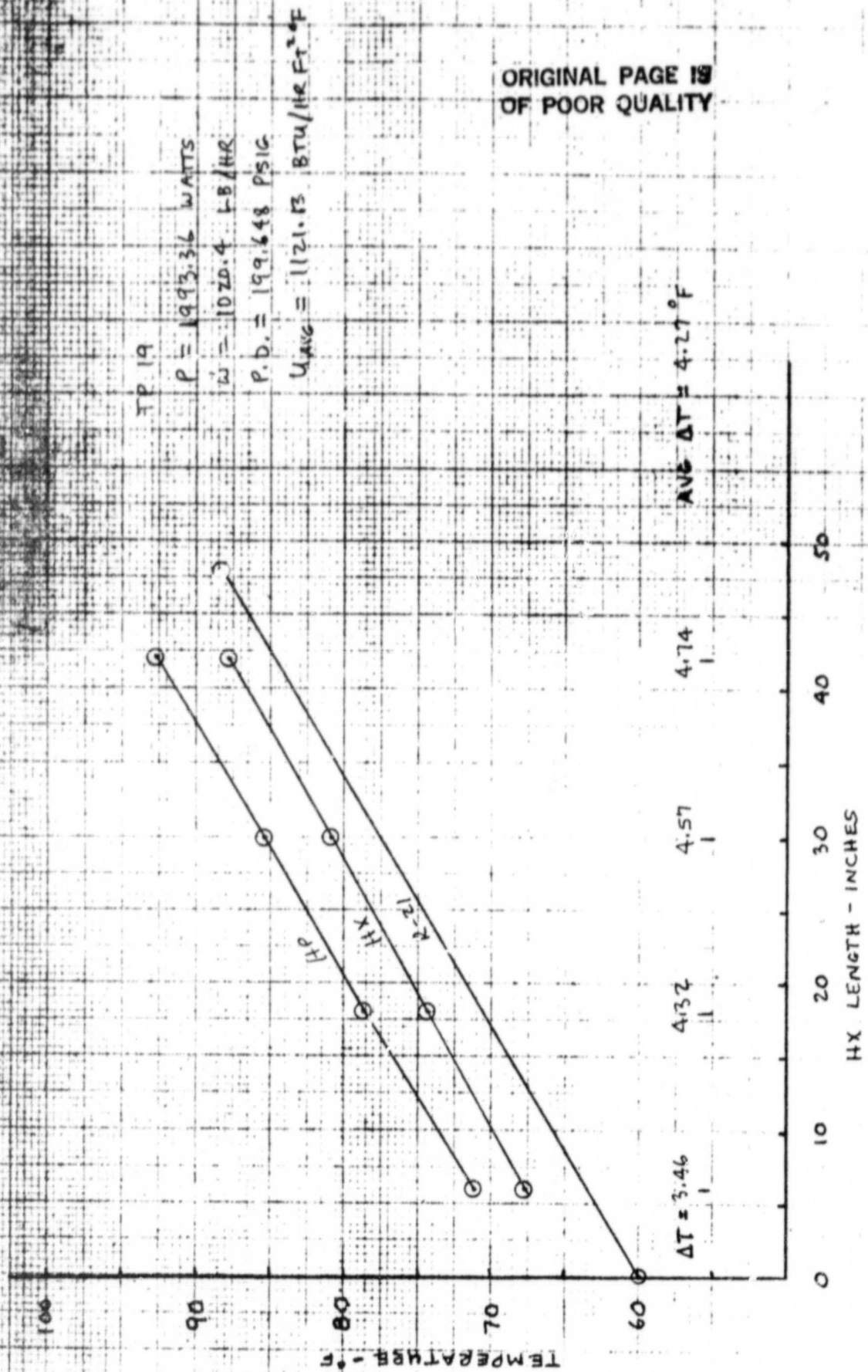
$\dot{m} = 974.003$ LB/HR

$P.D. = 100.153$ PSIG

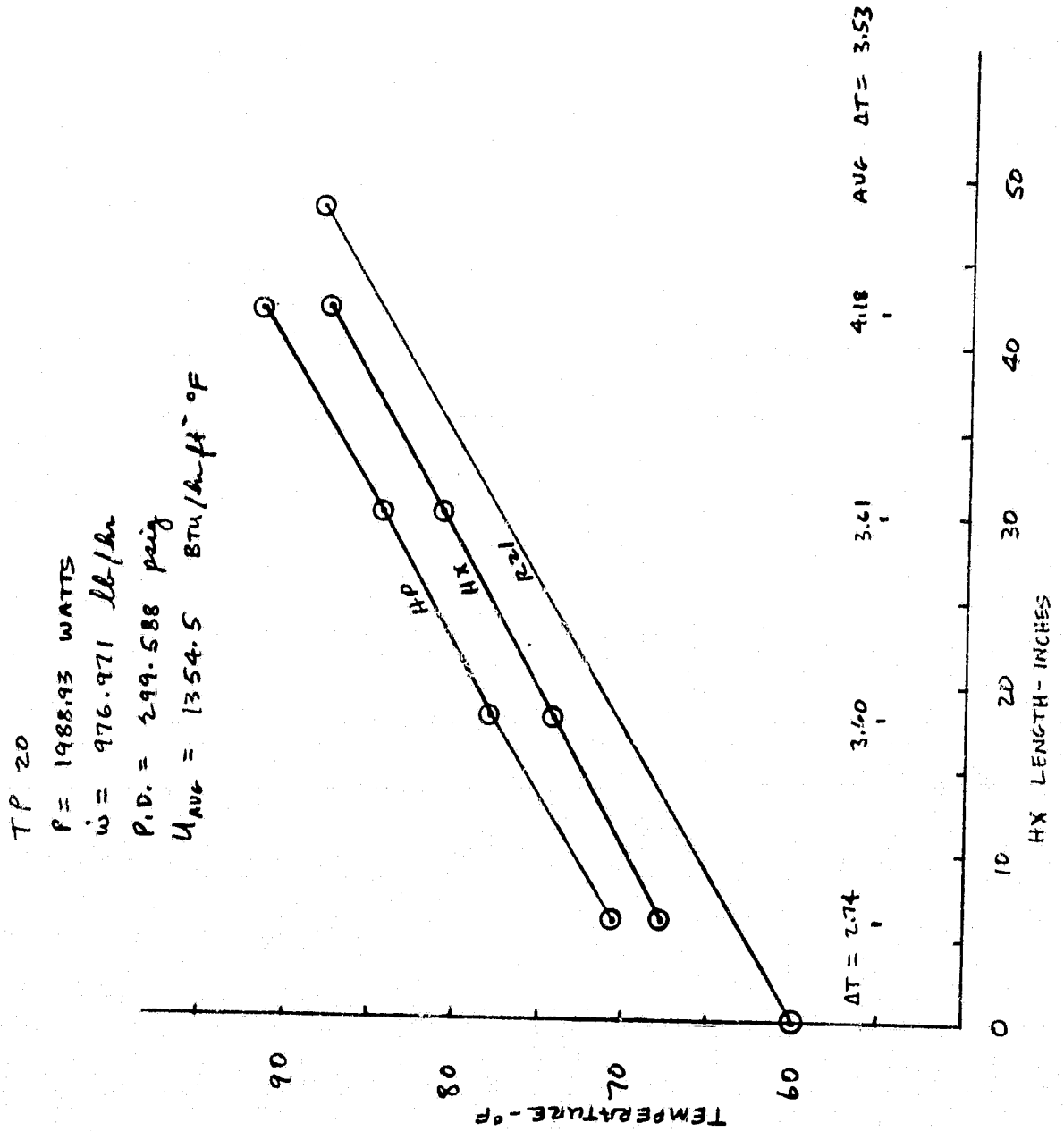
$U_{AVE} = 6.72, 31$ BTU/HR FT² °F



ORIGINAL PAGE 19
OF POOR QUALITY



ORIGINAL PAGE 18
OF POOR QUALITY



ORIGINAL PAGE IS
OF POOR QUALITY

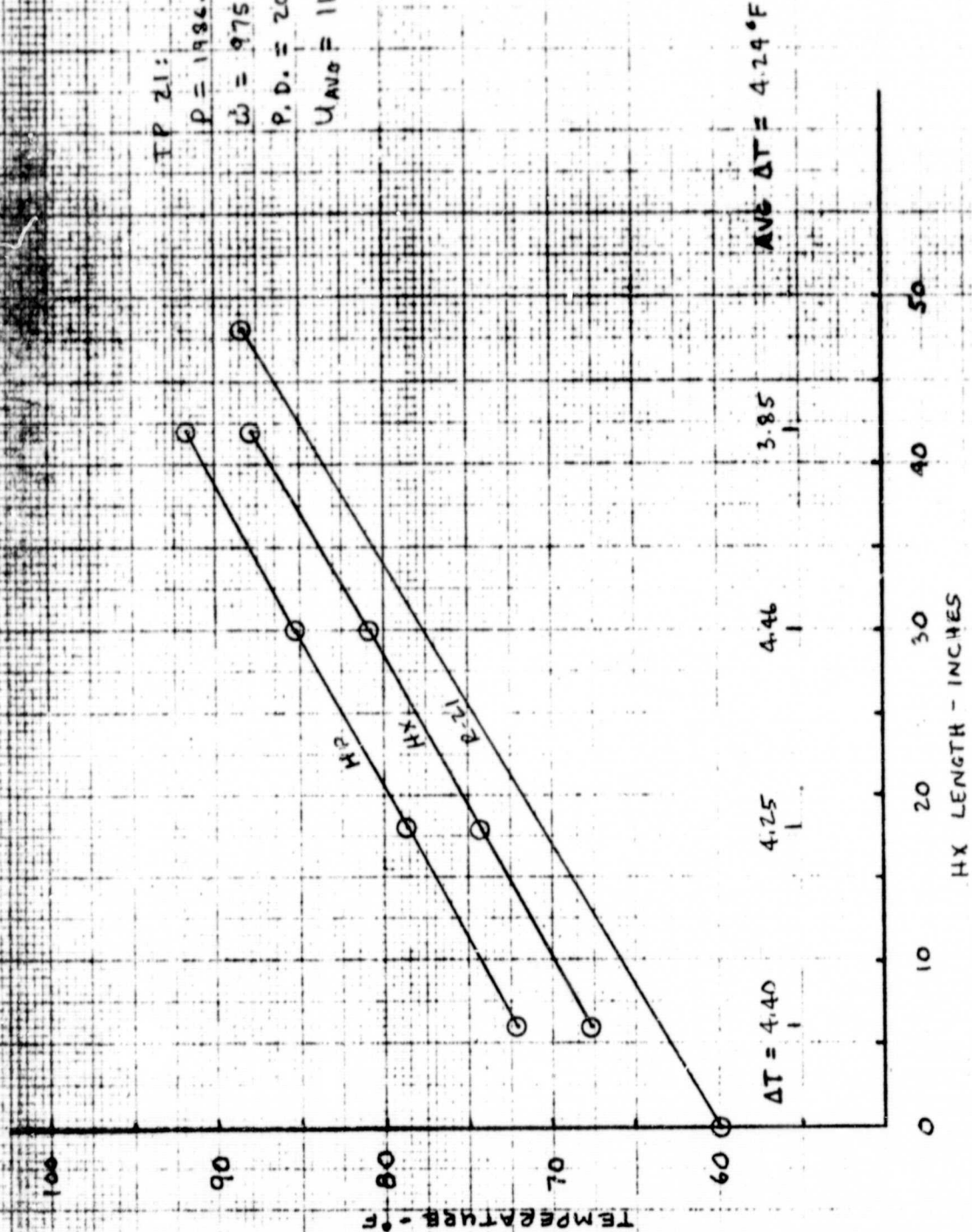
TP 21:

$P = 1986.13 \text{ WATTS}$

$\dot{W} = 975.439 \text{ LB/HR}$

$P.D. = 200.151 \text{ PSIG}$

$U_{AVG} = 1126.10 \text{ BTU/HR FT}^2 \text{ } ^\circ\text{F}$



TP 221

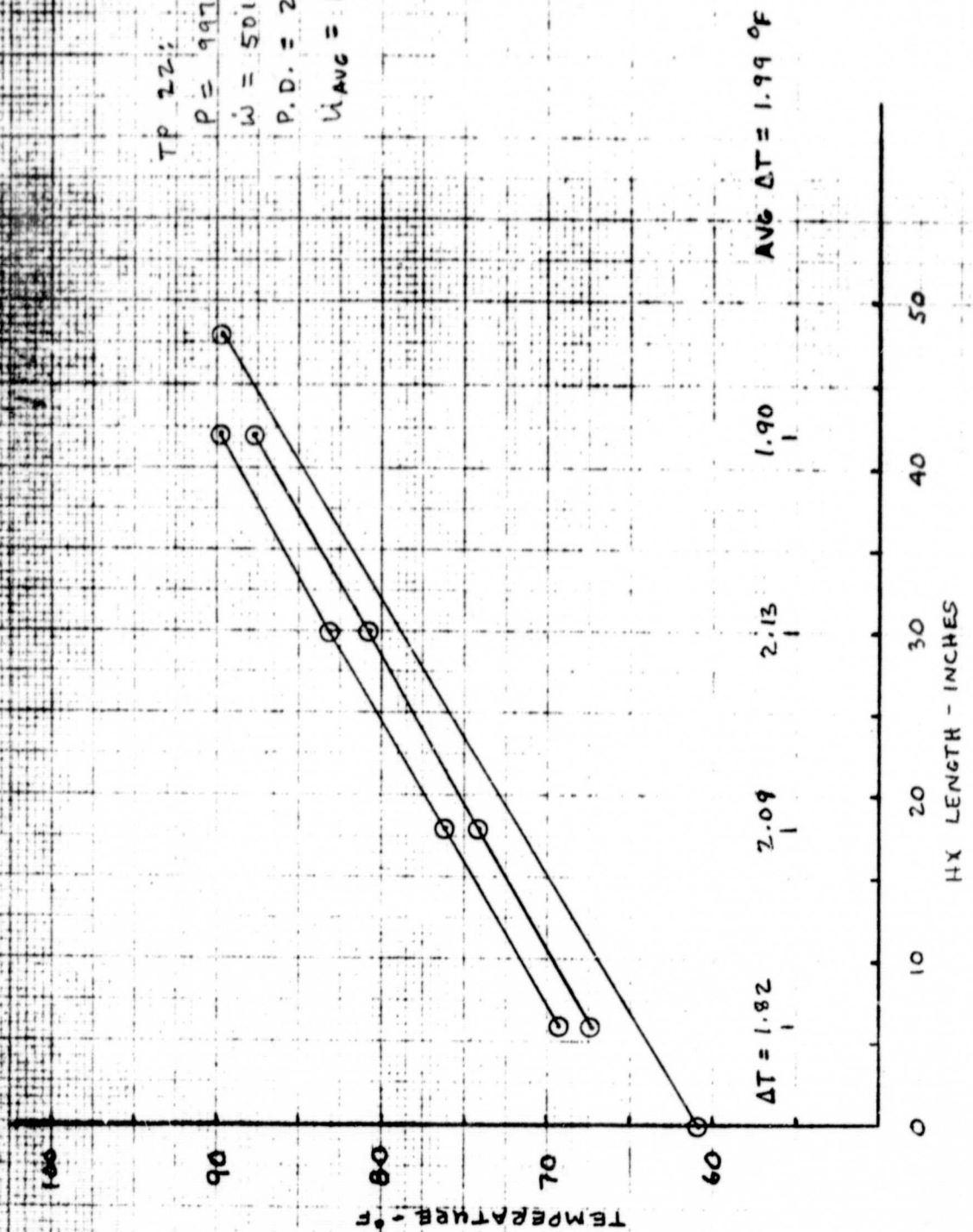
P = 997.385 WATTS

$\dot{W} = 501.083 \text{ LB/HR}$

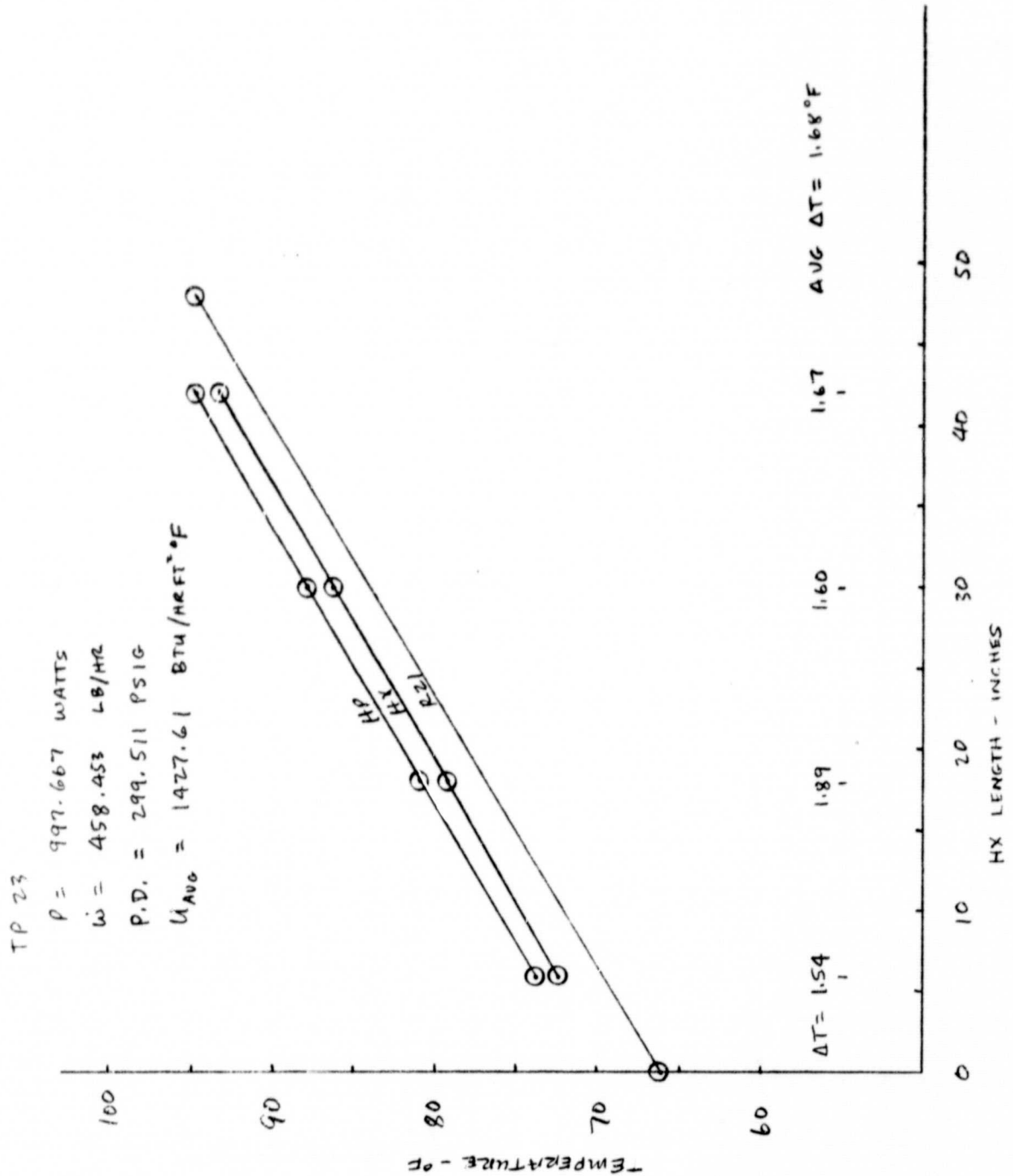
P.D. = 200.287 PSIG

$U_{AVG} = 1204.88 \text{ BTU/HR FT}^2 \text{ } ^\circ\text{F}$

ORIGINAL PAGE IS
OF POOR QUALITY



ORIGINAL PAGE 18
OF POOR QUALITY



ORIGINAL PAGE 13
OF POOR QUALITY

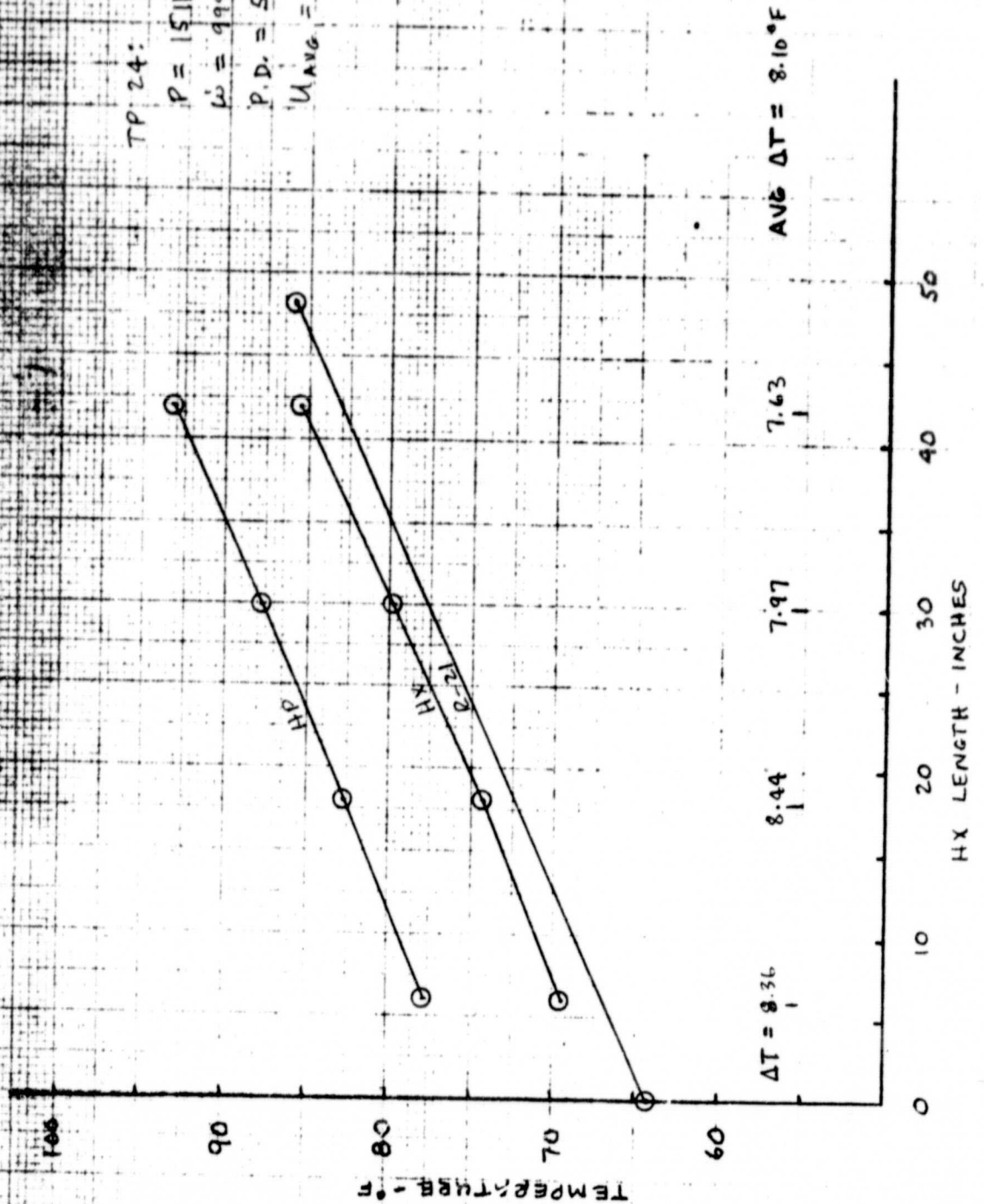
TP 24:

$P = 1511.53$ WATTS

$\dot{m} = 999.977$ LB/HR

P.D. = 50.5205 PSIG

$U_{avg} = 448.61$ BTU/HR FT² °F



ORIGINAL PAGE IS
OF POOR QUALITY

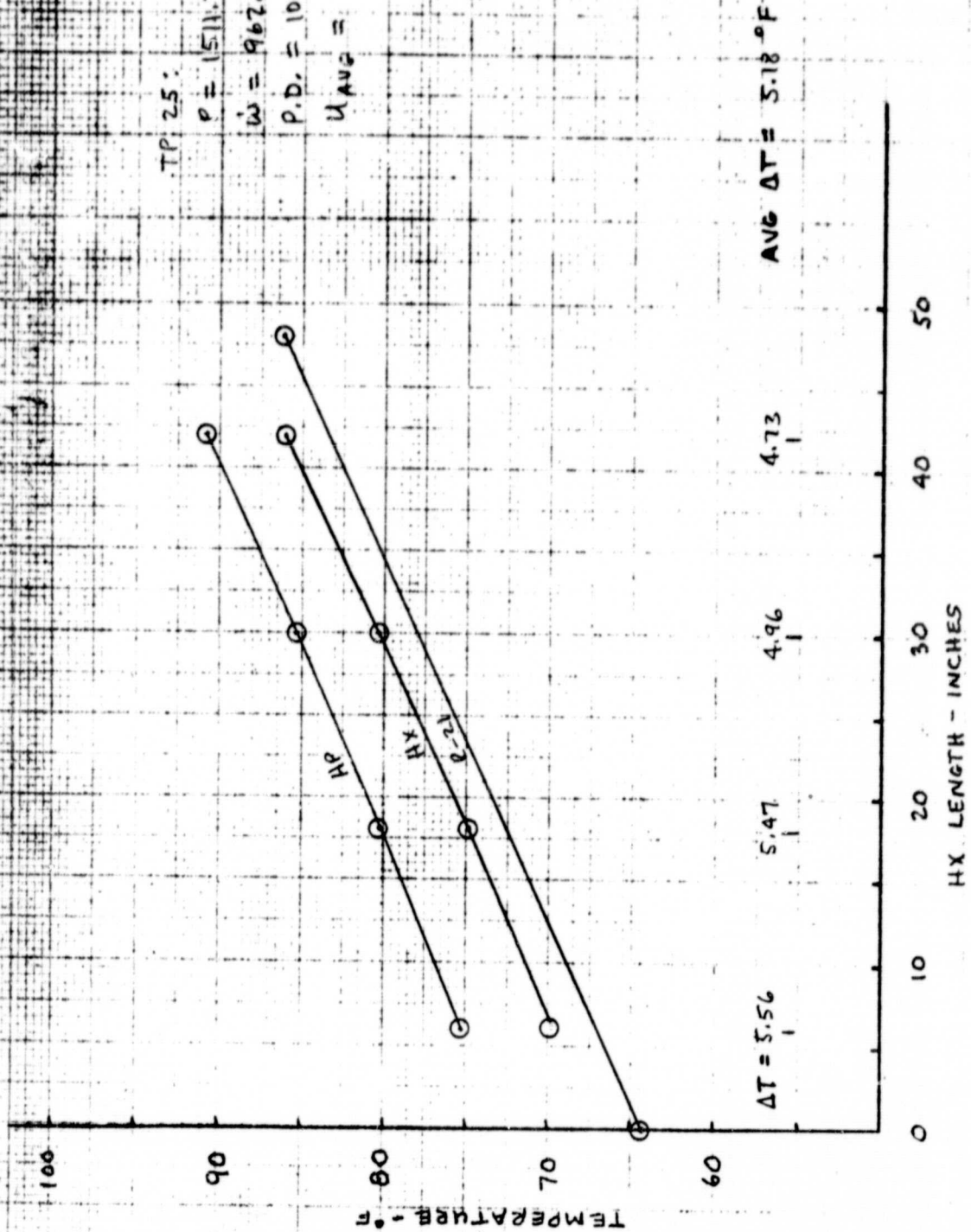
TP 25:

$P = 1511.39$ WATTS

$\dot{W} = 962.03$ LB/HR

P.D. = 100.347 PSIG

$U_{AVG} = 701.43$ BTU/HR FT² °F



ORIGINAL PAGE IS
OF POOR QUALITY

TP 26:

$P = 1510.98$ WATTS

$\dot{W} = 1000.25$ LB/HR

P.D. = 199.551 PSIG

$U_{AVE} = 987.06$ BTU/HR FT² OF

AVE $\Delta T = 3.68^\circ F$

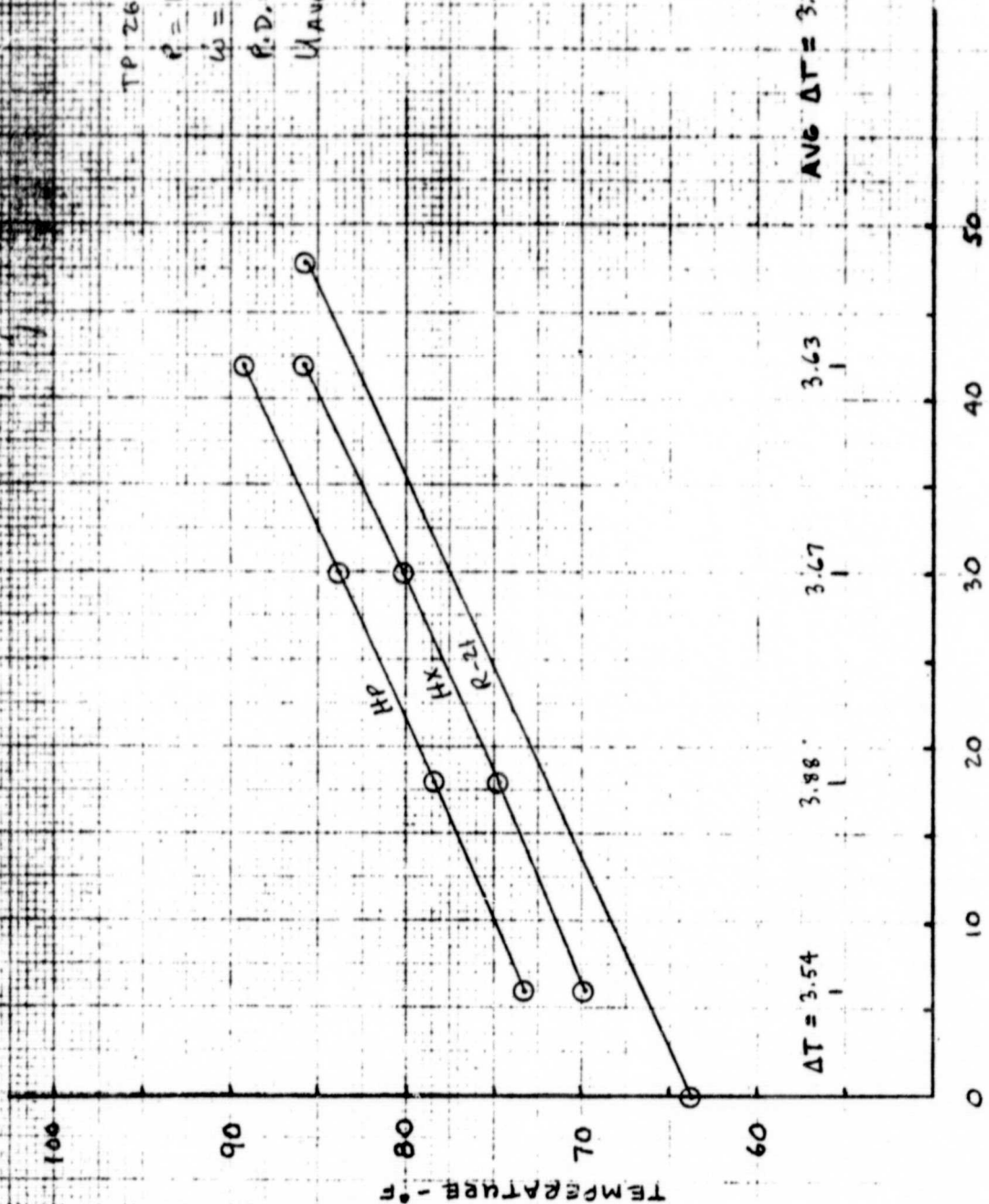
3.63

3.67

3.88

$\Delta T = 3.54$

HX LENGTH - INCHES



ORIGINAL PAGE IS
OF POOR QUALITY

TP 27:

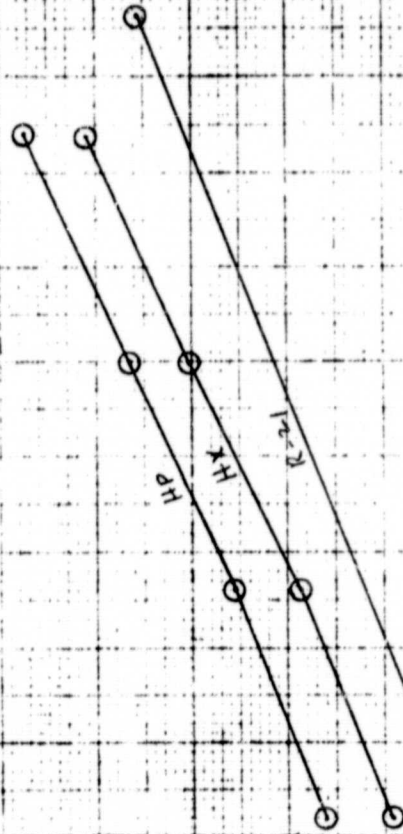
$P = 1510.62 \text{ WATTS}$

$\dot{M} = 992.35 \text{ LB/HR}$

$P.D. = 299.027 \text{ PSIG}$

$U_{\text{AVE}} = 1190.46 \text{ BTU/HC FT}^2 \text{ °F}$

AVE $\Delta T = 3.30 \text{ °F}$

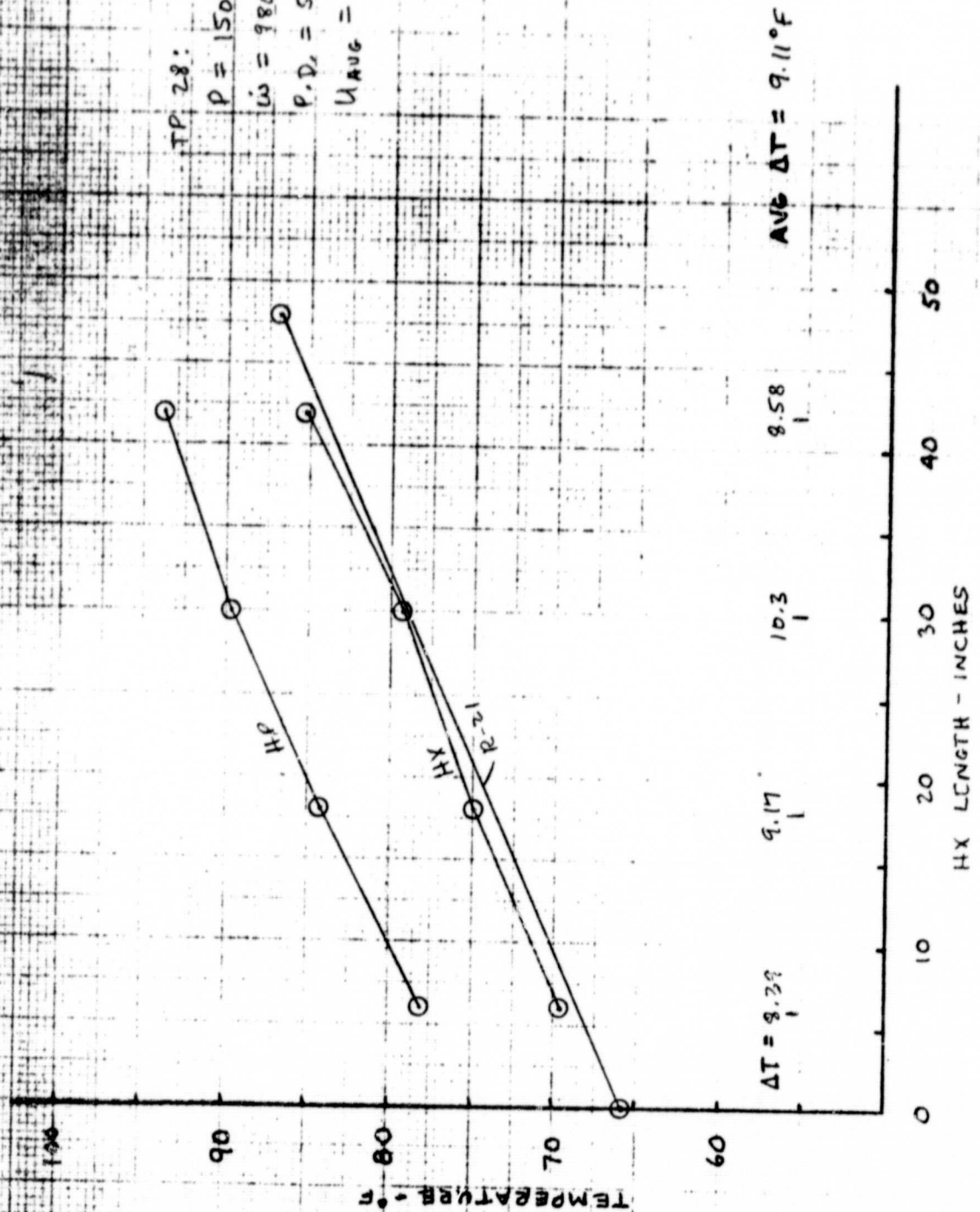


3.19

3.18

3.47

$\Delta T = 3.36$



ORIGINAL PAGE IS
OF POOR QUALITY

TP 29:

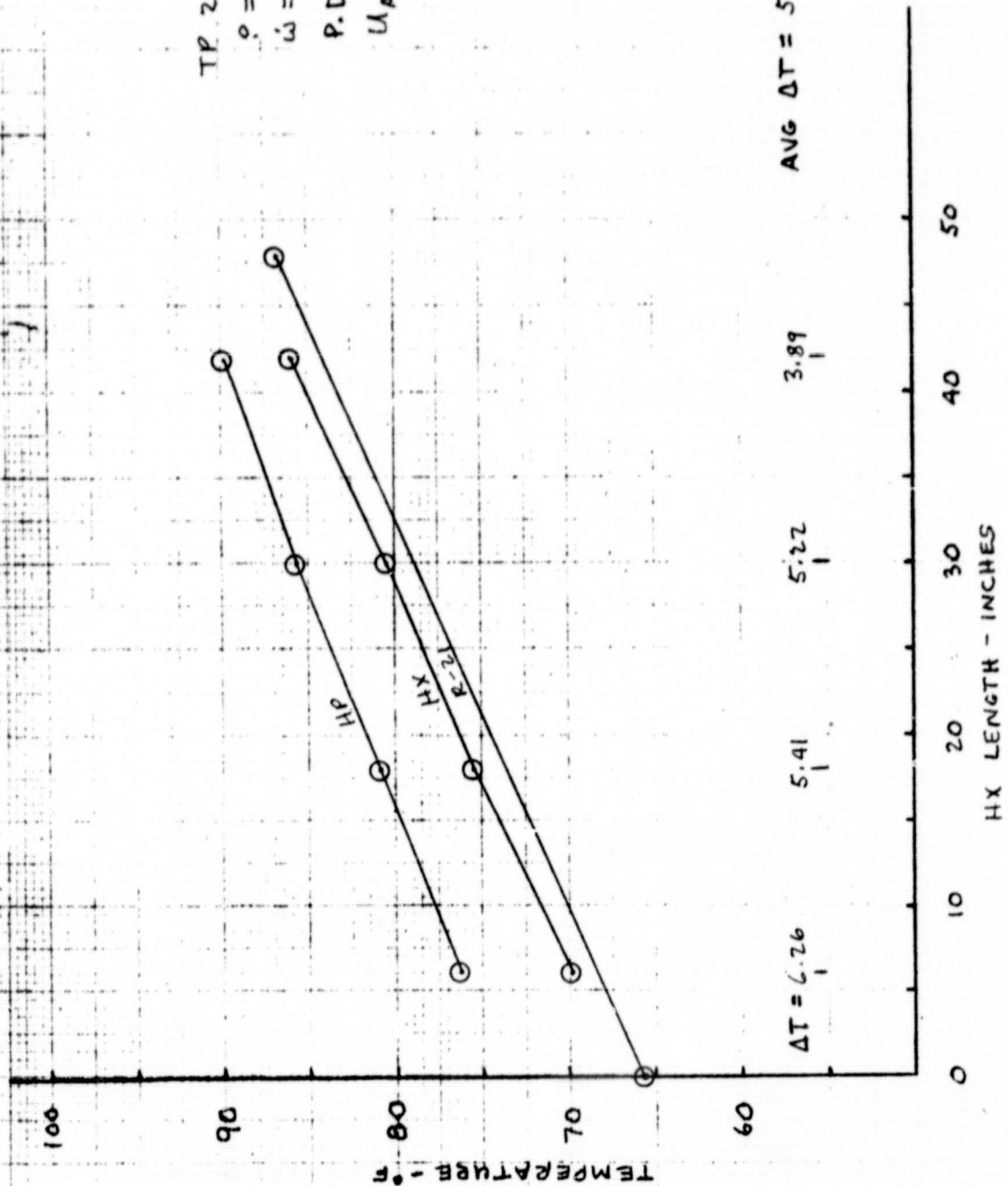
$$\dot{Q} = 1503.79 \text{ WATTS}$$

$$\dot{W} = 1003.32 \text{ LB/HR}$$

$$P.D. = 99.9595 \text{ PSIG}$$

$$U_{AVG} = 695.21 \text{ BTU/HR FT}^2 \text{ } ^\circ\text{F}$$

$$AVG \Delta T = 5.20^\circ\text{F}$$



ORIGINAL PAGE IS
OF POOR QUALITY

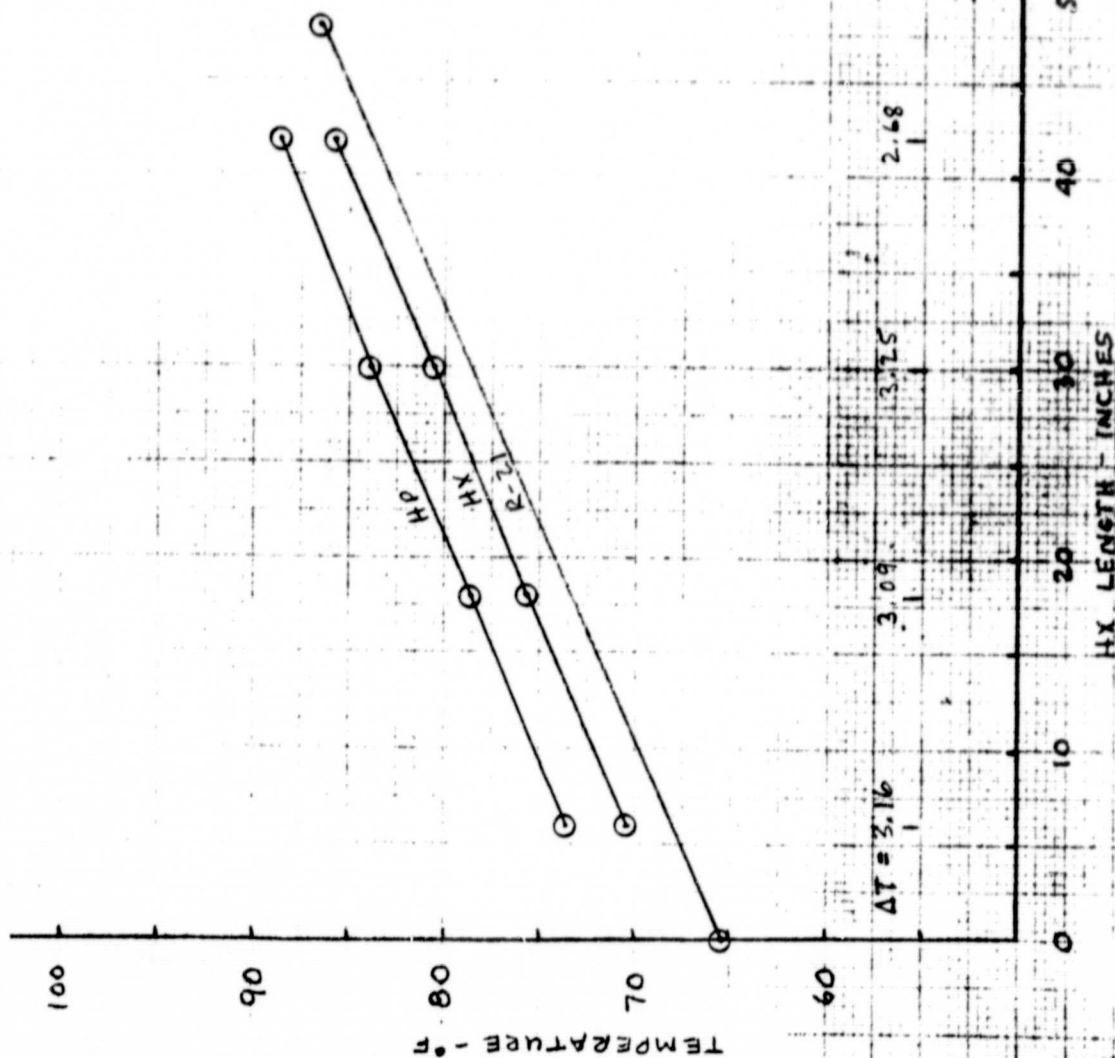
TP 30:

$P = 1504.61$ WATTS

$\dot{W} = 974.584$ LB/HR

P. D. = 199.958 PSIG

$U_{AVG} = 1185.93$ BTU/HR FT² °F



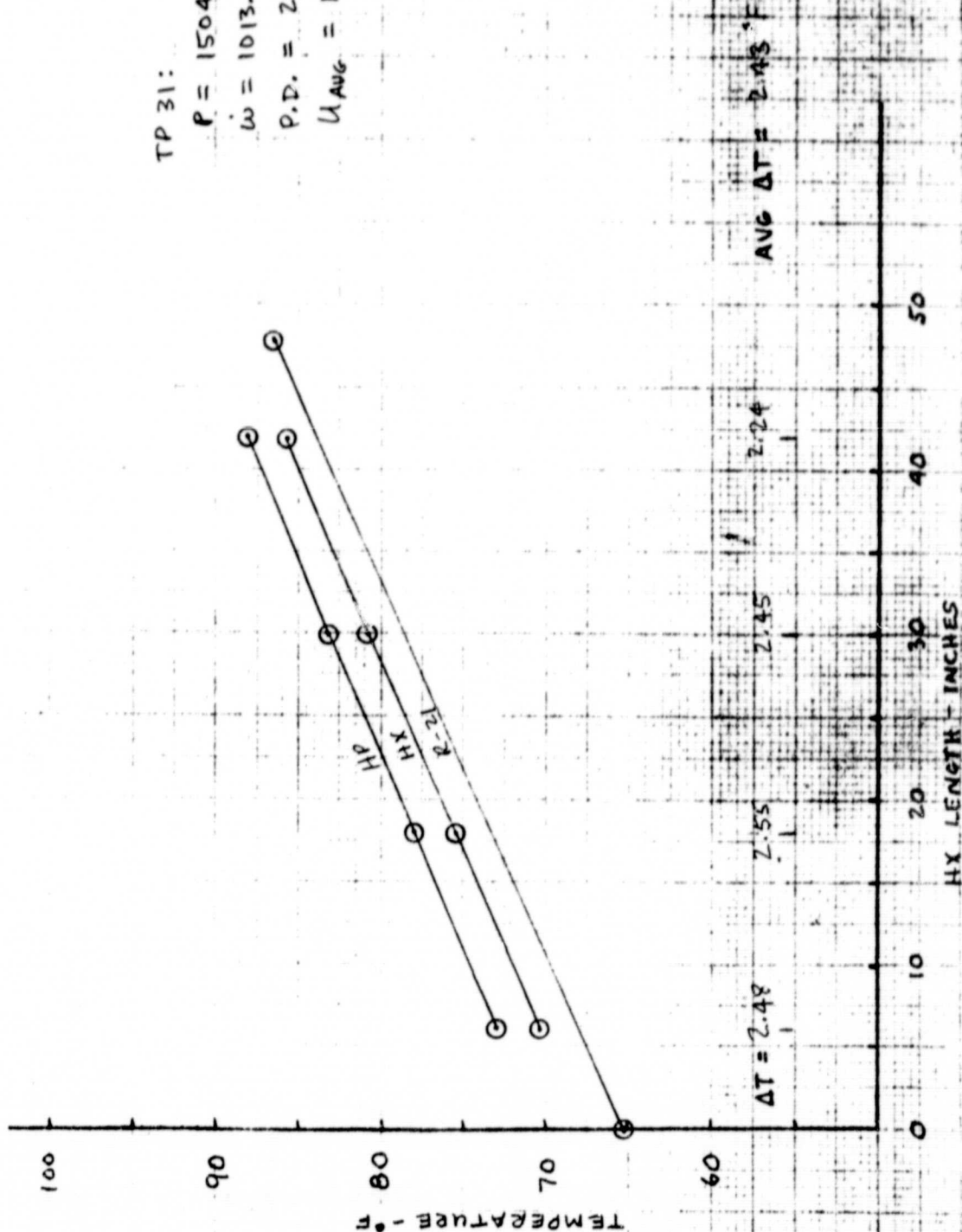
TP 31:

$$P = 1504.9 \text{ WATTS}$$

$$\dot{m} = 1013.26 \text{ LB/HR}$$

$$P.D. = 299.298 \text{ PSIG}$$

$$U_{\text{AVG}} = 1488.80 \text{ BTU/HE FT}^2\text{°F}$$



ORIGINAL PAGE IS
OF POOR QUALITY

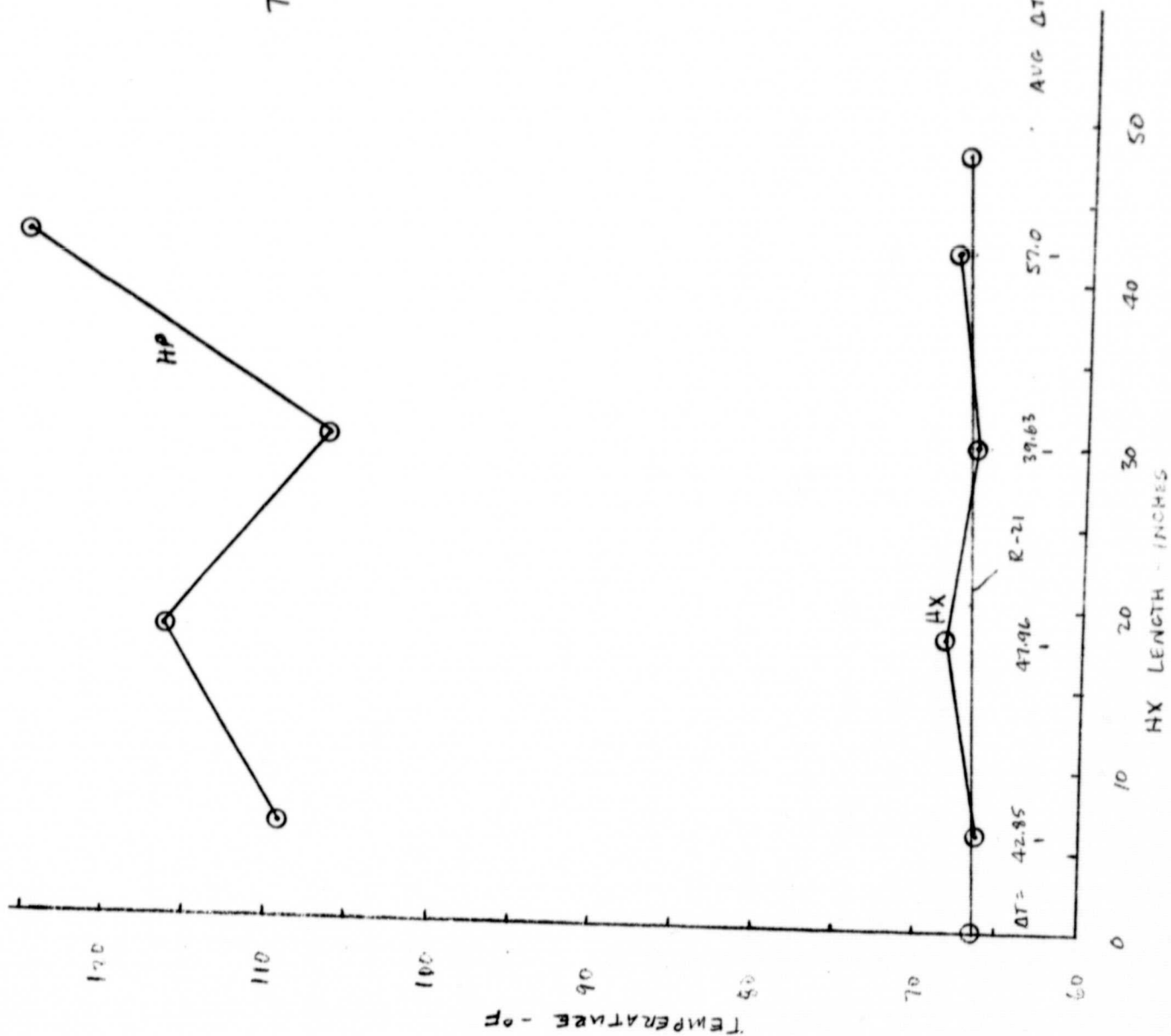
TP 32;

$P = 105.505$ watts

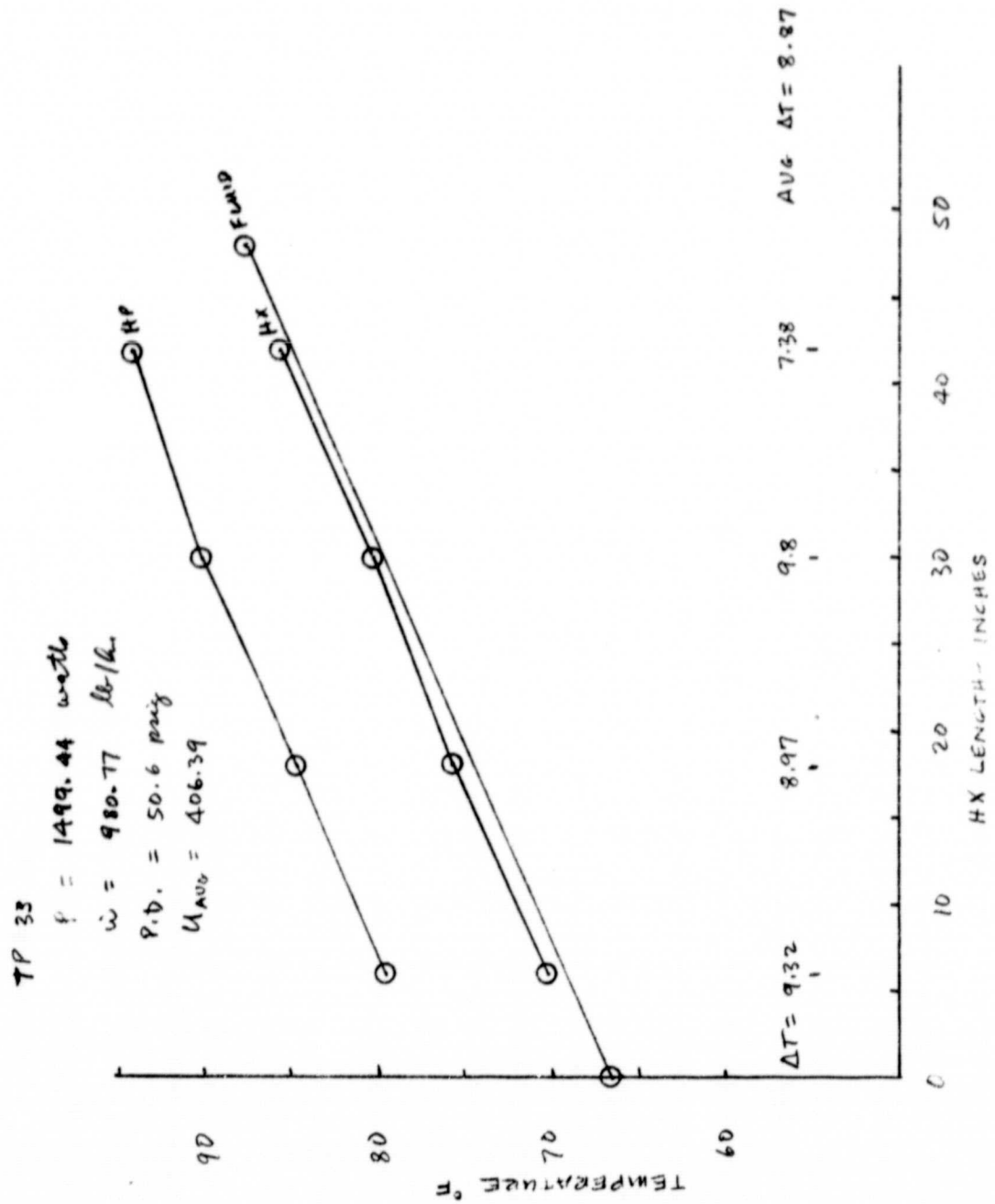
$\dot{m} = 987.71$ lb/hr.

P.D. = 3.5×10^{-6} hr

$U_{avg} = 5.41$ BTU/hr ft² °F



ORIGINAL PAGE IS
OF POOR QUALITY



ORIGINAL PAGE IS
OF POOR QUALITY

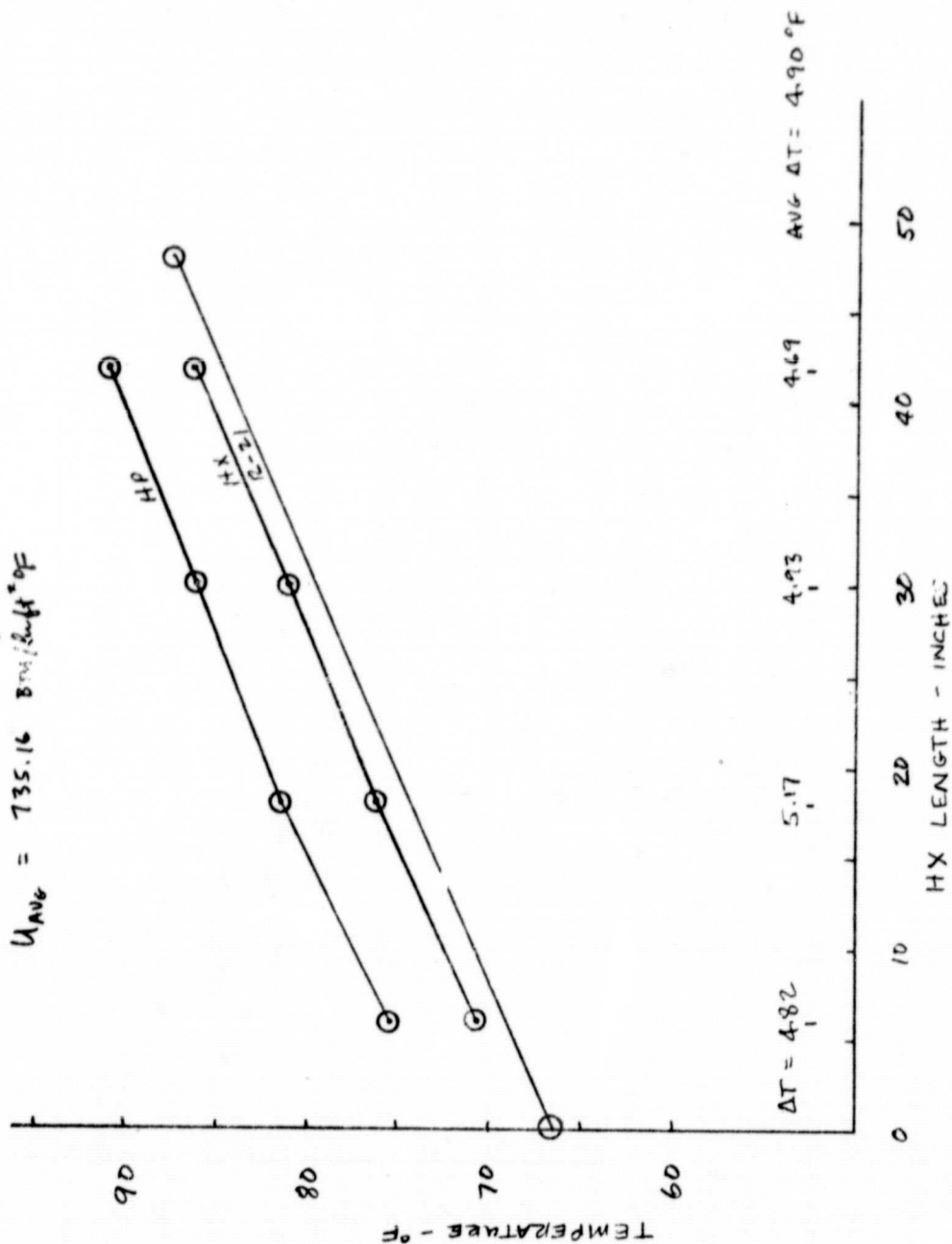
TP 34:

$P = 1498.46$ with

$\dot{W} = 978.287$ lb/hr

P.D. = 100.114 pair

$U_{AVE} = 735.16$ Btu/ft²°F



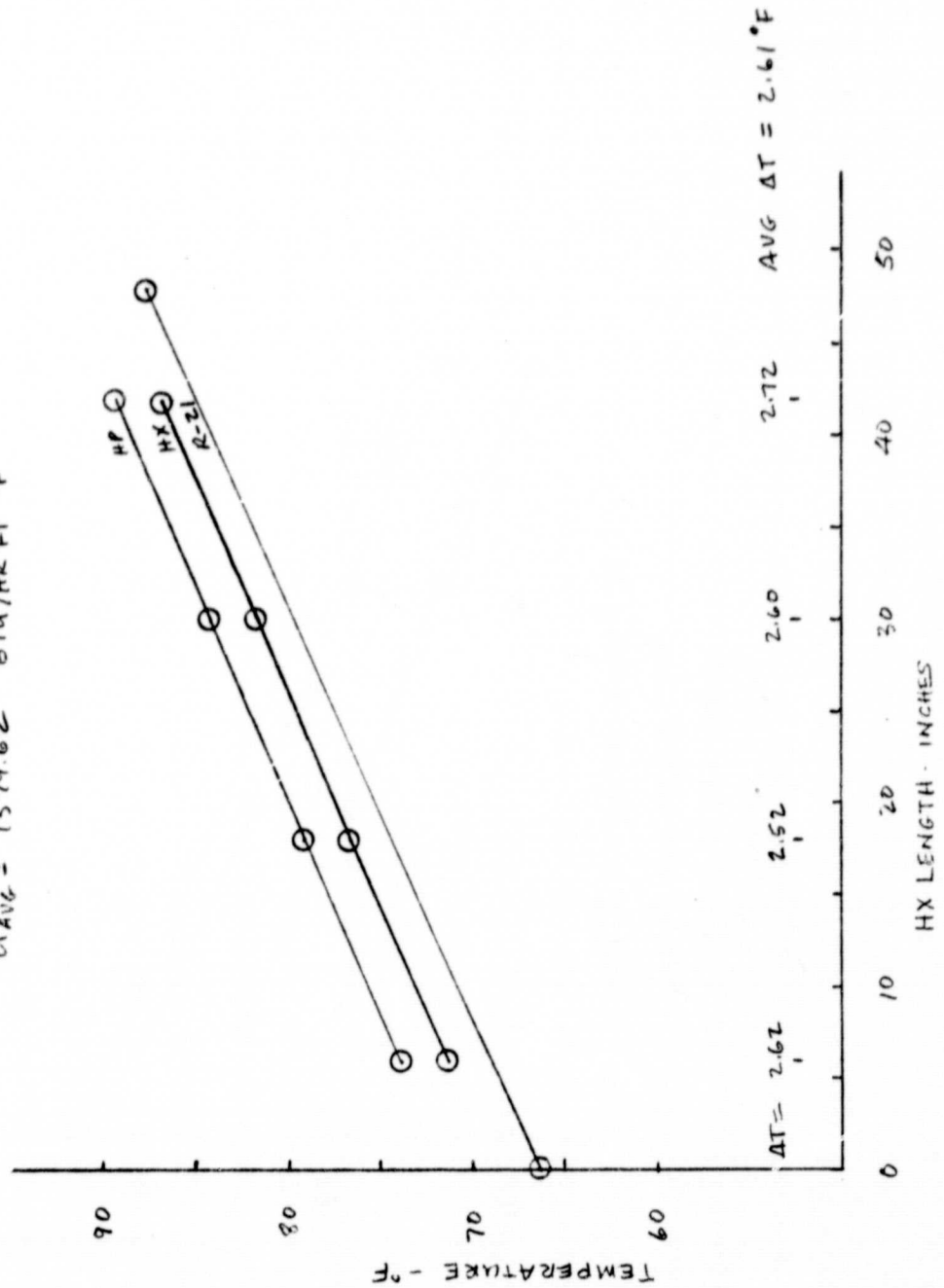
TP 35

$P = 1497.84 \text{ watts}$

$P.D = 199.57 \text{ paug}$

$\dot{W} = 994.94 \text{ lb/hr}$

$U_{AVE} = 1379.62 \text{ BTU/HR FT}^2 \text{ } ^\circ\text{F}$



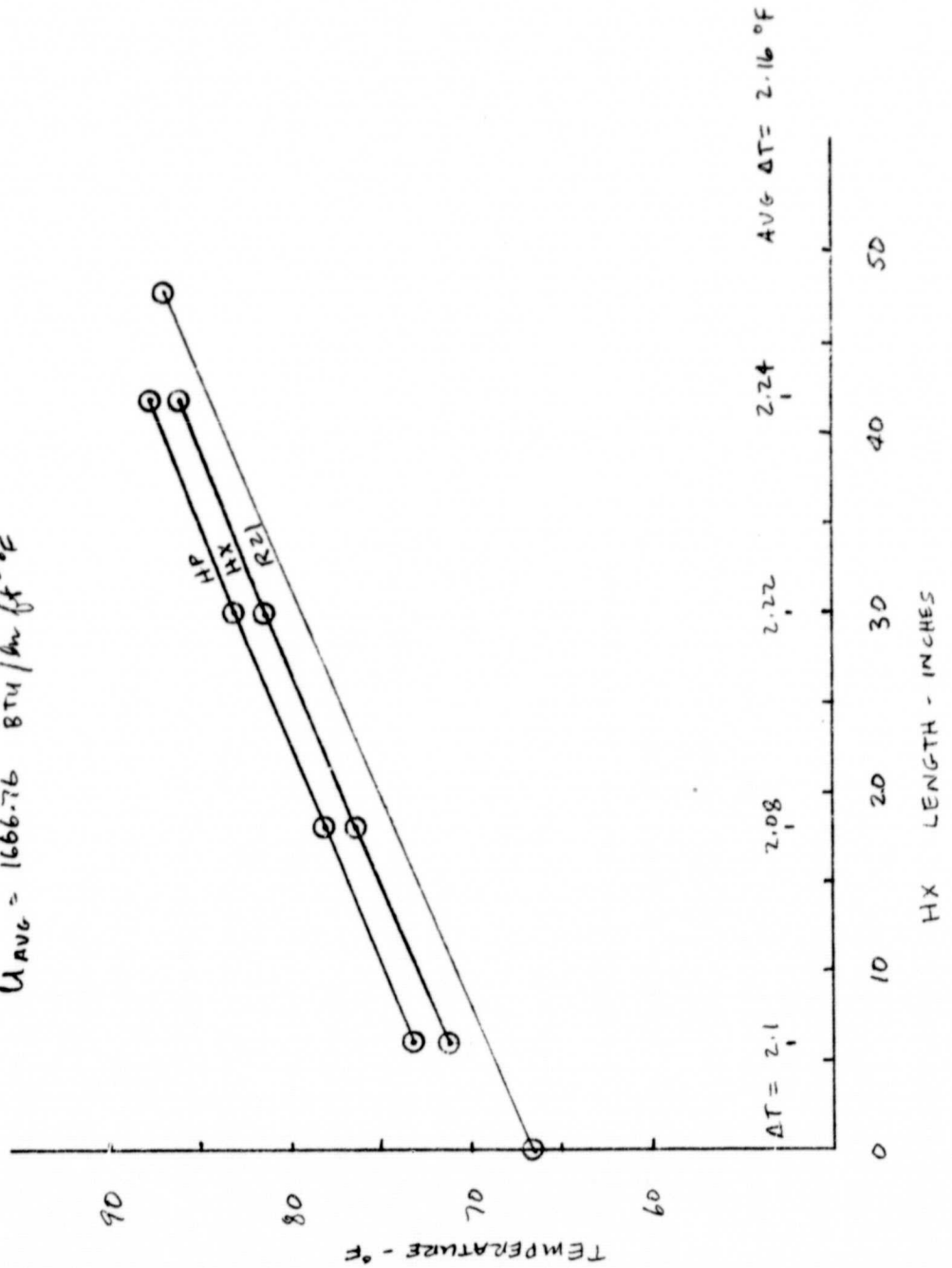
TP 36

$P = 1497.59$ watts

$\dot{m} = 1051.39$ lb/hr.

$P.D. = 299.259$ psig

$U_{AVE} = 1666.76$ BTU/hr ft² °F



ORIGINAL PAGE IS
OF POOR QUALITY

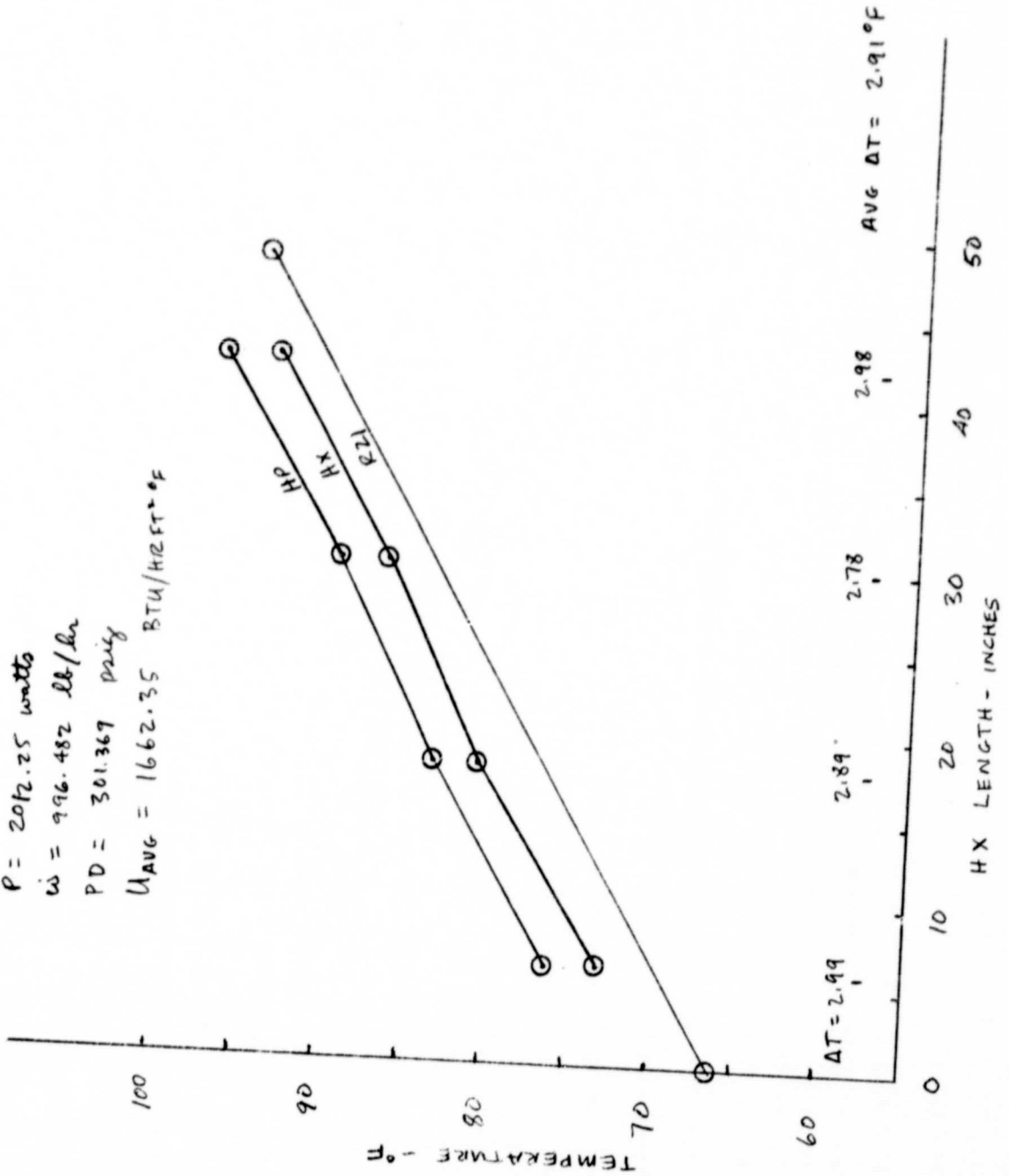
TP 37

$P = 2042.25 \text{ watts}$

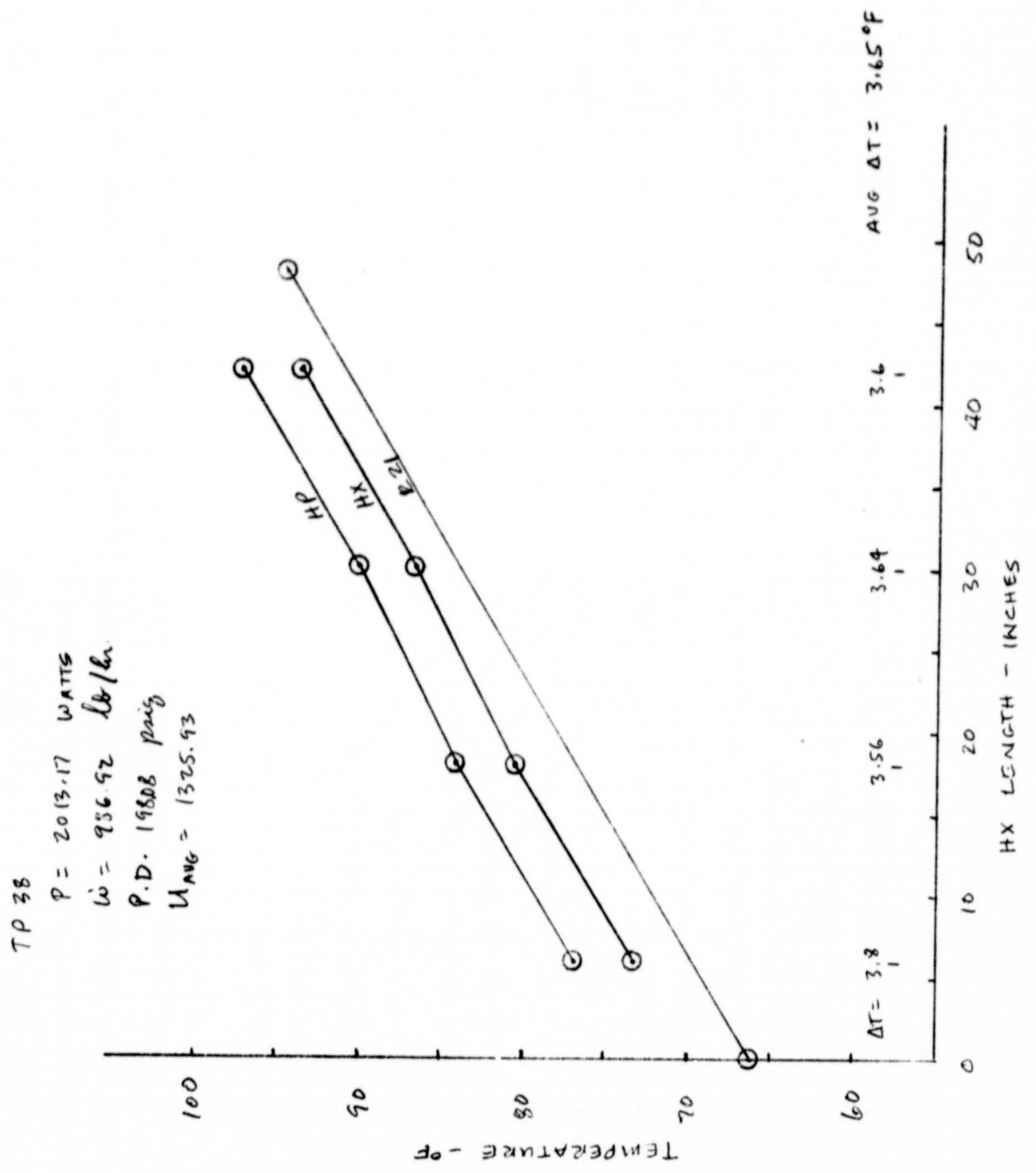
$\dot{m} = 996.482 \text{ lb/hr}$

$PD = 301.367 \text{ psig}$

$U_{AVG} = 1662.35 \text{ BTU/H2FT}^2\text{°F}$



ORIGINAL PAGE 13
OF POOR QUALITY



ORIGINAL PAGE
OF POOR QUALITY

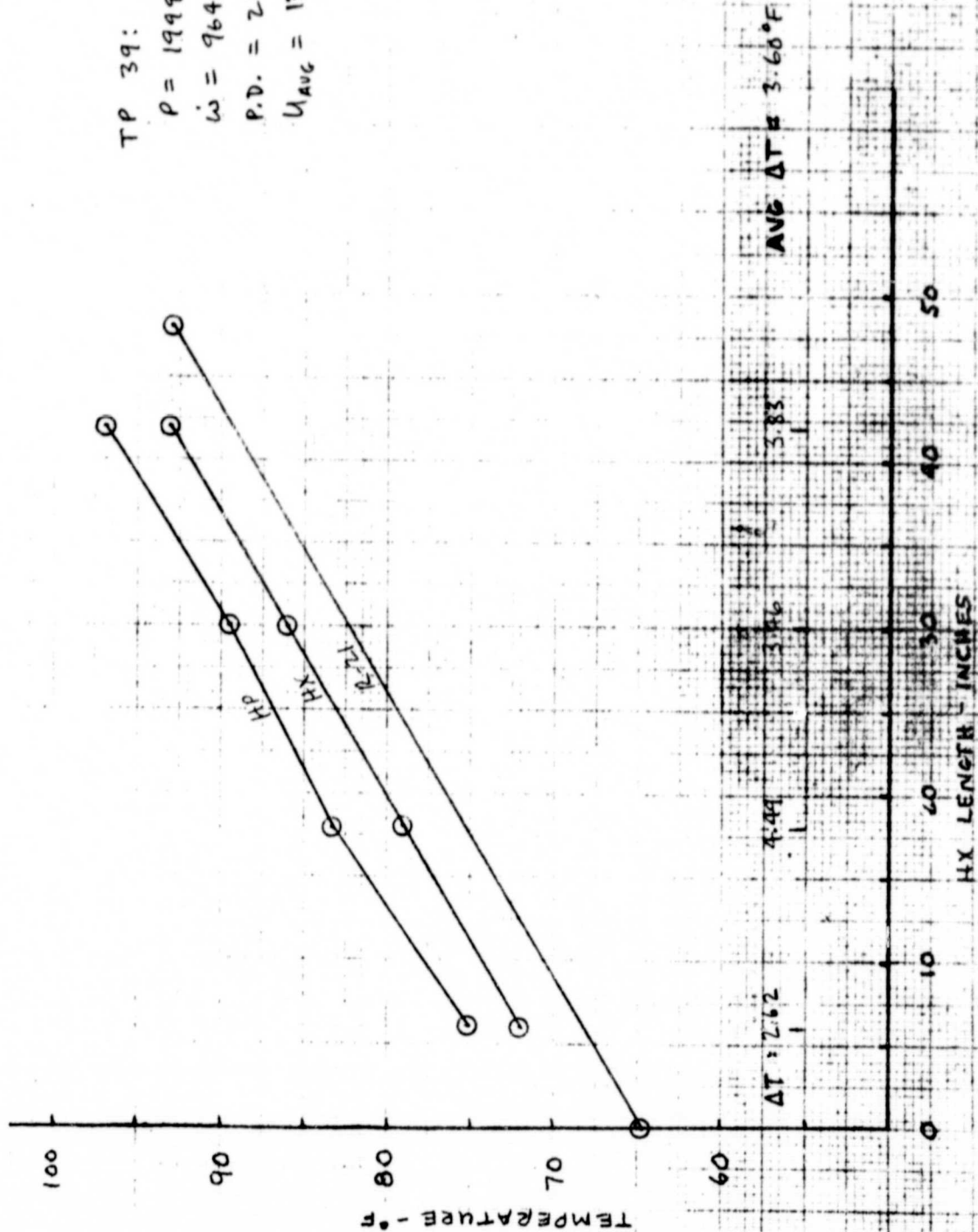
TP 39:

$$P = 1999.9 \text{ WATTS}$$

$$\dot{W} = 964.699 \text{ LB/HR}$$

$$P.D. = 299.724 \text{ PSIG}$$

$$U_{AUC} = 1335.49 \text{ BTU/HC FT}^2 \cdot ^\circ\text{F}$$



ORIGINAL PAGE IS
OF POOR QUALITY

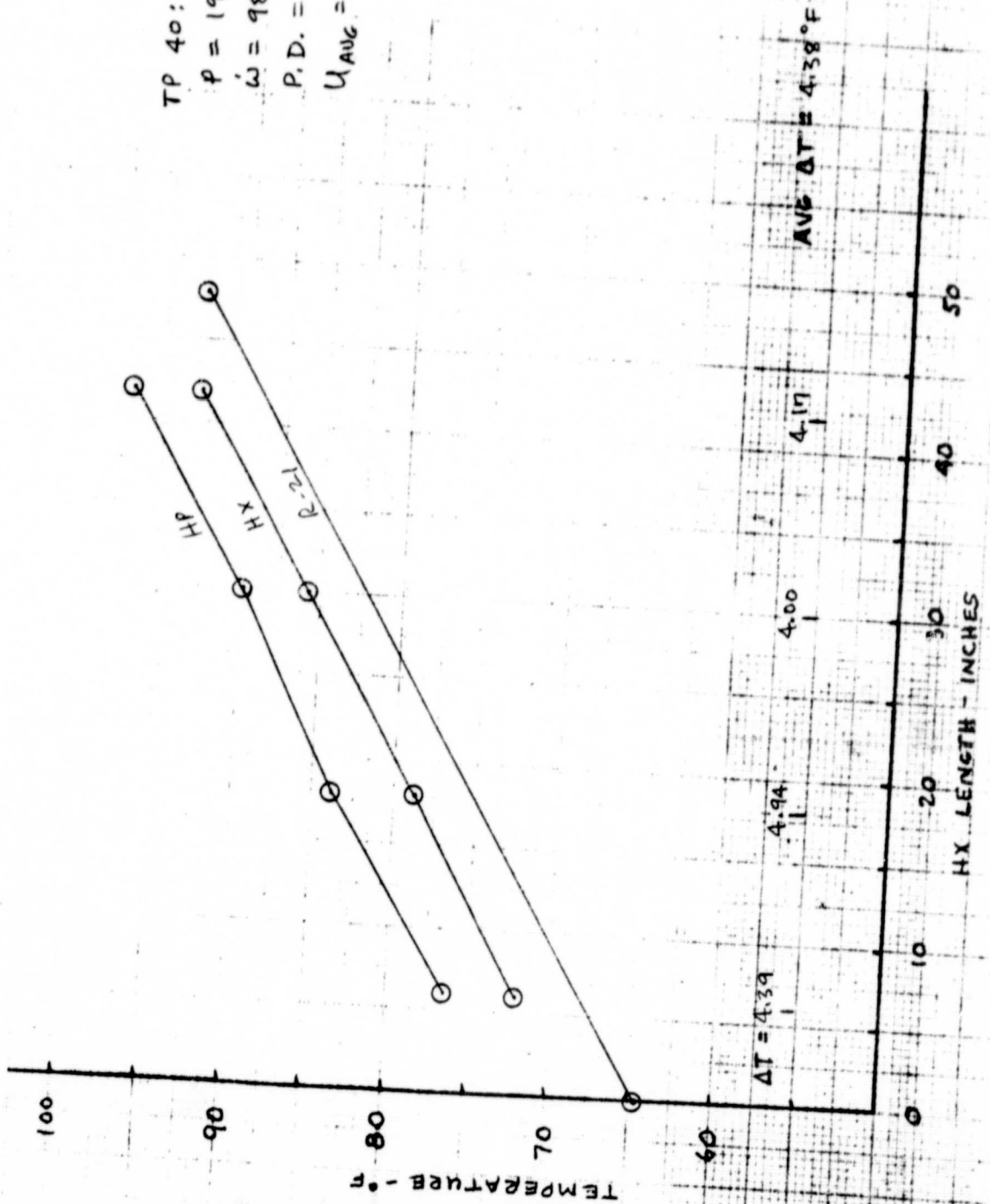
TP 40:

$$\dot{P} = 1999.53 \text{ WATTS}$$

$$\dot{W} = 980.948 \text{ LB/HR}$$

$$P.D. = 200.209 \text{ PSIG}$$

$$U_{AUG} = 1097.66 \text{ BTU/HR FT}^2 \text{ } ^\circ\text{F}$$



ORIGINAL PAGE IS
OF POOR QUALITY

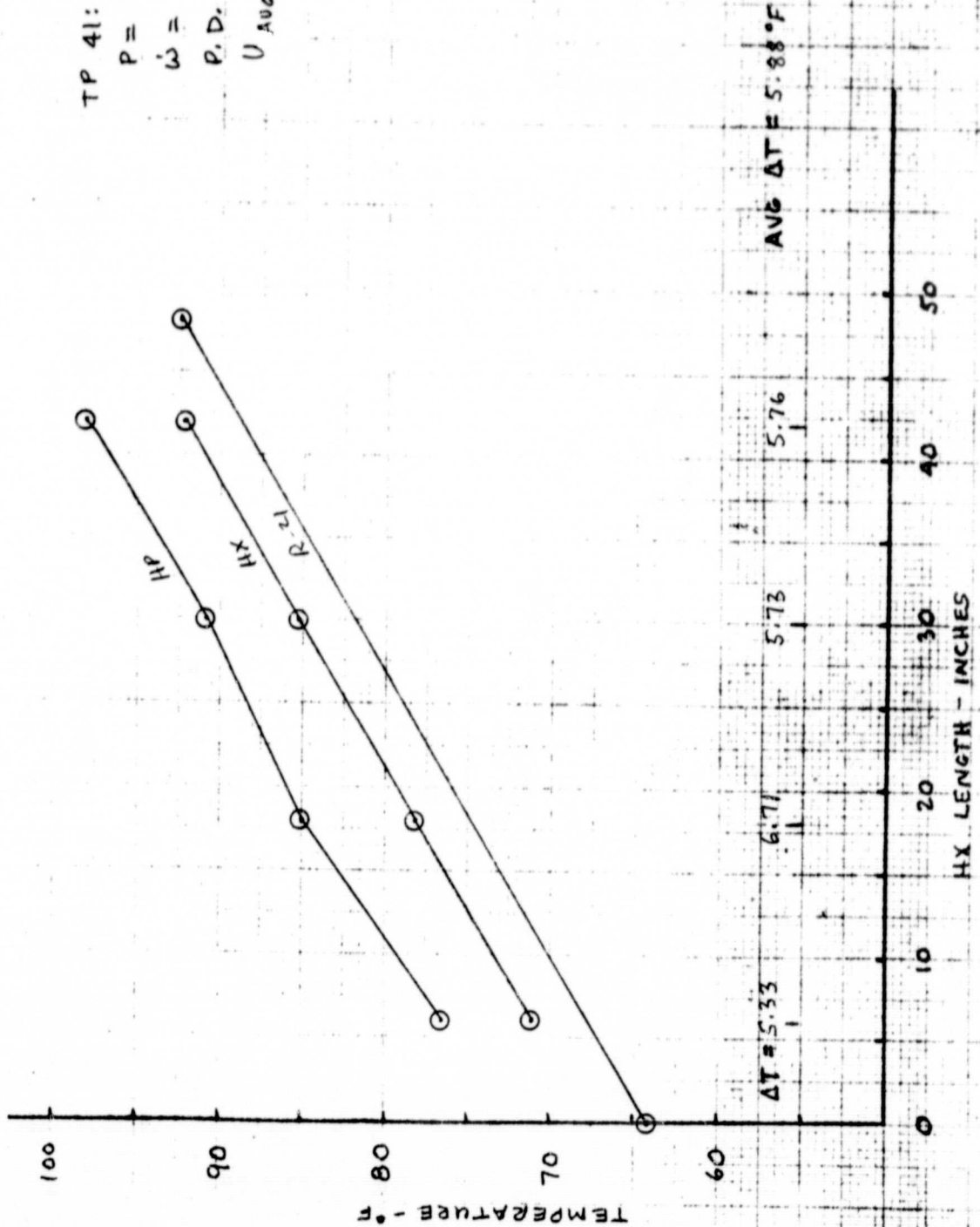
TP 41:

$$P = 2000.63 \text{ WATTS}$$

$$\dot{m} = 1018.88 \text{ LB/HR}$$

$$P.D. = 99.3788 \text{ PSK}$$

$$U_{AVE} = 817.94 \text{ BTU/HR FT}^2 \text{ } ^\circ\text{F}$$



ORIGINAL PAGE IS
OF POOR QUALITY

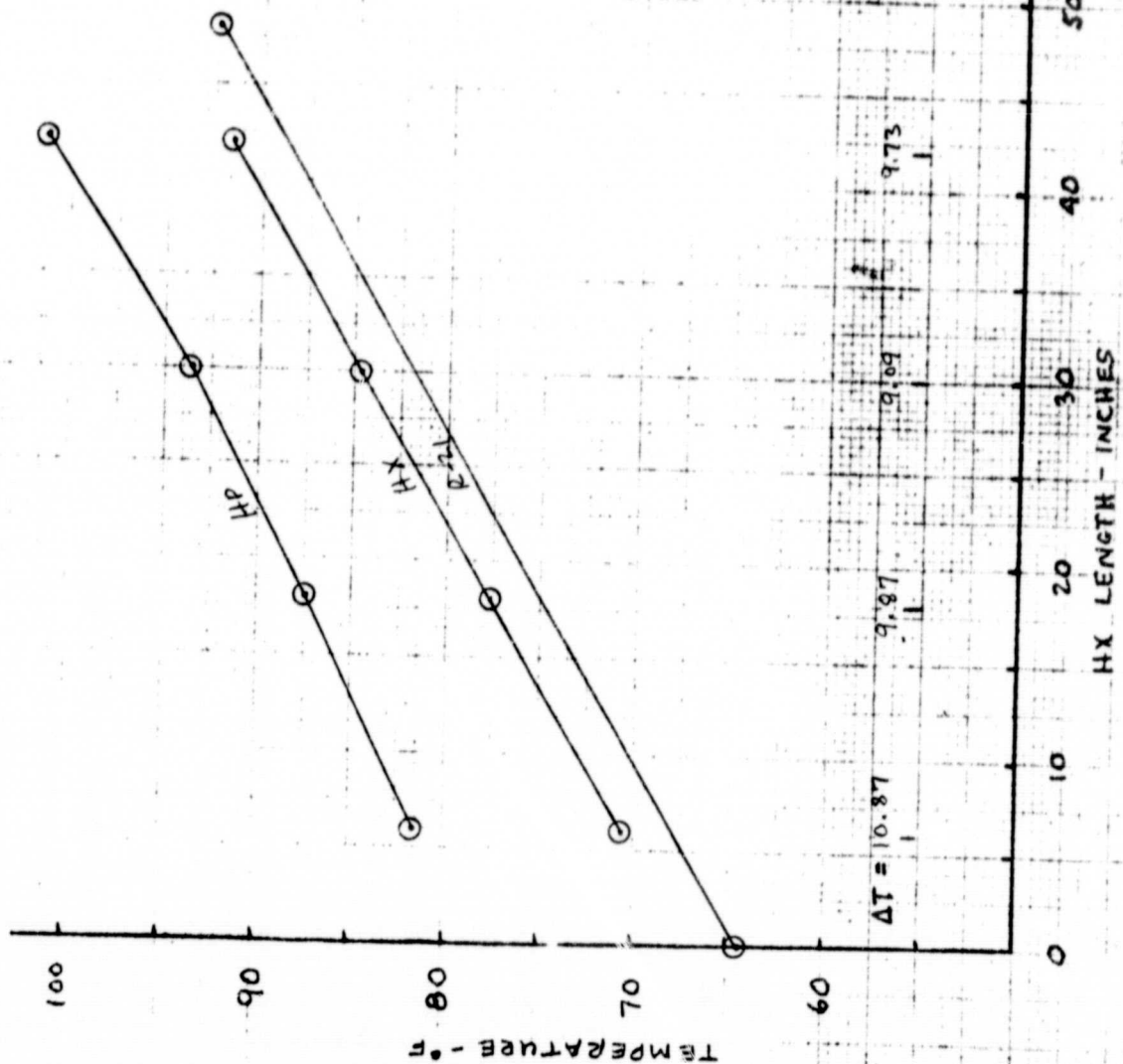
TP 42:

$P = 2001.55$ WATTS

$\dot{m} = 989.519$ LB/HR

P.D. = 49.492 PSIG

$U_{Avg} = 486.52$ BTU/HR FT² OF



ORIGINAL PAGE 13
OF POOR QUALITY

TP 43:

$$P = 195.815 \text{ WATTS}$$

$$\dot{m} = 980.794 \text{ LB/HR}$$

$$P.D. = .729371 \text{ PSIG}$$

$$U_{AVG} = 66.77 \text{ BTU/HR FT}^2 \text{ } ^\circ\text{F}$$

